Journal which deals with research, Innovation and Originality

Table of Content

CHIEF EDITOR BOARD

Message from IJERGS

This is the Third Issue of the Sixth Volume of International Journal of Engineering Research and General Science. A total of 11 research articles are published and we sincerely hope that each one of these provides some significant stimulation to a reasonable segment of our community of readers.

In this issue, we have focused mainly on the Innovative Ideas. We also welcome more research oriented ideas in our upcoming Issues.

Author's response for this issue was really inspiring for us. We received many papers from many countries in this issue but our technical team and editor members accepted very less number of research papers for the publication. We have provided editors feedback for every rejected as well as accepted paper so that authors can work out in the weakness more and we shall accept the paper in near future.

Our team have done good job however, this issue may possibly have some drawbacks, and therefore, constructive suggestions for further improvement shall be warmly welcomed.

IJERGS Team,

International Journal of Engineering Research and General Science

E-mail – feedback@ijergs.org

Static and Dynamic Wind Force Analysis of Self Supporting Flare Base Circular Steel Stacks with Variable Height

Babita Devi[1], Shashi Shekhar Singh[2]

Lecturer, Civil Engineering Department, Government Polytechnic Education Society, Mandkola, Palwal, India [1]

Associate Professor, Department of Civil Engineering, Madda Walabu University, Bale Robe, Ethiopia [2]

Abstract: This paper deals with the behaviour of Flare base circular steel stacks with variable height of 30m, 40m, and 50m respectively. The study aim is to find out the structural behaviour of Flare base steel stack under the equivalent static and dynamic wind forces. The static & dynamic wind analysis is done by using the Staad.Pro Vi8 ss5 software with assumptions as per IS 6533:1989(part1 & part2). The study parameter of static and dynamic forces, maximum deflection due to static & dynamic wind forces for flare base circular steel stacks for the different height with constant wind speed 47m/s (Location:- Agra, India) was compared.

Keywords— Steel stacks, Static wind force, Dynamic wind force, Maximum deflection and Variable height.

INTRODUCTION:

A steel stack is a vertical channel through which smoke and combustion gases pass out of a building. Steel stacks are used to emit and exhaust gases in atmosphere at higher elevation. Failure of steel stacks is prime issue in most of industries. The cause behind the failure is analyzed by the static & dynamic wind analysis of stacks. The steel stacks less than 80m are called short steel stacks. The first mode is sufficient for the analysis for the short circular steel stacks.

ANALYSIS OF STEEL STACKS:

Wind analysis include the effect of static and dynamic wind forces .Geometry of flare base is given in Table-1 as per accordance IS 6533 Part-1&2.

    A. *Geometry for flare base steel stacks:*

        Basic geometry of steel stacks is governed by top diameter (D_t), base diameter (D_b) and effective height (H_e). Following IS code are used for the analysis of steel stacks.

        a)   IS 6533 (part-1):1989, "Indian standard code of practice for design and construction of steel chimney –code of practice-Mechanical aspects."

        b)   IS 6533 (part-2):1989, "Indian standard code of practice for design and construction of steel chimney –code of practice-Structural aspects."

        c)   IS 875:1987(part-3) used for the wind force analysis.

Minimum top diameter of unlined chimney should be one twentieth of effective Height of chimney/stacks and minimum outside diameter at base should be equal to 1.6 times the top diameter of stack. (As per IS 6533(part2):1989(reaffirmed in 2003) cl.7.2.4 (b) &(c).

Table: 1 Geometry of Flare base steel stacks

Steel stacks	Total Height of stack (Meters) (H)	Basic wind speed (m/s)	Effective Height (He) = (2/3xH) (meter)	Top Diameter (Dt) = (H/30) (meter)	Bottom diameters (Db) = (1.6 * Dt) (meter)
1	30	47	20	1	1.6
2	40	47	26.67	1.33	2.128
3	50	47	33.33	1.66	2.656

PROBLEM -STATEMENT

Analyse the behaviour of self supporting flare base circular steel stacks under the static and dynamic wind forces of variable height as per Indian standard code of practice.

Detail of steel stack

- Type: self-supported unlined industrial flare base circular steel stacks with constant shell thickness as IS 6533 Part-1.

- Total 3 steel stacks (Wind speed constant with variable Height)

- Height of steel stack: 30m, 40m, and 50m.

- Top diameter for each stack is taken as minimum $h_e/20$ as per provision in IS 6533:1989.

- Variation in base diameter for each stack for fixed value of top diameter will be in following incremental ratio (ratio D_b/D_t) : 1.6

- Base condition : Rigid support at base

- Location of stack :Agra (L: 78*1'0", D: 27*10'0")

- Basic wind speed at location : 47m/s

- Shell thickness : 16mm (constant for all stacks)

- Materials for steel stack are conforming to IS2062:2006.

Results:

A. Static& dynamic wind Responses for Flare base circular steel stacks for 47m/s wind speed:

Deflection of FBC SS considering Static and dynamic wind force at basic wind speed 47m/s is given in table-2 & table-3.

Table: 2 Static wind responses for Flare base circular steel stacks for 47m/s wind speed

FBC SS	Height (m)	Top Diameter (m)	Bottom Diameter (m)	Static Wind Force (KN)	Maximum Deflection (mm)
30 m	10	1m	1.6 m	6.048	21.893
	20			6.408	
	30			5.880	
40m	10	1.33m	2.128 m	6.588	71.351

	20			7.342	
	30			7.203	
	40			5.880	
50 m	10	1.66m	2.656 m	6.634	116.233
	20			7.591	
	30			7.644	
	40			6.938	
	50			7.008	

Table: 3 Dynamic wind responses for Flare base circular steel stacks for 47m/s wind speed

FBC SS	Height (m)	Top Diameter (m)	Bottom Diameter (m)	Dynamic Wind Force (KN)	Maximum Deflection (mm)
30 m	10	1.00m	1.600 m	5.6461	25.411
	20			5.3753	
	30			5.6171	
40m	10	1.33m	2.128 m	8.1018	86.280
	20			7.1670	
	30			7.8879	
	40			7.8872	
50 m	10	1.66m	2.656 m	10.4716	141.123
	20			10.3180	
	30			9.8742	
	40			9.8716	
	50			11.0877	

B. *Graphical representation of static and dynamic wind Force:*

The static and dynamic wind forces are given below in Fig-1 and Fig-2.
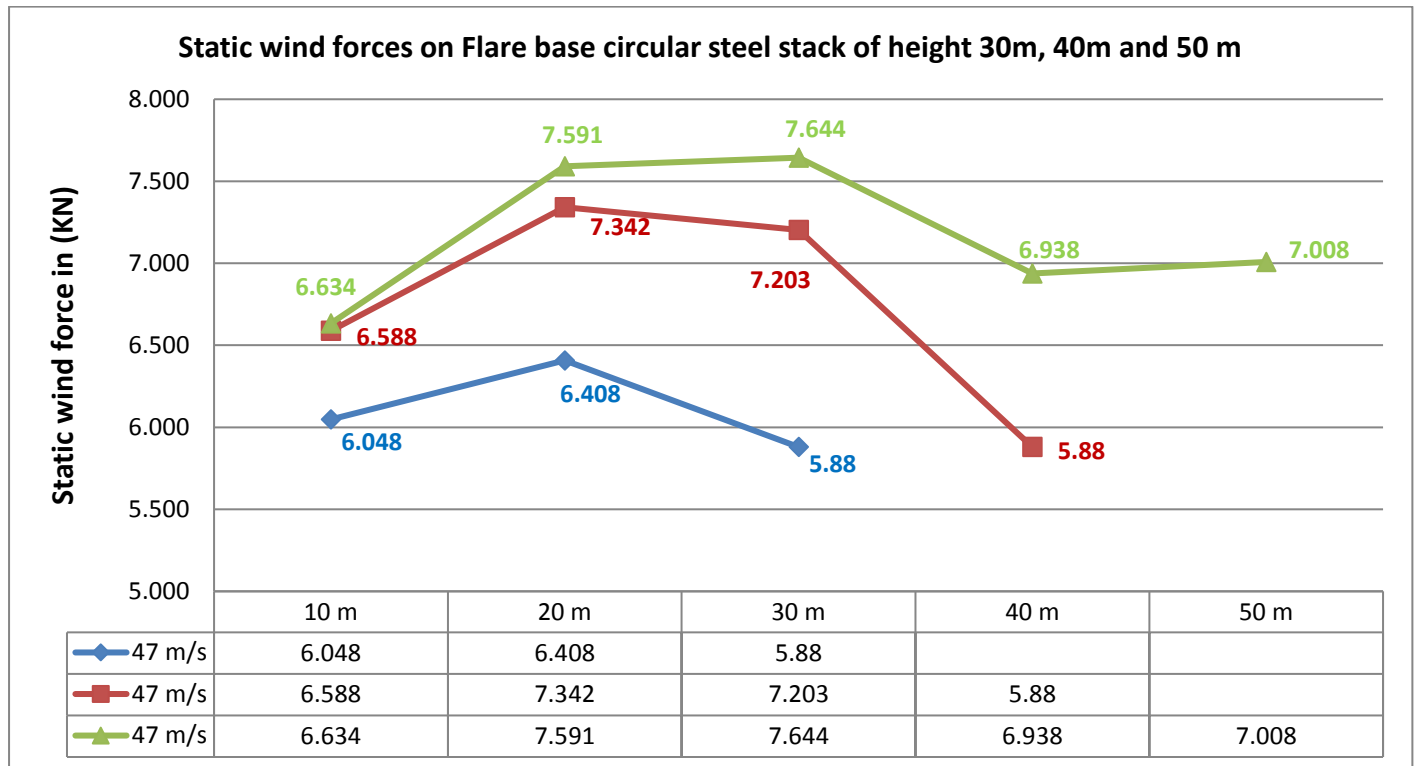
Static wind forces on Flare base circular steel stack of height 30m, 40m and 50 m

	10 m	20 m	30 m	40 m	50 m
47 m/s	6.048	6.408	5.88		
47 m/s	6.588	7.342	7.203	5.88	
47 m/s	6.634	7.591	7.644	6.938	7.008

Fig-1 Static wind forces on flare base circular steel stack of wind speed 47 m/s with height (30m, 40m and 50m)

Dynamic wind forces on Flare base circular steel stack of height 30m, 40m and 50m.

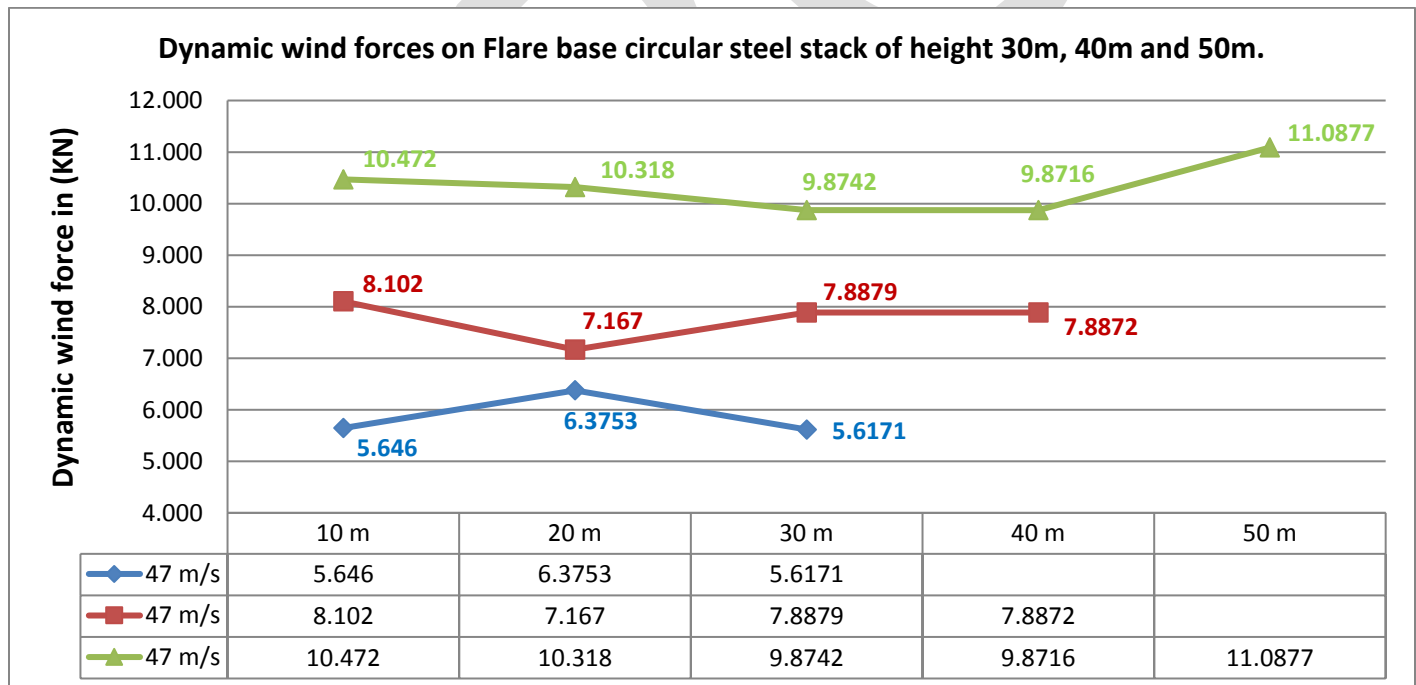|	10 m	20 m	30 m	40 m	50 m
47 m/s	5.646	6.3753	5.6171		
47 m/s	8.102	7.167	7.8879	7.8872	
47 m/s	10.472	10.318	9.8742	9.8716	11.0877

Fig-2 Dynamic wind forces on flare base circular steel stack of wind speed 47 m/s with height (30m, 40m and 50m)

C. *Maximum deflection due to static and dynamic wind responses:*

Maximum deflection due to static and dynamic wind forces increases along the increment in height. Maximum deflections at variable height (30, 40 & 50m) are given in figure -3.
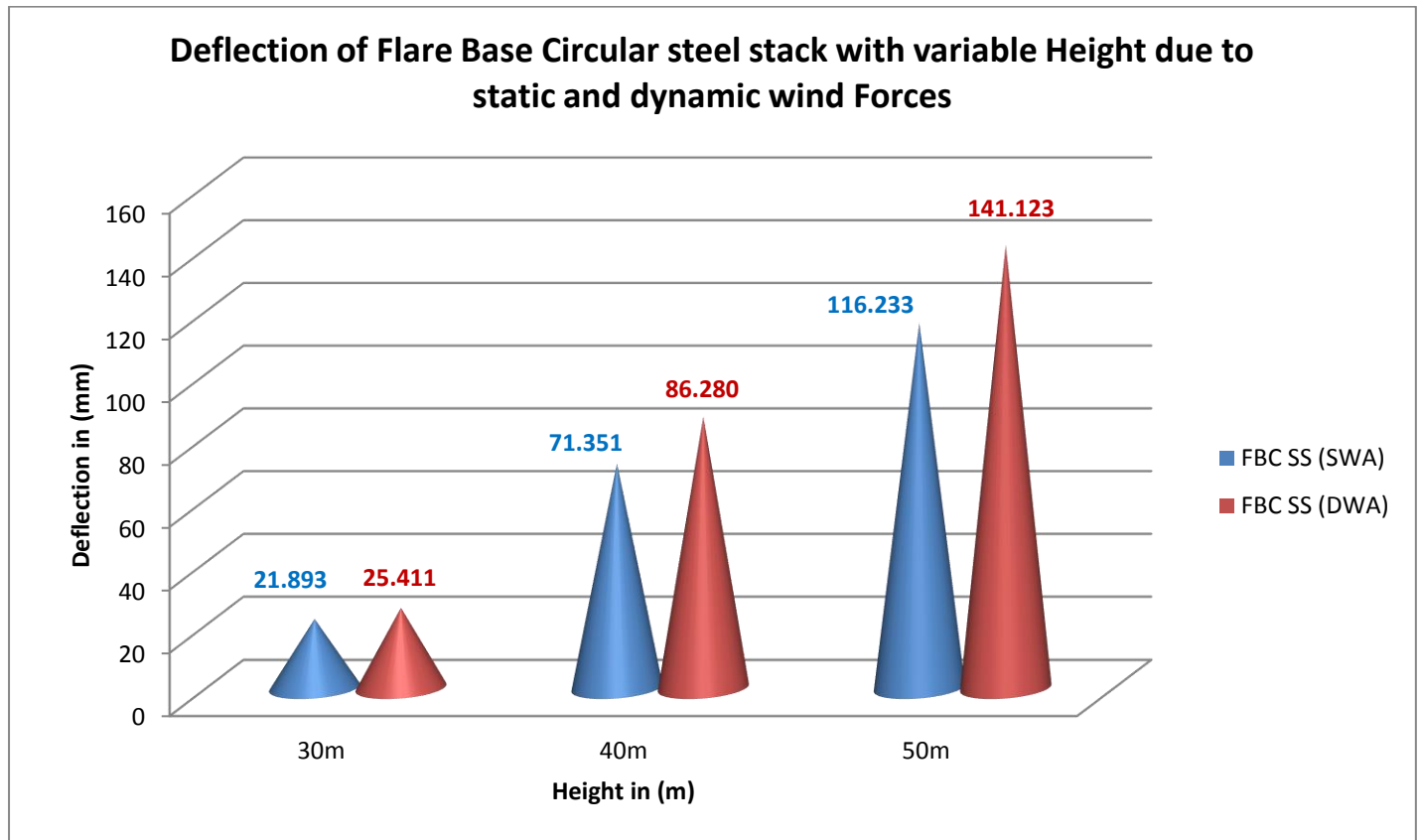
Fig-3 Maximum Deflection due to Static wind response with variable height (Basic mode)

CONCLUSION:

Following results are obtained from all above graphical representations:

1. Maximum deflection due to static wind force increase with the increase in height of steel stacks. At 30m, 40m and 50m height maximum deflection are 21.893mm, 71.351mm and 116.233mm respectively.

2. Maximum deflection due to dynamic wind force increase with the increase in height of steel stacks. At 30m, 40m and 50m height maximum deflection are 25.411 mm, 86.280mm and 141.123mm respectively.

3. Maximum deflection is more due to dynamic wind force as compare with static wind force at their respective height.

4. Maximum deflection difference is increasing due to static and dynamic wind force with the increase in height of steel stacks. At 30m, 40m and 50m height maximum deflection difference are 3.518mm, 14.929mm and 24.890mm respectively.

REFERENCES:

1. **IS 6533 (Part 2): 1989**, "*Code of Practice for Design and Construction of Steel Chimney*", Bureau of Indian Standards, New Delhi.
2. **IS 6533 (Part 1): 1989**, "*Design and Construction of Steel Chimney-Code of practice*", Bureau of Indian Standards, New Delhi.
3. **M Gaczek, J Kawecki(1996)**, "*Analysis of cross-wind response of steel chimneys with spoilers*", Journal of Wind Engineering and Industrial Aerodynamics. 65, pp.87-96.
4. **G. Murali *et al.*, (2012)**, "*Response of Mild Steel chimney Under Wind Loads*", International Journal of Engineering Research and Applications, 2(2), pp. 490-498.

5. **Harshal Deshpande ,Roshni John (2015)**, "*correlation of geometry and dynamic response of self-supporting circular steel stacks* ", International Journal of Engineering Technology Science and Research IJETSR, Vol. 2,special Issue 8 (september 2015), pp. 133- 144.

6. **Babita Devi, (2016),** "*Analysis of Self supporting Steel Stacks with Variable Geometrical Configuration under the seismic loading for different shapes",* International Journal of Engineering Research and general science.

Influence of PET bottle mesh in Flexural behaviour of concrete beam

Teena Thomas [1], Faisal K. M [2]

[1] PG Scholar, Dept of Civil Engineering, Universal Engineering College, Vallivattom, Thrissur, Kerala, India.

[2] Assistant professor, Dept of Civil Engineering, Universal Engineering College, Vallivattom, Thrissur, Kerala, India.

Abstract— Polyethylene Terephthalate (*PET*) is among the most widely used plastic resins around the world with increased recycling rates every year. Many studies have been done using waste plastic fibers in short, dispersed and continuous forms to reinforce concrete. Test of beams with PET fiber in mesh form and that in tension zone region has not yet reported. This paper presents a study of the flexural behaviour of concrete beams with PET mesh in tension zone. The results of 28 days flexural strength test and its comparison with ordinary concrete on 6 simply supported beams are presented.

Keywords — PET, PET mesh, Tension zone, Flexural behaviour, Flexural strength test

INTRODUCTION

Concrete is one of the most widely used construction   material in the world and it is strong in compression but weak in tension and brittle one. The ductility of concrete can be increased by reinforcing with fibers. In recent year all over the world, there is increased production of the plastic waste and improper disposal of this plastic leads to a serious environmental problem. Plastic is composed of various toxic chemicals and materials thereby pollutes air, soil and also water because plastic is a non biodegradable material. Due to slow degradation rate plastic is dangerous to nature and also it can block the plant roots movement. Therefore, it is necessary to find alternatives about recycling and reusing the waste plastic materials. The potential of PET waste in replacing aggregates in concrete which represents a better option than landfill. Number of studies has been conducted using waste plastic as components in cement pastes, mortar and concrete. It has been reported that, concrete reinforced with short, dispersed and continuous plastic fibers drastically improves the performance of concrete and eliminates its disadvantages.

METHODOLOGY

In the present research, experimental investigations were conducted for assessing the flexural strength of concrete provided with continuous PET fiber in mesh form which was incorporated in the tension zone. PET fibers were extracted from washed bottles collected from household waste. A hand tool made of wood was used to extract continuous fibers. Uniform width of 10mm was fixed for fiber as shown in Fig 1. Thickness of PET fiber was found to be 0.5mm using a vernier scale. Mesh size obtained is 25mm x 25mm as the size of coarse aggregate used is 20mm. For transforming continuous fibers to mesh form, a synthetic based adhesive called Fevibond were used. The tensile strength of PET strip obtained is 460 N/mm². Totally 2 types of concrete beam specimens of size 500 x 100 x 100 mm were used for the research. Control beams are those which were made with plain concrete of M25 mix without any reinforcement. Second type is beam with plain concrete of same M25 mix with the PET mesh in tension zone. Test setup has shown in Fig.2. Beams were casted with design mix ratio of 1:1.45:2.68 with w/c ratio 0.45. The mix was prepared and evenly filled till thickness reached 25mm. Prepared mesh was then placed over it as shown in Fig 3. Slowly rest of the mould portion was filled. The beams were then tested under two point loading test after 28 days water curing.
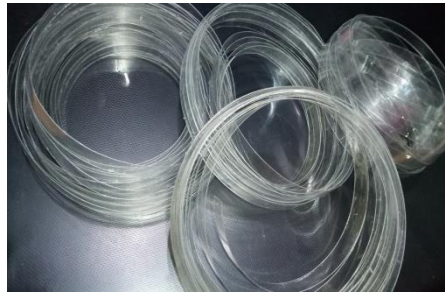
Fig. 1 Peeled PET fiber
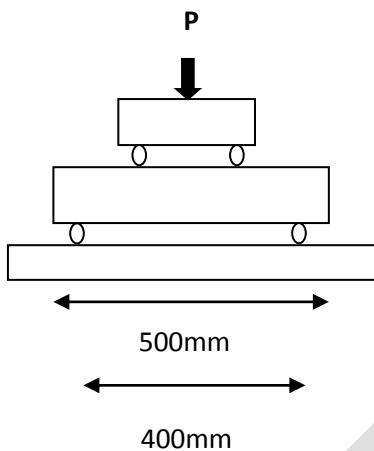
Fig. 2 Schematic Setup for Testing

Fig. 3 Placing of mesh during casting

RESULTS

The failure modes of control beams and beams with PET are shown in fig 4 and fig 5 respectively. Control beams showed the pure brittleness of concrete by giving sudden collapse.

Fig. 4 Failure of control beam

Fig. 5 Failure of Beam with PET mesh

The beams with PET mesh showed flexural failure without any collapse. Beams with PET mesh showed much higher load carrying capacity when compared with control beams. Crack propagation rate was very less when PET mesh was introduced to tension zone of beams.

DISCUSSION

The ultimate loading carrying capacity of control beam was obtained as 8.5 kN and the ultimate load carrying capacity of beams with PET mesh was obtained as 13 kN. Flexural strength for control beams and beams with PET was found to be 4.25 N/mm^2 and 6.5 N/mm^2 respectively.
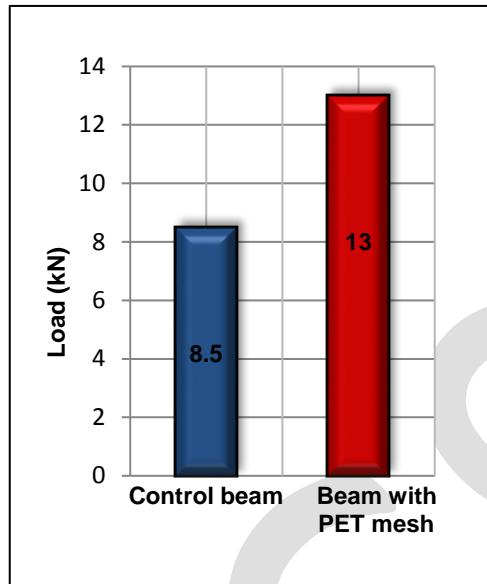
Fig. 6 Ultimate Load Carrying Capacity

CONCLUSIONS

The research work included the testing of concrete beams, each having a span of 500 mm and incorporated PET mesh in tension zone to increase the flexural strength of beams. Flexural strength comparison between control beam and other types of beams casted for the present investigation is illustrated as follows:

a) The flexural strength of concert beam with PET mesh is far greater than that of control beams and also the crack propagation rate of the concrete beam with PET mesh is greatly decreased due to the tensile property of PET fiber whereas the control beam exhibited brittle failure.
b) The post cracking behaviour of the beam with PET mesh shows the nature of PET fibers with hardened concrete offering little more resistance even after the failure.
c) The ultimate load carrying capacity of beam with PET mesh is around 50% more than the conventional RC beams.
d) A high adherence between PET fibers and concrete matrix was achieved.
e) Waste PET bottle fibers could be considered for the reinforcement of concrete; further studies could elucidate if these fibers may be used as structural material like reinforced beams, slabs, etc, and for other construction works.

Furthermore, the fact of using waste PET bottles as reinforcing material contributes to generate a benefit to the environmental preservation.

REFERENCES:

[1] Azad A. M "Flexural behaviour and analysis of reinforced concrete beams made of recycled PET waste concrete" Construction and Building Materials 155 (2017)593–604 Elsevier
[2] Dora Foti "Use of recycled waste pet bottles fibers for the reinforcement of concrete" Composite Structures 96 (2013) 396–404
[3] Dora Foti "Preliminary analysis of concrete reinforced with waste bottles PET fibers" Construction and Building Materials 25 (2011) 1906–1915
[4] E. Rahmani , M. Dehestani , et al "On the mechanical properties of concrete containing waste PET particles" Construction and Building Materials 47 (2013) 1302–1308 Elsevier
[5] H. Ataei, M; K. Kalbasi Anaraki, and Rui Ma "Mechanical Properties of Polyethylene Terephthalate Particle-Based Concrete: A Review" Airfield and Highway Pavements 2017

[6] J. Baldenebro, J.H. Castorena, C.D. Gómez,et.al "Influence of continuous plastic fibers reinforcement arrangement in concrete strengthened" IOSR Journal of Engineering (IOSRJEN) Vol. 04, Issue 04 (April. 2014), ||V1|| PP 15-23

[7] M.A. Al-Kubaisy, Mohd Zamin Jumaat "Flexural behaviour of reinforced concrete slabs with ferrocement tension zone cover" Construction and Building Materials 14 (2000) 245-252

[8] Karim S. R, J Member, S P. Serhal, and David W.F "Structural behaviour of polymer concrete beams using recycled plastic" Journal of Materials in Civil Engineering, Vol. 6, No.1 1994. 9 ISSN 0899-1561/94/0001-015 Paper No. 4733

[9] R J Rinu Isah, M.V.Shruthi "Utilization of waste pet bottle fibres in reinforced concrete" International Journal of Pure and Applied Mathematics volume 116 No. 13 2017, 579-584

[10] Santosh D. Nagare, Prof. S.A.Karale "The Flexural Strength of Plastic Concrete and PET Reinforced Concrete" International Journal of Innovations in Engineering Sciences and Technology: Civil, volume. 2, issue. 2

[11] Sampada Chavan, Pooja Rao "Utilization of Waste PET Bottle Fibers in Concrete as an Innovation in Building Materials" International Journal of Engineering Research ISSN: 2319 Volume No.5, Issue Special 1 pp: 304-307

[12] S.Soji, P. Anima, (2016) "Experimental and Analytical investigation on partial replacement of concrete below neutral axis in beams", IJERGS, Vol4 (4), pp 23-32.

[13] S. Gowri, N. Rajkumar, (2011) "Behaviour of Plastic Mixed Reinforced Concrete Columns Under Axial Compression", NBMCW

[14] Siddique, J Khatib , I Kaur "Use of recycled plastic in concrete: A review" Waste Management 28 (2008) 1835–1852 Elsevier

Experimental Study on Pineapple Leaf Fiber Reinforced RCC Beams

Riya Johnson [1], Amritha E. k [2]

[1] PG Scholar, Dept of Civil Engineering, Universal Engineering College, Vallivattom, Thrissur, Kerala, India.

[2] Assistant professor, Dept of Civil Engineering, Universal Engineering College, Vallivattom, Thrissur, Kerala, India.

Abstract - Concrete made with Portland cement is comparatively strong in compression but weak in tension and tends to be brittle. The weakness in tension can be overcome by the use of conventional rod reinforcement and to some extent by including sufficient volume of certain fibers. There has been a growing interest in utilizing natural fibers for making low cost construction materials in recent years. For environmental protection purposes, the use of natural fibers rather than synthetic fibers is highly recommended. Pineapple leaf fiber (PALF) is more compatible natural fiber resource and constitutes a good chemical composition and has highest tensile strength when compared to other natural fibers.

However, the main disadvantages of natural fibers in composites are the poor compatibility between fiber and matrix and the relative high moisture sorption. The chemical treatment of fiber improves the adhesion between the fiber surface and the matrix may not only modify the fiber surface but also increase fiber strength.

In this study combined dilute alkali and polymer treated pineapple leaf fiber are provided as secondary reinforcement in concrete beams. The concrete members were experimentally studied. The ultimate Load carrying capacity of beams were obtained and compared with the ordinary RCC beams.

Keywords – Natural fiber**,** Pineapple leaf fiber, Secondary reinforcement, Ultimate Load, Combined dilute alkali and polymer treatment , Tensile strength, RCC beam.

INTRODUCTION

Concrete made with Portland cement is comparatively strong in compression but weak in tension and tends to be brittle. The weakness in tension can be overcome by the use of conventional rod reinforcement and to some extent by including sufficient volume of certain fibers. There has been a growing interest in utilizing natural fibers for making low cost construction materials in recent years. [12], [17]

Fibers are thread like materials which can be used for different purposes. Fibers produced by plants (vegetable, leaves and wood), animals and geological processes are known as natural fibers. Researchers have used plant fibers as an alternative source of steel and/or artificial fibers to be used in composites (such as cement paste, mortar and/or concrete) for increasing its strength and ductility. Natural fibers have the advantages of low density, low cost, and biodegradability. When concrete cracks, the randomly oriented fibers start functioning, arrest crack formation and propagation, and thus improve strength and ductility [2], [5]

Pineapple leaf fiber is more compatible natural fiber resource and constitutes a good chemical composition. Pineapple leaf fiber (PALF) is vital natural fiber, which have high specific strength, rigidity, flexural and torsional rigidity than other fibers. Pineapple-Leaf Fiber-Reinforced concrete beam is a structural model designed to address three major problems: waste management, pollution control and climate change. [1]

However, the main disadvantages of natural fibers in composites are the poor compatibility between fiber and matrix and the relative high moisture sorption. Therefore, chemical treatments are considered in modifying the fiber surface properties. The chemical treatment of fiber aimed at improving the adhesion between the fiber surface and the matrix may not only modify the fiber surface but also increase fiber strength. Water absorption of composites is reduced and their mechanical properties are improved. For homogeneous distribution of natural fiber into the cement matrix both the chemical composition as well as surface properties of natural fiber have to be modified by a combined dilute alkali and polymer emulsion treatment [14]

EXPERIMENTAL WORK

A. General

The experimental work includes the casting of conventional RCC beams and the same set of specimens added with combined dilute alkali and polymer treated pineapple leaf fibers. The beams are casted in the size 150 mm x 200 mm x 1250 mm.

B. Mix Proportions and Materials Used

The characteristic compressive strength of the concrete after 28 days of curing is assumed to be 25 i.e. the fck value is 25. The cement used is ordinary Portland cement with 53 as grade. The coarse aggregate is 20 mm in size and the fine aggregate is well sieved. The mix proportion is designed as per the IS code for the M25 grade of cement.

TABLE 1

MIX PROPORTION

Material	Cement	Fine Aggregate	Coarse Aggregate	Water
Weight (kg/m^3)	437.77	636.396	1174.931	197
Ratio	1	1.45	2.68	0.45

The fiber that is used is pineapple leaf fiber and the mechanical properties of fiber are listed below in the form of a table

TABLE 2

MECHANICAL PROPERTIES OF PALF

Type	Tensile Strength (Mpa)	Youngs Modulus (Gpa)	Density (g/cm^3)	Length (cm)
Natural	387-1486	29.8-81	1.3	12.5

C. Experimental process

RC beams of size 150mm width, 200mm depth and 1250mm length were casted using M25 conventional mix and fiber added mix. Combined dilute alkali and polymer treated PALF fiber are added in the mix. Combined polymer alkali treatment was done by

soaking the required amount of PALF in 0.5% alkali solution following which the spent alkali solution was decanted out after 24 h of soaking. Next the respective amounts of Sika latex containing solid (carboxylated styrene butadiene (SBR) was diluted with 1000 ml of water and added to the alkali soaked wet PALF. The fiber that is added along with the mix is in the percentage of 0.75 (by weight).The beams were designed for flexural failure with 2#12mm bars as the bottom longitudinal reinforcement and 2#8mm bars as the top longitudinal reinforcement. Two legged 8mm stirrups were provided as shear reinforcement at spacing of 130 mm from the supports. The beams were tested under two point loading test after 28 days water curing.
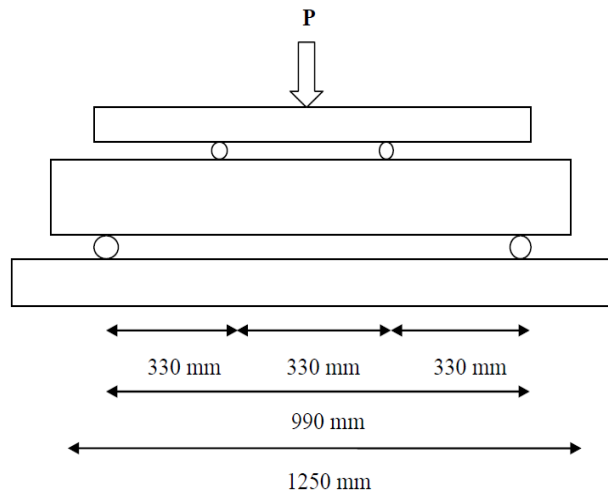

Fig. 1 Schematic Setup for Testing

RESULTS

The mode of failure of control beam and beam reinforced with treated PALF are shown in Fig. 2 and Fig. 3 respectively.

Fig. 2 Failure of control beam

The mode of failure was found to be flexural in both control beam and fiber added beam. It was also observed that the crack width increased with the increase of load.

Fig. 3 Failure of beam with treated PALF

DISCUSSION

The ultimate loading carrying capacity of control specimen was obtained as 147.15 kN. The ultimate load carrying capacity of beams reinforced with treated PALF was obtained as 191.29 kN which is greater than that of the control beam.
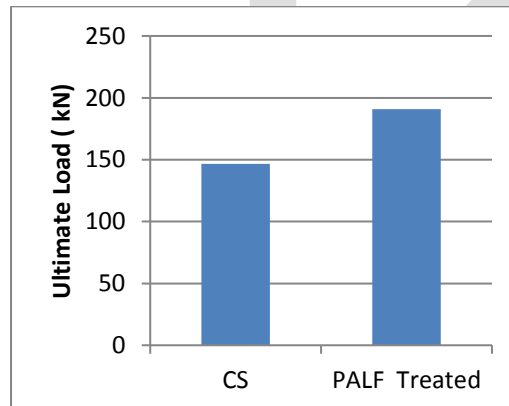
Fig. 4 Ultimate Load Carrying Capacity

CONCLUSION

The flexural behavior of concrete beams with PALF as secondary reinforcement has been presented in this study. Based on the findings from the beam flexure tests performed, the following conclusions can be drawn,

1. The ultimate load bearing capacity of the PALF reinforced beam was very much higher than the conventional type specimens in the flexural test that was carried out. In combined dilute alkali polymer treated beams the load carrying capacity is increased by 24%.
2. Both control beam and treated PALF added beams failed in flexure.
3. Beam without fiber or normal concrete start cracking at lower loads, and the cracks continue towards compression region. However, beam with fiber start cracking in higher loads because of higher tensile strength due to fiber addition.

REFERENCES:

[1] A.Khalina et.al, A Review on Pineapple Leaves Fibre and Its Composites, International Journal of Polymer Science,2016

[2] A.Majid, Natural fibres as construction materials, Journal of Civil Engineering and Construction Technology, Vol. 3(3), pp. 80-89,2012

[3] C.Andressa et.al, Mechanical behavior of natural fiber composites, Sciencedirect, journal of cement & concrete composite,Vol. 10, pp. 2022-2027,2011

[4] E.Mello et.al, Improving Concrete Properties with Fibers Addition, International Journal of Civil and Environmental Engineering, Vol. 8, pp. 249-254,2014

[5] E.Sinha et.al, Influence of fibre-surface treatment on structural, thermal and mechanical properties of jute, Springer, Journal of Material Science , Vol.43, pp.2590–2601,2008

[6] F.Faizal, Properties and Applications of Fiber Reinforced Concrete, *JKAU: Eng. Sci.,* Vol. 2, pp. 49-63,2005

[7] G. Ramakrishna et.al , Studies on the durability of natural fibers and the effect of corroded fibers on the strength of mortar, Science Direct, journal of cement & concrete composite,Vol. 27, pp. 575-582,2005

[8] H. Ujwala et.al, Effect of Maleic Anhydride Grafted Polypropylene on the Mechanical and Morphological Properties of Chemically Modified Short-Pineapple-Leaf-Fiber-Reinforced Polypropylene Composites, Journal of Applied Polymer Science, Vol. 107, pp. 1507–1516,2007

[9] L.Natinee et.al, Performance of Pineapple Leaf Fiber–Natural Rubber Composites: The Effect of Fiber Surface Treatments**,** Journal of Applied Polymer Science, Vol. 102, pp.1974–1984,2005

[10] M.G. Aruan Efendy et.al, A review of recent developments in natural fibre composites and their mechanical performance, Elsevier, journal of cement & concrete composite,Vol. 83, pp. 98-112,2016

[11] M.Linto et.al, Mechanical Properties of Pineapple Fibre Reinforced Concrete Subjected to High Temperature, Global Research and Development Journal for Engineering,Vol. 2,pp. 200-205,2017

[12] M.R. Sanjay et.al, Study on properties of Natural-Glass fibre reinforced Polymer Hybrid Composites, Science Direct, journal of cement & concrete composite,Vol.2, pp. 2959-2967,2015

[13] P.Satyanarayan et.al, Chemical Treatments of Natural Fiber for Use in Natural Fiber-Reinforced Composites: A Review, J Polym Environ Vol.15, pp. 25–33,2007

[14] R.M. Vignesh et.al, Experimental study on natural fibers in RCC beams, International Journal of Civil Engineering and Technology, Vol.8, pp.179-184,2017

[15] S.Aiswarya et.al, fiber addition and its effect on concrete strength, International Journal of Innovative Research in Advanced Engineering, Vol. 1, pp.144-149,2014

[16] S.Chattopadhyay et.al, Influence of Varying Fiber Lengths on Mechanical, Thermal, and Morphological Properties of MA‐g‐PP Compatibilized and Chemically Modified Short Pineapple Leaf Fiber Reinforced Polypropylene Composites, Journal of Applied Polymer Science, Vol. 113, pp.3750–3756,2009

[17] V.Sandeepani et.al, Study On Addition Of The Natural Fibers Into Concrete, International journal of scientific & technology research ,Vol. 2, pp. 213-218,2013

[18] W.O. Soboyejo et.al , Fracture and fatigue of natural fiber-reinforced cementitious composites, Science Direct, journal of cement & concrete composite,Vol. 31, pp. 232-243,2009

Mechanical characteristics of Hardened concrete with mineral admixtures Silica fume and fly ash

D.SYAMALA (M.Tech scholar), P.SILUS(Associate professor)

A.CHANDANA JYOTHI(Assistant professor) ,

Chebrolu engineering college, chebrolu, Guntur

Abstract - In the present day construction practice where large quantities of concrete are being poured daily, accelerated curing techniques are quite popular to predicting the 28 days strength within a short time. The accelerated strength procedure given by the IS Code are being adopted in the case of normal concrete without admixtures. In the present experimental investigation silica fume admixture& fly ash has been employed as a replacement at various percentages, Like 0, 14,28,42,56 for M20 are considered and the 7,28 day strengths are predicted using the codal procedure and the co-relation formula. The co-efficient of variation is useful in the strength prediction of silica fume concrete mixes are considered. The investigation has high practical importance and use.

Literature Review

Balendran, et al(2001) demonstrated the effect of quick and slow cooling on residual compressive strengthsof various high strength concrete grades (60, 90, 110, 130 MPa) cured for 28 days with an optimum dosage ofmicro silica as 10% of cementations material, 10 mm maximum size of coarse aggregate and water binder ratio ranging from 0.5 to 0.24.

Belaoura Mebarek, et al (2013) explained the use of super plasticizers, and ultrafine particles such as silicafume, has significantly minimized the amount of mixing water in concrete while improving workability.Owning to this water reduction (and thus the w/c ratio), the mechanical strength of such concretes hasconsiderably increased. The compressive strength may exceed 80 MPa. Therefore, their use is very promisingfrom an economic point of view and quality of civil engineering an hydraulics works.

Borys and Patrick (2004) completed a study on several ultra-fines used to produce very high performance concrete and ultra-high performance concrete. The ultrafine powders used were met kaolin (MK), pulverized fly ash (PFA), limestone micro filler (LM), siliceous micro filer (SM) and micronized phonolith (PF). Despite

a significant higher dosage of super plasticizer in comparison of those with silica fume, the UHPC with metkaolin shows poor workability with a slump of 17 cm. the fluidity of met kaolin blended cement become poorer than that of Portland cement at the same dosage of super plasticizer and the same w/c ratio. The UHPCwith pulverized fly ash required significant higher water content. All the compressive strength of UHPC was above 150 MPa at the age of 28 days except for those with pulverized fly ash.

Dilip Kumar Singha Roy (2012) has investigated on the strength parameters of concrete made with partial replacement of cement by SF.

Duval and Kadri (2000) results show that partial cement replacement up to 10% silica fume does not reduce the concrete workability. Moreover, the super plasticizer dosage depends on the cement characteristics. Atlow water-cementitious materials ratios, slump loss with time is observed and increased with highreplacement levels. Silica fume at replacement contents up to 20% produce higher compressive strength thancontrol concretes; nevertheless, the strength gain is less than 15%. Models to evaluate the compressive strength.

OBJECTIVE OF THE STUDY: Objectives of the study. The main objective of this study is to determine the suitable percentage of fly ash, and silica fume in CC that gives the highest value of concrete compressive strength. As well as studying the influence of different curing conditions

Fly ash is one of the residues generated in the combustion of coal. Fly ash is generally captured from the chimneys of coal-fired power plants, and is one of two types of ash that jointly are known as coal ash; the other, bottom ash, is removed from the bottom of coal furnaces. Depending upon the source and makeup of the coal being burned, the components of fly ash vary considerably, but all fly ash includes substantial amounts of silicon dioxide (SiO_2) (both amorphous and crystalline) and calcium oxide (CaO). Fly ash is classified as Class F and Class C types. The replacement of Portland cement with fly ash is considered to reduce the greenhouse gas "footprint" of concrete, as the production of one ton of Portland cement produces approximately one ton of CO_2 as compared to zero CO_2 being produced using existing fly ash. New fly ash production, i.e., the burning of coal, produces approximately twenty to thirty tons of CO_2 per ton of fly ash. Since the worldwide production of Portland cement is expected to reach nearly 2 billion tons by 2010, replacement of any large portion of this cement by fly ash could significantly reduce carbon emissions associated with construction

Silica fume is a byproduct in the reduction of high-purity quartz with coke in electric arc furnaces in the production of silicon and ferrosilicon alloys. Silica fume consists of fine particles with a surface area on the order of 215,280 ft²/lb (20,000 m²/kg) when measured by nitrogen adsorption techniques, with particles approximately one hundredth the size of the average cement Because of its extreme fineness and high silica content, silica fume is a very effective pozzolanic material particle

Silica fume is added to Portland cement concrete to improve its properties, in particular its compressive strength, bond strength, and abrasion resistance. These improvements stems from both the mechanical improvements resulting from addition of a very fine powder to the cement paste mix as well as from the pozzolanic reactions between the silica fume and free calcium hydroxide in the paste

Silica fume	ASTM-C-1240	Actual Analysis
SiO2	85% min	84.7%
LOI	6% max	2.2%
Moisture	3%	0.8%
Pozz Activity Index	105% min	134%
Sp Surface Area	>15 m2/gm	22 m2/gm
Bulk Density	550 to 700	556

TEST RESULTS:

COMPRESSIVE STRENGTH RESULTS

CSA REPLACMENT (0 TO 56 %)

Mix type	Trail	Peak Load (kN)		Compressive Strength (Mpa)		Avg Compressive Strength (Mpa)	
		7 days	28 days	7 days	28 days	7days	28 days
M (0%)	1	773.2	821	14.31	26.8	14.3	26.4
	2	697.2	880.2	14.23	26.3		
	3	738.6	613.9	14.56	26.2		
M-1(14)	1	778.4	826.3	15.26	21.40	15.23	21.48
	2	773	842.1	15.20	21.52		
	3	768	808	15.23	21.53		
M-2 (28)	1	830.2	647.7	16.12	21.75	16.08	21.77
	2	788.9	714.9	16.00	21.73		
	3	433.7	862.9	16.12	21.83		
M-3(42)	1	620.1	601	16.56	21.92	16.7	22.00
	2	447.4	792	16.73	22.00		
	3	753.2	922	16.83	22.31		
M-4(56)	1	578	863.5	16.92	22.36	16.96	22.43
	2	597.1	902.2	16.98	22.45		
	3	721.3	913.2	16.98	22.48		

SILICA FUME COMPRESSIVE STRENGTH
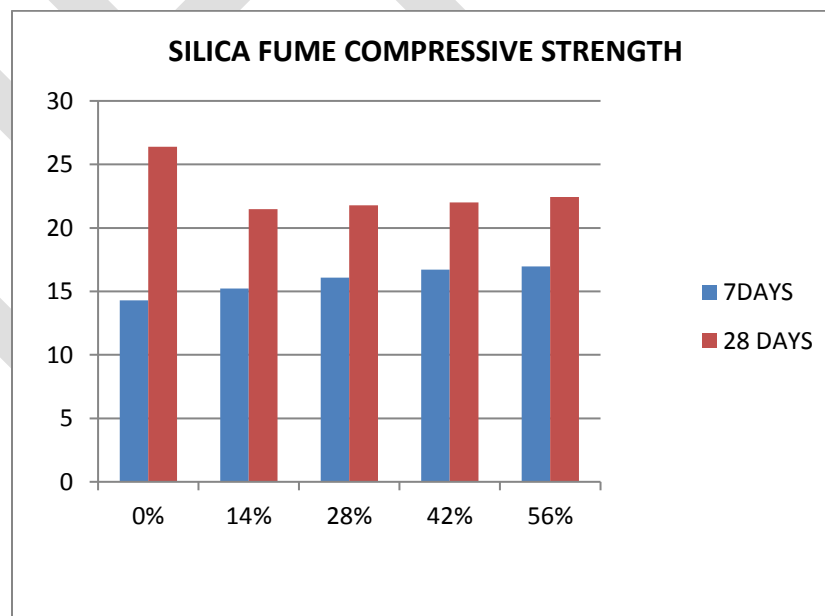
FLY ASH REPLACEMENT (0 TO 56%)

CUBE ID	TRAIL	PEAK LOAD(7 DAYS)	PEAK LOAD (28 DAYS)	COMPRSSIVE STRENGTH(7 DAYS & 28 DAYS)		AVERAGE COMPRESSIVE STRENGTH	
M-5 (14%)	1	613.3	921	12.23	18.48	12.34	18.44
	2	476.5	922	12.48	18.42		
	3	713.6	770.9	12.32	18.43		
M-6 (28%)	1	764.8	768.4	13.12	18.96	13.17	18.92
	2	539.8	713.7	13.25	18.91		
	3	455	918.2	13.15	18.90		
M-7 (42%)	1	918.1	808.4	13.45	19.56	13.44	19.4
	2	715.6	917.3	13.48	19.56		
	3	741.6	917.9	13.39	19.28		
M-8 (56%)	1	646.4	917.6	13.83	19.83	13.86	19.83
	2	718.2	757.8	13.89	19.82		
	3	743.6	718.1	13.86	19.84		

FLY ASH COMPRESSIVE STRENGTH
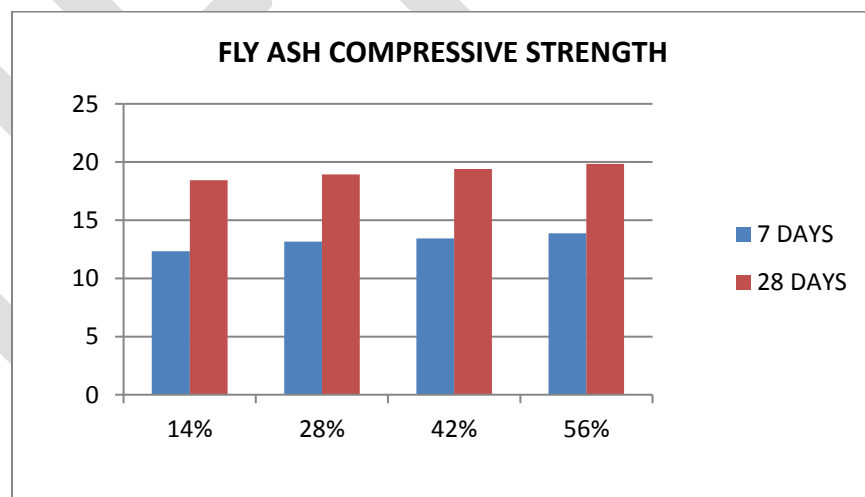
CSA & FLY ASH REPLACEMENTS RESULTS

CUBE-ID	TRAIL	PEAK LOAD(7 DAY)	PEAK LOAD(28 DAY)	CS. (7 DAY)	CS .28 DAY)	AVG.CS(7 DAY)	AVG .CS(28 DAY)
M-9 (14%)	1	710.2	720.3	16.79	27.38	16.82	27.13
	2	711.2	728.9	16.83	27.01		
	3	712.8	728.6	16.84	27.00		
M-10 (28%)	1	694.06	740.8	17.86	27.86	18.08	27.86
	2	698.8	740.3	17.89	27.83		
	3	712.6	752.4	17.89	27.89		
M-11 (42%)	1	750.3	780.36	18.46	28.83	18.45	28.82
	2	754.2	790.62	18.42	28.82		
	3	758.3	788.36	18.49	28.83		
M-12 (56%)	1	798	800.1	19.47	28.91	19.45	28.91
	2	792.3	810.23	19.42	28.91		
	3	798.12	810.58	19.48	28.91		
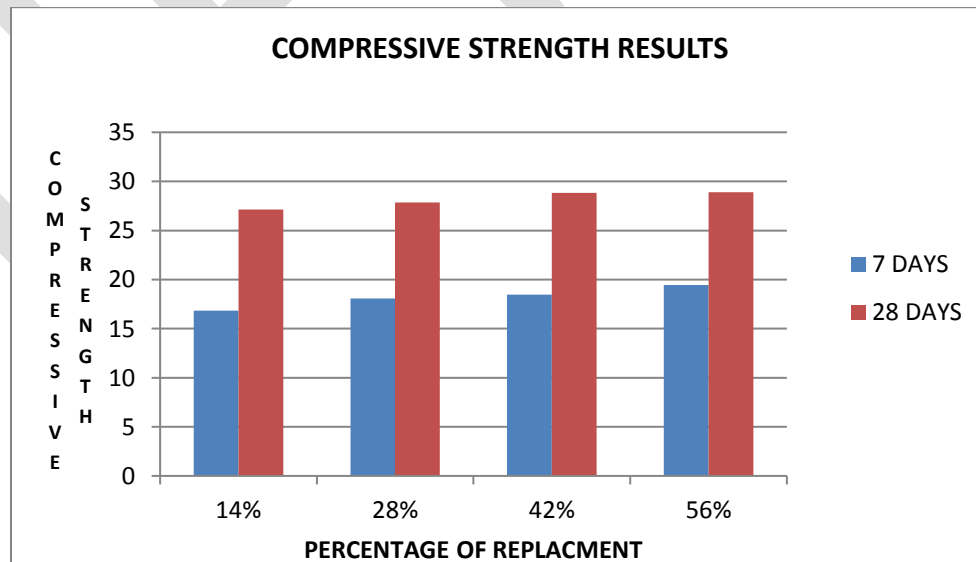
SPLIT TESNILE STRENGTH: CONDENSED SILICA FUME

MIX TYPE	% Of CONDENSED SF	7 DAYS	28 DAYS
M-0	0	1.8	2.56
M-1	14	1.893	3.145
M-2	28	1.274	3.185
M-3	42	1.843	3.896
M-4	56	1.179	3.893
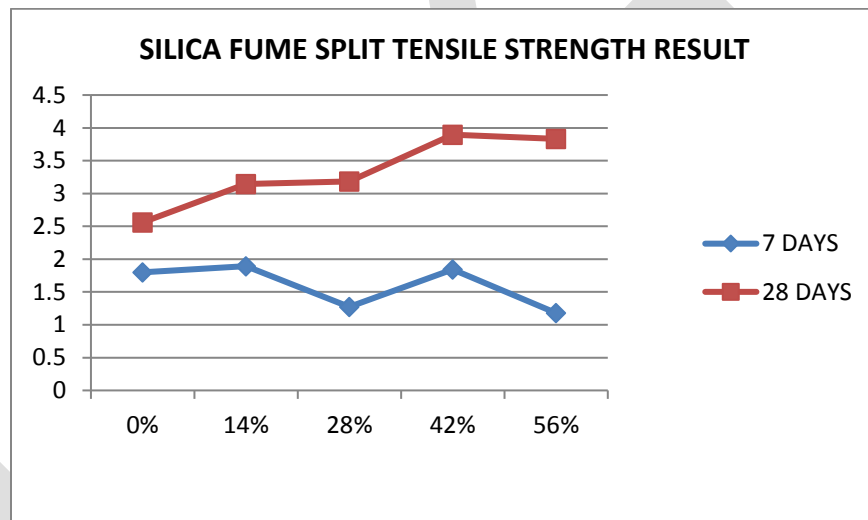
MIX TYPE	% Of FLY ASH	7 DAYS	28 DAYS
M-5	14	0.98	2.346
M-6	28	1.26	2.389
M-7	42	1.28	2.41
M-8	56	1.268	2.458

SPLIT TESNILE STRENGTH FLY ASH

FLY ASH SPLIT TENSILE STRENGTH RESULT
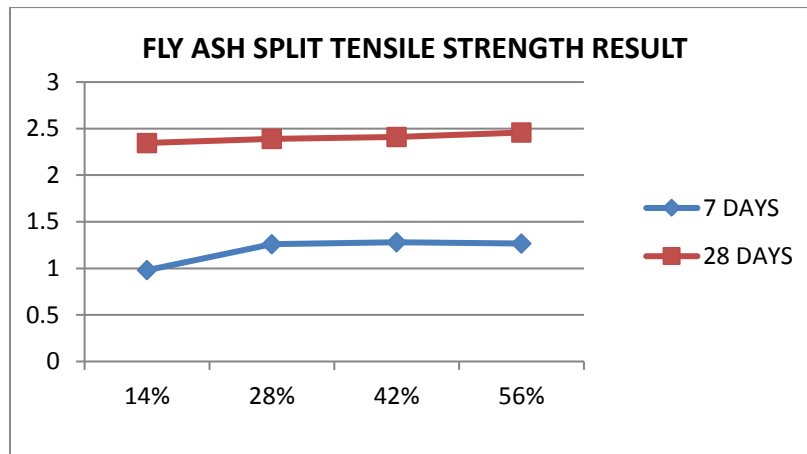
MIX TYPE	% Of CSA & FLY ASH	7 DAYS	28 DAYS
M-9	14	3.12	3.92
M-10	28	3.189	4.12
M-11	42	3.46	4.35
M-12	56	3.28	4.32

SILICA & FLY ASH SPLIT TENSILE STRENGTH RESULT
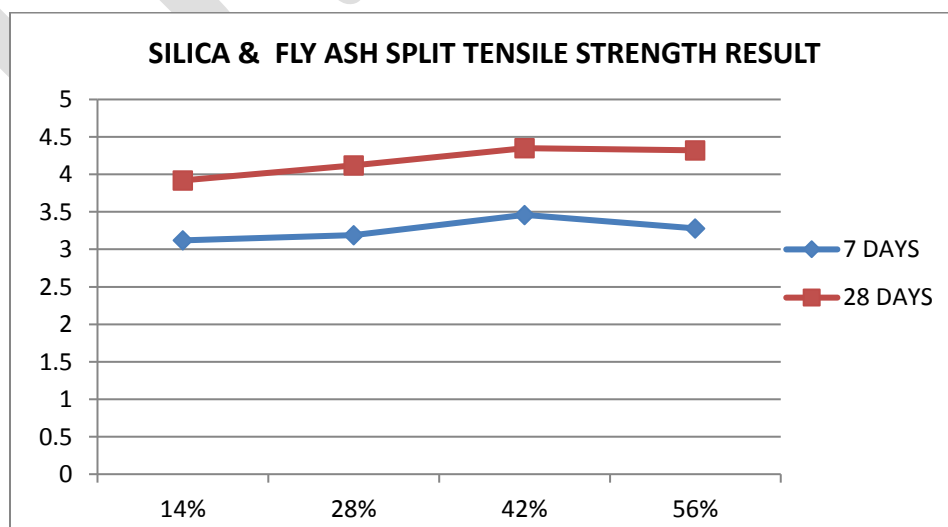
ULTRA SONIC PULSE VELOCITY TEST

S NO	% of CSA & FLY ASH	Obtained average velocity(m/s)	Quality of Concrete
M-0	0	3500	GOOD
M-9	14	3512	GOOD
M-10	28	3670	GOOD
M-11	42	3689	GOOD
M-12	56	3900	GOOD

FLEXTURAL STRENGTH OF CONCRETE

S.NO	CSA & FLY ASH	7 DAYS	28DAYS
M-0	0	4.83	5.37
M-9	14	4.87	5.39
M-10	28	4.93	5.34
M-11	42	4.98	5.89
M-12	56	4.96	5.87

SILICA FUME & FLY ASH FLEXURE RESULT
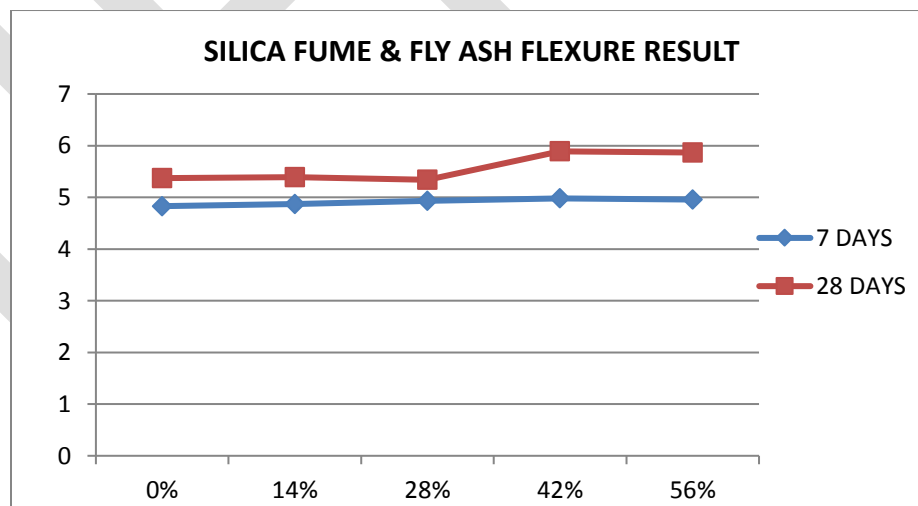
<u>CONCULSIONS</u>

.

- ❖ The optimum percentage of cement replacement by fly ash & CSA for achieving maximum cube compressive strength, cylinder compressive strength, split tensile and beam flexural strengths

- ❖ With the above replacement, concrete with a strength of **30Mpa** canbe produced with water to cementitious materials ratio of 0.3 withAppropriate dosages of compatible superplasticisers.

- ❖ Substantial savings can be achieved through total replacement levelsof 50-55% of cement with locally available fly ash and silica fume.

- ❖ The maximum 28 days split tensile strength was obtained with 28%fly ash 14% silica fume mix, the strength is about 31% more at 28Days of curing compared.

- ❖ The maximum 28 days flexural strength was obtained again with28% fly ash and 14% silica fume mix, a strength gain about 34%More than that of reference.

- ❖ The transition zone gets improved and densified with the use of Ternary mix concretes containing micro silica and fly ash.

REFRENCES:

- ❖ GopalaKrishnan. S., "Use of Supplementary Cementitious Materialsin Concrete Mixtures towards Sustainable Development in ConcreteConstruction", ICFRC National seminar on HPCC, 28-29December2000, Chennai, India; pp.KNP 423.

- ❖ Reported by ACI committee 226, "Silica Fume In Concrete", ACIMaterial Journal, April 1987; pp.217-223.

- ❖ Ziad Bayasi and Jing Zhou, "Properties Of Silica Fume Concrete andMortar" ACI Material Journal, JULY – AUGUST 1993; PP349-356.

- ❖ Ravindra. S.R., and DR. Mattur C. Narasimhan, "Experimentalstudies on High Strength Micro Silica Concrete", ICI Journal, JULYAUGUST2003; PP.19-22.

- ❖ V.Yogendra, B.W.langan, M.N. Haque and M.A. ward, "Silica FumeIn High Strength Concrete", ACI Material MARCH-APRIL1987;PP. 124-129

Effect of Acid Attack on Rice Husk Ash-Filtered Sand Self-Compacting Concrete

Manjunath N K[1], Dr. Annapurna B P[2], Dr. K Naresh[3], Shashi Shekhar Singh[4]

Assistant Professor, Professor, Sri Krishna Institute of Technology, Department Of Civil Engineering, Bangalore [1] [3]

Associate Professor, University Visvesvaraya College of engineering, Faculty of Engineering - Civil, Bangalore [2]

Associate Professor, Madda Walabu University, Department of Civil Engineering, Bale Robe, Ethiopia [4]

ABSTRACT-This paper deals with the effect of rice husk ash and filtered sand on the durability property acid attack. In this study M_{70} grade concrete with rice husk ash, filtered sand and superplasticizer were used. Cement and sand was replaced at the levels of 5%, 10%, 15%, 20% and 25%, 50%, 75%, 100% respectively. From the test results, it was observed that rice husk ash SCC and rice husk ash filtered sand SCC has shown better performance than conventional concrete.

KEYWORDS

Fresh Properties, Durability properties, Self-Compacting Concrete (SCC), Rice Husk Ash (RHA), Filtered Sand (FS), Acid Resistance, Hydrochloric Acid (Hcl).

INTRODUCTION

Concrete is a widely used construction material for various types of structures due to structural stability and strength. All the materials required producing such huge quantities of concrete come from the earth's crust. Thus, it deflects its resources every year creating ecological strains. On the other hand, human activities on earth produce solid wastes in considerable quantities of over 2500/MT per year, including industrial wastes, agricultural wastes and wastes from rural and urban societies. Recent technological development has shown that these materials are valuable as inorganic and organic resources and can produce various useful products. Amongst the solid wastes, the most prominent ones are fly ash, blast furnace slag, rice husk ash, silica fume and demolished construction materials.

From the middle of 20th century, there had been an increase in the consumption of mineral admixtures by the cement and concrete industries. This increasing demand for cement and concrete is met by partial cement replacement. Substantial energy and cost savings can result when industrial by-products are used as a partial replacement for the energy intense Portland cement. The use of by-products is an environmental–friendly method of disposal of large quantities of materials that would otherwise pollute land, water and air. The current cement production rate of the world, which is approximately 1.2 billion tones/year, is expected to grow exponentially to about 2 billion tones/year by 2015. Most of the increase in demand will be met by the use of supplementary cementing materials.

Prior to 1970, RHA was usually produced by uncontrolled combustion and the ash so produced was crystalline and possessed poor pozzolanic properties. In 1973, Mehta published the first of several papers describing the effect of pyro processing parameters on the pozzolanic reactivity of RHA. Based on his research, Pitt designed a fluidized bed furnace for controlled burning of rice husks. By burning the rice husks under a controlled temperature and atmosphere, a highly reactive RHA was obtained. The utilization of RHA as a pozzolanic material in cement and concrete provides several advantages, such as improved strength and durability properties, reduced materials cost due to cement savings and environmental benefits related to the disposal of waste materials.

The main components of concrete are cement, sand & coarse aggregate. The production of cement adds pollution to the environment is a well-known fact to civil engineers. River sand which is used as fine aggregate is becoming very scarce, sand mining is discouraged to save the rivers of our country. Because of these environmental and economic reasons it requires thinking about the use of industrial wastes as alternative materials in concrete production, which not only reduce the cost of production of concrete but also controls the pollution relatively.

Rice plant is one of the plants that absorbs silica from the soil and assimilates it into its structure during the growth (Smith et al., 1986). Rice husk is the outer covering of the grain of rice plant with a high concentration of silica, generally more than 80-85%.

Surface soils from tank beds, agricultural fields and village common lands have been excavated and washed to produce a kind of artificial sand in order to meet the enormous demand known as filtered sand. Only source materials with suitable strength, durability and shape characteristics should be considered. Production generally involves screening and possible washing. Separating into discrete fractions, recombining and blending may be necessary.

Therefore the utilization of Rice Husk Ash (RHA) & Filtered Sand (FS) in concrete for the replacement of cement & sand, environmentally and economically advantageous. In the present study Portland cement and sand was replaced by RHA and FS at various percentages to study strength and durability property acid attack.

EXPERIMENTAL PROGRAMME

MATERIALS USED

Cement: ordinary Portland cement of 53 grade confirming to IS: 12269-1987 was used for the present experimental investigation. The cement was tested as per the Indian standards IS: 4031-1988. The test results are given in Table 1.

Sl.No	PROPERTIES	Obtained Values	Requirement as per IS -12269
1	Fineness	2.59	Not more than 10%
2	Soundness	1.00 mm	Not more than 10 mm
3	1.Initial Setting Time	71.00 min	Not less than 30 min
	2. Final Setting Time	438.00 min	Not more than 600 min
4	Compressive strength	53.36 N/mm²	Not less than 53 N/mm²
5	Standard Consistency	31%	
6	Specific Gravity	3.12	

Table 1: Physical Properties of Cement

Fine Aggregates: Natural river sand as per IS: 383-1987 was used. The physical properties and sieve analysis of fine aggregate are presented in Table 2.

Sl.No	Properties	Results
1	Fineness Modulus	2.855
2	Specific Gravity	2.62
3	Water Absorption	1.0%
4	Zone	II

Table 2: Physical Properties of Fine Aggregates (Natural Sand)

Filtered Sand IS: 383-1987 was used. The physical properties obtained on conducting sieve analysis and specific gravity tests for Filter Sand and for different replacement levels of sand by Filter Sand is presented in Table 3. The amount of silt content in sand to be used in concrete should be less than 5% according to codal provisions (IS 383). If the amount of silt content is higher than 5% affects the strength of concrete. Hence the amount of silt content in the present filtered sand is investigated by using Hydrometer test (Table 4).

Sl. No	Fine Aggregate	Specific Gravity	Fineness Modulus	Zone
	Fine Aggregate (NS+FS)			
1	100% sand+0%FS	2.62	2.855	Zone II
2	75% sand+25% FS	2.61	3.76	Zone II
3	50% sand+50% FS	2.19	3.51	Zone II
4	25% sand+75% FS	2.22	3.42	Zone II
5	0% sand+100% FS	2.46	3.40	Zone II

Table 3: Test Results of Fine Aggregates (Natural sand & Filtered sand)

% of Filter Sand	% of Silt	% of Clay	% of Finer Sand
25	14.3	39.19	46.51
50	28.8	38.29	32.91
75	42.5	32.10	25.40
100	49.87	24.87	25.26

Table 4: Hydrometer Test Results

Coarse Aggregates: Crushed Granite jelly of size 12.5mm down confirming to IS: 383-1987 was used (Table 5).

Sl. No	Particulars of the test	Results
1.	Fineness modulus	6.54
2.	Specific Gravity	2.65

Table 5: Physical characteristics of Coarse Aggregates (12.5 mm down size)

Rice Husk Ash: The rice husk ash obtained from Maddur (Mandya dist.).RHA used for investigation have tested in the Civil Aid and the chemical characteristics are given in Table 6.

Sl.No	Test Conducted	Results	Requirements as per IS:3812:2003	
			Siliceous Pulverized Fuel Ash	Calcareous Pulverized Fuel Ash
1	Silicon Dioxide(Si_o_2)+Aluminum oxide(Al_2O_3)+iron oxide Fe_2O_3),Percentage by mass(min)	98.92%	70%	50%
2	Silicon dioxide(Si_o_2),Percentage by mass(min)	94.08%	35%	25%
3	Magnesium oxide(Mgo),percent by mass,(max)	0.18%	5%	5%
4	Total Sulphur as sulphur trioxide(Si_o_3),Percentage by mass(max)	0.29%	3%	3%
5	Calcium oxide percentage by mass,(Cao)	0.28%	5%	5%

Table 6: Chemical characteristics of Rice Husk Ash

Superplasticizer: Polycarboxylic ether based super plasticizer Glenium 6100 has been used in present research work.

MIX PROPORTIONING

For the present investigation, High strength self-compacting concrete of grade $M_{70}$was aimed. To achieve this grade of concrete, OKAMURA (JAPANESE) METHOD of mix design was used.

Note: [C.SCC - Conventional Self Compacting Concrete with only Cement & Natural Sand without RHA & FS].
The mix proportions obtained for C.SCC of M_{70} grade is 1:1.12:1.17 is been replaced by RHA & FS in place of cement & natural sand by different percentages, which is tabulated in Table 7.

Note: C.SCC-Conventional Concrete (0%RHA, 0%FS);
A Series-5% RHA; B Series-10% RHA; C Series-15% RHA; D Series-20% RHA;
$A_o A_1 A_2 A_3 A_4$ − 5% RHA, (100%NS+0%FS, 75%NS+25%FS, 50%NS+50%FS, 25%NS+75%FS, 0%NS+100%FS);
$B_o B_1 B_2 B_3 B_4$ − 10% RHA, (100%NS+0%FS, 75%NS+25%FS, 50%NS+50%FS, 25%NS+75%FS, 0%NS+100%FS);
$C_o C_1 C_2 C_3 C_4$ − 15% RHA, (100%NS+0%FS, 75%NS+25%FS, 50%NS+50%FS, 25%NS+75%FS, 0%NS+100%FS);
$D_o D_1 D_2 D_3 D_4$ − 20% RHA, (100%NS+0%FS, 75%NS+25%FS, 50%NS+50%FS, 25%NS+75%FS, 0%NS+100%FS).

Mix	Cement		RHA		NS		FS		CA		Water	SP	
	% age	Wt in Kgs	% age	Wt in Kgs	% age	Wt in Kgs	% age	Wt in Kgs	% age	Wt in Kgs	Water in Ltrs	% age	SP in ml
CHCC	100	649.0	0	0	100	726.6	0	0	100	759.5	208.0	0.8	5192
A_0	95	616.5	5	32.4	100	726.6	0	0	100	759.5	208.0	0.8	5192
A_1	95	616.5	5	32.4	75	545.0	25	181.6	100	759.5	208.0	0.8	5192
A_2	95	616.5	5	32.4	50	363.3	50	363.3	100	759.5	208.0	0.8	5192
A_3	95	616.5	5	32.4	25	181.6	75	545.01	100	759.5	208.0	0.8	5192
A_4	95	616.5	5	32.4	0	0	100	726.6	100	759.5	208.0	0.8	5192
B_0	90	584.1	10	64.9	100	726.6	0	0	100	759.5	208.0	0.8	5192
B_1	90	584.1	10	64.9	75	545.0	25	181.6	100	759.5	208.0	0.8	5192
B_2	90	584.1	10	64.9	50	363.3	50	363.3	100	759.5	208.0	0.8	5192
B_3	90	584.1	10	64.9	25	181.6	75	545.0	100	759.5	208.0	0.8	5192
B_4	90	584.1	10	64.9	0	0	100	726.6	100	759.5	208.0	0.8	5192
C_0	85	551.6	15	97.3	100	726.6	0	0	100	759.5	208.0	0.8	5192
C_1	85	551.6	15	97.3	75	545.0	25	181.6	100	759.5	208.0	0.8	5192
C_2	85	551.6	15	97.3	50	363.3	50	363.3	100	759.5	208.0	0.8	5192
C_3	85	551.6	15	97.3	25	181.6	75	545.0	100	759.5	208.0	0.8	5192
C_4	85	551.6	15	97.3	0	0	100	726.6	100	759.5	208.0	0.8	5192
D_0	80	519.2	20	129.8	100	726.6	0	0	100	759.5	208.0	0.8	5192
D_1	80	519.2	20	129.8	75	545.0	25	181.6	100	759.5	208.0	0.8	5192
D_2	80	519.2	20	129.8	50	363.3	50	363.3	100	759.5	208.0	0.8	5192
D_3	80	519.2	20	129.8	25	181.6	75	545.0	100	759.5	208.0	0.8	5192
D_4	80	519.2	20	129.8	0	0	100	726.6	100	759.5	208.0	0.8	5192

Table 7: Mix proportions of RHA-FS SCC and Conventional SCC per m³ by weight

TESTING OF SCC

It is important to mention that none of the test methods for SCC have yet been standardized and included in Indian Standard Code for the present. The following are some of the features of SCC mentioned in Indian standard code IS: 456-2000.

1. Slump flow: Minimum 600mm.

2. Sufficient amount of fines (<12.5mm) preferably in the range of 400kg/m³ to 600kg/m³. This can be achieved by having sand content more than 38% and using mineral admixture to the order of 25% to 50% by mass of cementitious materials.

3. Use of high range water reducing (HRWR) admixture and viscosity modifying agent (VMA) in appropriate dosages are permitted. European guidelines for testing, covers number of parameters ranging from material selection, mixture design and testing methods like slump flow test, L-box test and V-funnel test as recommended by EFNARC for determining properties of SCC in fresh state. Most of Indian researchers are following these guidelines to determine the rheological properties of SCC mixes.

TESTING METHODS OF SCC

Different methods have been developed to characterize the rheological properties of SCC. No single method has been found until date, which characterizes all the relevant workability aspects. Each mix has been tested by more than one test method for the different workability parameters. Following are the tests recommended by European guidelines.

A. **Slump flow test**- The slump flow test is used to assess the horizontal flow of SCC in the absence of obstructions. The test also indicates resistance to segregation. On lifting the slump cone, filled with concrete the average diameter of spread of the concrete is measured. It indicates the filling ability of the concrete.

B.V-funnel test- The flowability test of the fresh concrete can be tested with the V-funnel test, where by the flow time is measured. The funnel is filled with about 22kgs of concrete and the time taken for it to flow through the apparatus is measured. Shorter flow time indicate greater flowability.

C. L-Box test- This is a widely used test, suitable for laboratory and site use. It accesses filling and passing ability of SCC and serious lack of suitability can be detected visually. The vertical section of the L-box is filled with concrete, and then the gate is lifted to let the

concrete flow into the horizontal section. Blocking ratio, it indicates passing ability of concrete or the dosage to which the passage of concrete through the bars is restricted.

TESTS CONDUCTED

Acid Attack Test:

A total number of 126 cubes of size of 100 mm were casted and stored in a place at a temperature of 27°C±2°C for 24 hours and then the demoulded specimens were water cured for 28 and 56 days. After curing, the specimens were taken out and allowed to dry for one day. Weights of the cubes were taken. For acid attack, 5% dilute hydrochloric acid (Hcl) with PH value of about 2 was used. After that, cubes were immersed in the above said acid water for a period of 28 days.

The concentration of the solution was maintained throughout this period. After 28 days, the specimens were taken from the acid water. The surfaces of the cubes were cleaned, weights of the specimens were registered and then they were tested in the compression testing machine of 2000kN capacity under a uniform rate of loading of 140 kg/cm^2/min. The loss in compressive strength of the concrete cubes without RHA and the improvement of resistance of resistance of acid attack of RHA along with FS concrete cubes were analyzed.

RESULTS AND DISCUSSIONS

The slump flow characteristics, V-funnel & L-box of the mixtures satisfies the EFNARC requirement. Slump flow decreases with increase in RHA content along with FS. The RHA indicates the increase in the viscosity of concrete. The blocking ratio in L-box test were as per requirement of SCC mixes as laid down by EFNARC guidelines. The results are presented in Table 8.

Sl.No	Designation	Slump Values, mm	EFNARC Values	T_{500}, Slump	EFNARC Values	V-Funnel, Sec	EFNARC Values	H2/H1 Ratio	EFNARC Values
1	C.SCC	768		2.95		8.54		0.95	
2	A0	760		3.18		8.72		0.84	
3	A1	743		3.23		9.12		0.81	
4	A2	725		3.29		9.16		0.92	
5	A3	708		3.68		9.34		0.87	
6	A4	694		4.05		9.51		0.81	
7	B0	690		3.32		9.36		0.88	
8	B1	683		3.41		9.52		0.87	
9	B2	680	650-800 mm	3.62	2-5 Secs	9.48	6-12 Secs	0.89	0.8-1.0
10	B3	676		3.91		9.56		0.87	
11	B4	672		3.98		9.66		0.86	
12	C0	686		3.94		9.32		0.90	
13	C1	681		4.01		9.50		0.86	
14	C2	673		4.17		9.52		0.92	
15	C3	670		4.23		9.60		0.90	
16	C4	661		4.47		9.88		0.90	
17	D0	680		4.17		10.09		0.92	
18	D1	672		4.36		10.26		0.90	
19	D2	666		4.64		10.36		0.93	
20	D3	658		4.92		10.44		0.92	
21	D4	653		5.12		10.83		0.86	

Table 8: Test results of Fresh concrete

The fresh concrete properties compared to EFNARC specifications, the slump obtained from RHA-FS SCC is between 768 mm to 653mm. The V-Funnel time obtained from RHA-FS SCC is between 2.95 sec to 5.12 sec. The H$_2$/H$_1$ ratio obtained from RHA–FS SCC is between 0.945 to 0.862.The fresh concrete properties of RHA-FS SCC obtained are within the EFNARC specifications.

Compressive Strength:

Sl. No	Concrete	Percentage Replacement of		Designation	Weight of C.SCC specimens and RHA-FS SCC specimens, Kg		Ratio of weight of RHA-FS SCC with respect to C.SCC	
		RHA	FS		28 Days	56 Days	28 Days	56 Days
1	C.SCC	0%	0%	C.SCC	2.380	2.400	1.000	1.000
2	RHA-FS SCC (with 5% RHA & different levels of FS)	5%	0%	A_0	2.320	2.340	0.975	0.975
3		5%	25%	A_1	2.200	2.210	0.924	0.921
4		5%	50%	A_2	2.220	2.230	0.933	0.929
5		5%	75%	A_3	2.180	2.190	0.916	0.913
6		5%	100%	A_4	2.170	2.180	0.912	0.908
7	RHA-FS SCC (with 10% RHA & different levels of FS)	10%	0%	B_0	2.100	2.110	0.882	0.879
8		10%	25%	B_1	1.990	2.000	0.836	0.833
9		10%	50%	B_2	2.000	2.100	0.840	0.875
10		10%	75%	B_3	1.980	1.990	0.832	0.829
11		10%	100%	B_4	1.970	1.980	0.828	0.825
12	RHA-FS SCC (with 15% RHA & different levels of FS)	15%	0%	C_0	1.960	2.000	0.824	0.833
13		15%	25%	C_1	1.900	1.950	0.798	0.813
14		15%	50%	C_2	1.950	1.990	0.819	0.829
15		15%	75%	C_3	1.800	1.900	0.756	0.792
16		15%	100%	C_4	1.780	1.860	0.748	0.775
17	RHA-FS SCC (with 20% RHA & different levels of FS)	20%	0%	D_0	1.890	1.990	0.794	0.829
18		20%	25%	D_1	1.700	1.900	0.714	0.792
19		20%	50%	D_2	1.800	1.920	0.756	0.800
20		20%	75%	D_3	1.690	1.840	0.710	0.767
21		20%	100%	D_4	1.600	1.800	0.672	0.750

Table 9: Weight of Conventional SCC mix (C.SCC) & RHA-FS SCC with different replacement levels of RHA and FS specimens with respect to different curing periods
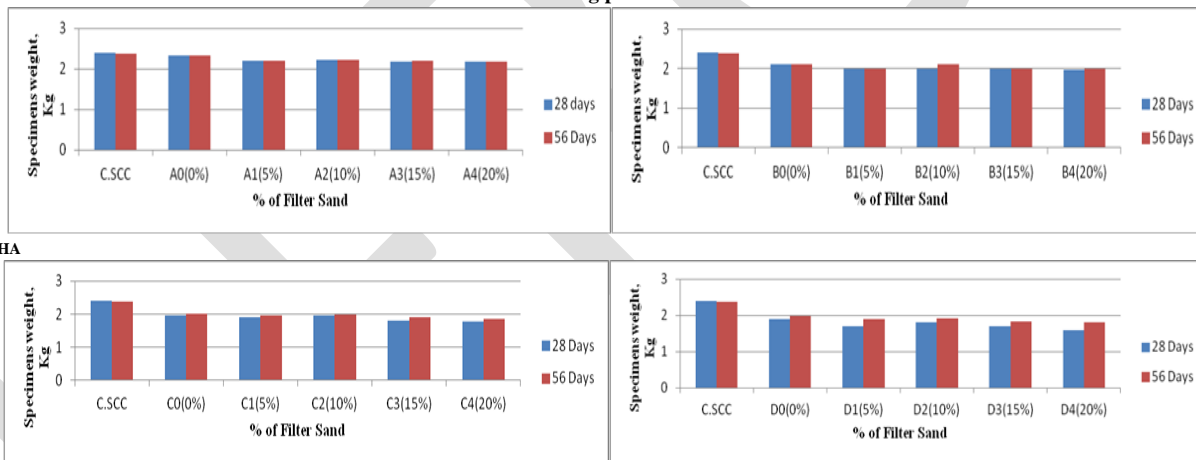

5% RHA 10% RHA

15% RHA 20% RHA

Fig 1: Comparison of specimen's weight of conventional SCC mix (C.SCC) & RHA-FS SCC of different replacement levels of RHA and FS for curing periods of 28 and 56 days

From above Table and Fig following observations are made:

The partial replacement of cement by RHA alone in C.SCC (RHA-FS SCC) reduces the weight of C.SCC, with increase in percentage of RHA the reduction in weight also increases. The weight of RHA-FS SCC with RHA of 5%, 10%, 15% and 20% and FS of 0% (A_0, B_0, C_0 and D_0) is 2.34, 2.11, 2.00 and 1.99 kgs respectively, whereas weight of C.SCC is 2.4 kg.

In addition to the replacement of cement by RHA, the natural sand partially replaced by FS in SCC (A_1, A_2, A_3, A_4 series), reduces the weight of RHA-FS SCC specimen further, for a typical case of RHA-FS SCC with 10% RHA and FS of 25%, 50%, 75% and 100% (B_1, B_2, B_3, B_4 series) the weights are 2.00, 2.10, 1.99 and 1.98 kgs respectively, whereas the weight of RHA-FS SCC of B_0 (10% RHA and 0% FS) is of 2.11 kg.

Hence from the above observations the replacement of cement and natural sand by RHA and FS respectively in SCC (RHA-FS SCC) reduces the weight of SCC in comparison to C.SCC.

Sl. no	Concrete	Percentage Replacement of		Designation	Comp Strength of C.SCC specimens and RHA-FS SCC specimens, N/mm^2		Ratio of Comp Strength of RHA-FS SCC with respect to C.SCC	
		RHA	FS		28 Days	56 Days	28 Days	56 Days
1	C.SCC	0%	0%	C.SCC	78.12	79.69	1.000	1.000
2	RHA-FS SCC (with 5% RHA & different levels of FS)	5%	0%	A_0	55.90	73.18	0.716	0.918
3		5%	25%	A_1	52.65	68.44	0.674	0.859
4		5%	50%	A_2	53.33	70.81	0.683	0.889
5		5%	75%	A_3	49.48	64.88	0.633	0.814
6		5%	100%	A_4	42.07	58.36	0.539	0.732
7	RHA-FS SCC (with 10% RHA & different levels of FS)	10%	0%	B_0	52.44	67.54	0.671	0.848
8		10%	25%	B_1	49.18	63.40	0.630	0.796
9		10%	50%	B_2	50.66	65.77	0.648	0.825
10		10%	75%	B_3	40.88	55.99	0.523	0.703
11		10%	100%	B_4	37.03	50.36	0.474	0.632
12	RHA-FS SCC (with 15% RHA & different levels of FS)	15%	0%	C_0	46.20	53.77	0.591	0.675
13		15%	25%	C_1	41.77	44.00	0.535	0.552
14		15%	50%	C_2	42.96	45.92	0.550	0.576
15		15%	75%	C_3	39.10	43.35	0.501	0.544
16		15%	100%	C_4	35.55	42.07	0.455	0.528
17	RHA-FS SCC (with 20% RHA & different levels of FS)	20%	0%	D_0	35.84	45.75	0.459	0.574
18		20%	25%	D_1	31.55	43.84	0.404	0.550
19		20%	50%	D_2	32.73	45.48	0.419	0.571
20		20%	75%	D_3	30.51	43.10	0.391	0.541
21		20%	100%	D_4	27.99	37.03	0.358	0.465

Table 10: Compressive strength of Conventional SCC mix (C.SCC) & RHA-FS SCC with different replacement levels of RHA and FS with respect to different curing periods

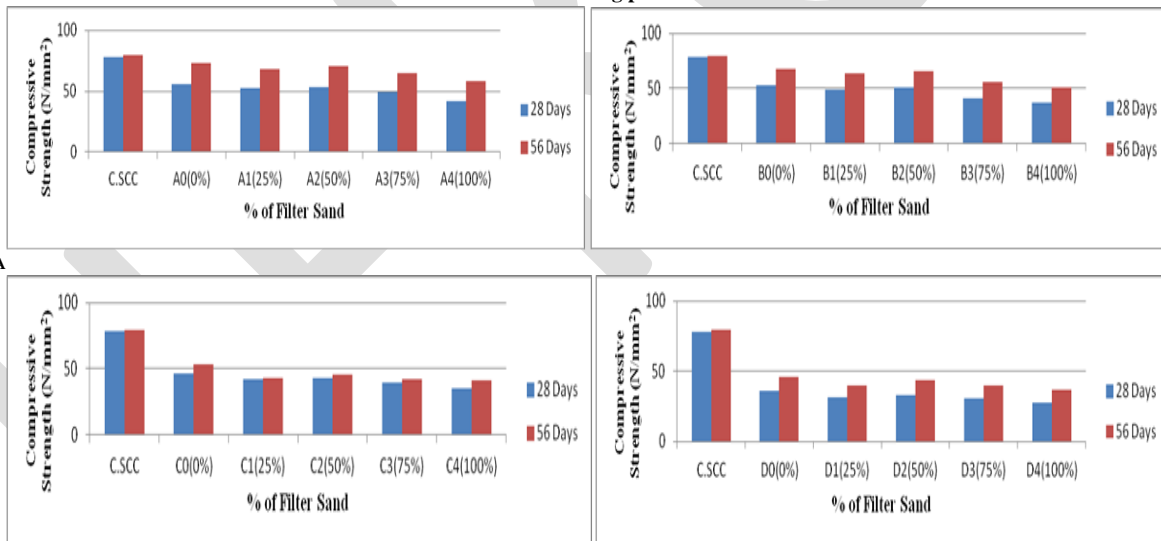5% RHA   10% RHA

15% RHA   20% RHA

Fig 2: Comparison of Compressive strength of conventional SCC mix (C.SCC) & RHA-FS SCC of different replacement levels of RHA and FS for curing periods of 28 and 56 days

From Table and Fig the following observations are made:

The SCC with RHA attains significant strength only after 28 days of curing unlike Conventional Self Compacting Concrete (0% RHA, 0% FS) which attains its strength at 28 days of curing.

The compressive strength of RHA-FS SCC for different replacement level of FS from 0% to 100% with 5%, 10%, 15% and 20% of RHA varies between 73.18 N/mm^2 to 58.36 N/mm^2; 67.54 N/mm^2 to 50.36 N/mm^2; 53.77 N/mm^2 to 42.07 N/mm^2 and 45.75 N/mm^2 to 37.03 N/mm^2 respectively. Whereas compressive strength of Conventional SCC is 79.69N/mm^2.

The compressive strength of RHA-FS SCC of A-series SCC i.e. 5% RHA and FS of 0%, 25%, 50%, 75% and 100% are 73.18 N/mm^2, 68.44 N/mm^2, 70.81 N/mm^2, 64.88 N/mm^2 and 58.36 N/mm^2. Similar variations are observed for RHA of 10%, 15% and 20% i.e. B, C and D-series.

The RHA-FS SCC with replacement of 5%, 10%, 15% & 20% of RHA and replacement of FS of 50% (A$_2$, B$_2$, C$_2$ & D$_2$) the compressive strength compared to 0% FS (A$_0$, B$_0$, C$_0$ & D$_0$) reduces, it reduces by 3.24%, 2.62%, 14.60% & 0.60% respectively. And when compared to 25% of FS (A$_3$, B$_3$, C$_3$ & D$_3$) the compressive strength increases, it increases by 3.47%, 3.74%, 9.34% & 3.75% respectively.

The replacement of sand by FS in RHA-FS SCC influences in reduction of the compressive strength. However the replacement level of FS of 50% (A$_2$, B$_2$, C$_2$ & D$_2$) gives higher strength when compared to other replacement levels of FS.

Hence from the above observations replacement of cement partially by RHA reduces the compressive strength compared to C.SCC. The compressive strength of RHA-FS SCC is reduced further when natural sand is replaced partially by FS.

Acid Resistance:

Sl. no	Concrete type	Compressive strength of specimens before immersion in Hcl soln 'N/mm^2'		Compressive strength of specimens after immersion in Hcl soln 'N/mm^2'		% Reduction in Compressive strength after immersion in Hcl soln		Ratio of % change in strength wrt C.SCC	
		28 Days	56 Days	28 Days	56 Days	28 Days	56 Days	28 Days	56 Days
1	C.SCC	78.12	79.69	61.86	67.18	26.29	18.62	1.00	1.00
2	A$_0$	55.90	73.18	48.12	65.42	16.17	11.86	0.62	0.64
3	A$_1$	52.65	68.44	46.00	60.88	14.46	12.42	0.55	0.67
4	A$_2$	53.33	70.81	47.12	63.20	13.18	12.04	0.50	0.65
5	A$_3$	49.48	64.88	38.90	57.00	27.20	13.82	1.03	0.74
6	A$_4$	42.07	58.36	36.18	56.18	16.28	3.88	0.62	0.21
7	B$_0$	52.44	67.54	46.50	62.00	12.77	8.94	0.49	0.48
8	B$_1$	49.18	63.40	45.90	58.12	7.15	9.08	0.27	0.49
9	B$_2$	50.66	65.77	46.48	58.86	8.99	11.74	0.34	0.63
10	B$_3$	40.88	55.99	32.10	52.18	27.35	7.30	1.04	0.39
11	B$_4$	37.03	50.36	29.14	49.16	27.08	2.44	1.03	0.13
12	C$_0$	46.20	53.77	38.00	48.61	21.58	10.62	0.82	0.57
13	C$_1$	41.77	44.00	32.18	39.11	29.80	12.50	1.13	0.67
14	C$_2$	42.96	45.92	34.85	42.86	23.27	7.14	0.89	0.38
15	C$_3$	39.10	43.35	32.00	36.72	22.19	18.06	0.84	0.97
16	C$_4$	35.55	42.07	28.10	32.10	26.51	31.06	1.01	1.67
17	D$_0$	35.84	45.75	30.00	45.16	19.47	1.31	0.74	0.07
18	D$_1$	31.55	43.84	27.40	39.10	15.15	12.12	0.58	0.65
19	D$_2$	32.73	45.48	28.98	40.00	9.17	13.70	0.35	0.74
20	D$_3$	30.51	43.10	25.35	34.18	20.36	26.10	0.77	1.40
21	D$_4$	27.99	37.03	21.18	30.10	32.15	23.02	1.22	1.24

Table 11: The Compressive strengths of C.SCC and RHA-FS SCC specimens of different replacement levels of RHA and FS cured for 28 days and 56 days immersed in 5% Hcl solution
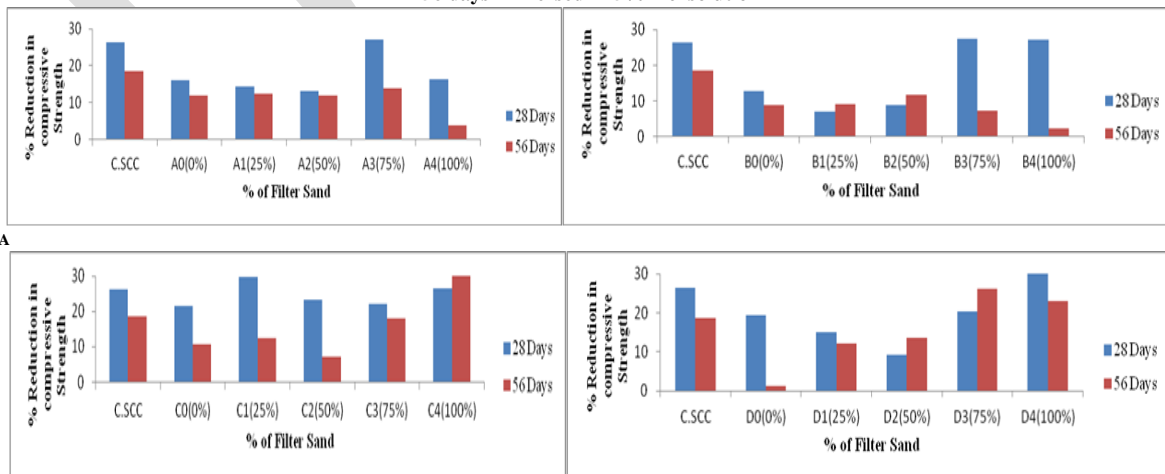

5% RHA 10% RHA

15% RHA 20% RHA

Fig 3: Percentage reduction in compressive strength of specimens immersed in 5% Hcl solution cured for 28 days and 56 days

From Table following observations are made on strength loss of SCC immersed in 5% Hcl solution.

Both C.SCC and RHA-FS SCC specimens when immersed in acid for 28 days, suffered loss in compressive strength.

The strength loss of C.SCC is 26.29% & 18.62% for 28 and 56 days water cured specimens immersed in acid for 28 days respectively. Similarly the loss in strength of RHA-FS SCC with different levels of RHA and FS are lesser in 56 days water cured specimens.

All RHA-FS SCC specimens with different levels of RHA and FS showed almost lower degree of loss in strength compared to that of C.SCC specimens at both 28 and 56 days water curing period, when immersed in 5% Hcl solution.

It is found that the % loss in strength of RHA-FS SCC as RHA replacement level increases from 5%-20% (A_0, B_0, C_0 and D_0) goes on decreasing. The % losses in strength are 11.86%, 8.94%, 10.62% and 1.31%.

It is seen that the % loss in strength of RHA-FS SCC specimens (A_0, B_0, C_0 and D_0) showed lesser values as compared to C.SCC of 18.62%. Increase in % replacement level of RHA increases the acid resistance.

It is found that with the partial replacement of FS from 25%-100% the % reduction in strength increases marginally than that of 0% replacement level of FS. However the C and D series with RHA of 15% and 20% and FS varying between 25%-100% the % reduction in the strength increases drastically, which shows that the RHA-FS SCC with RHA upto 10% and with different replacement levels of FS (25% to 100%) has better acid resistance compared to the other proportions of RHA and FS. The % reductions of A_1-A_4, B_1-B_4, C_1-C_4 and D_1-D_4 are 12.42-3.88%, 9.08-2.44%, 12.50-31.06% and 12.12-23.02% respectively.

From all the observations, it can be seen that the resistance to acid attack of RHA-FS SCC specimens is higher than that of C.SCC specimens and resistance goes on increasing as RHA and filter sand replacement level increases, except C and D series.

CONCLUSIONS

Fresh properties:

RHA contributes in the reduction of agricultural waste that is the main cause of environmental problems in agricultural countries. On the other hand, it is an approach to improve the quality of concrete without using costly additives such as silica fume, GGBFS etc.

Due to the presence of RHA in SCC along with FS, the required strength of SCC is obtained to actual values, after 56 days of curing unlike normal concrete which attains the strength at 28days.

The presence of RHA reduces the slump, with the increase in quantity of RHA in SCCs the reduction in slump also increases. The addition of FS along with RHA further reduces the slump. For D_4-Mix (20% RHA+100% FS) the slump reduced frrom768 mm (Conventional SCC mix) to 653 mm.

The T_{500} time increases with the increase in percentage of RHA. The presence of FS further increases the T_{500} time i.e., 2.95 sec to 5.12 sec.

The increase of RHA affects the consistency of flow of SCC. The presence of FS along with RHA, add to the increase in reduction of consistency of flow.

The V Funnel time increases with the increase in percentage of RHA. The presence of FS further increases the V Funnel time.

Durability properties:

The RHA-FS SCC when immersed in 5% Hcl solution (acid) the weight gets reduced, with increase in replacement levels of both RHA and filter sand in SCC the percentage weight loss also goes on increasing. However the % loss in weight is lesser than C.SCC.

The RHA-FS SCC with replacement level of RHA upto 10% shows better acid resistance with all % replacement level of FS (upto 100%). RHA-FS SCC with replacement level of RHA 15% and 20% shows better acid resistance with FS upto 50%. Hence the resistance to acid attack of RHA-FS SCC specimens is higher than that of C.SCC specimens and resistance goes on increasing as RHA and filter sand replacement level increases, except C_3, C_4 and D_3, D_4 specimens.

The RHA-FS SCC with only replacement of cement by RHA (upto 20%) and without the replacement of natural sand by filter sand increases the chemical resistance against acid attack, with replacement of natural sand by filter sand along with replacement of cement by RHA the durability factors becomes vice versa.

Hence the RHA-FS SCC with replacement of cement by RHA is more durable than the RHA-FS SCC with replacement of natural sand by filter sand.

REFERENCES:

1. V.Ramasamy[*]Dr.S.Biswas, "Durability Properties of Rice Husk Ash Concrete" ICI Journal, October-December 2009.

2. Salas[*], 1, M. A. Ospina1, S. Delvasto2 and R. Mejía de Gutierrez2, "Study on the Pozzolanic Properties of Silica Obtained from Rice Husk by Chemical and Thermal Process" 1 Materials Engineer, Ph.D Student, Composites Materials Group, CENM, Universidad del Valle, Cali, Colombia, 2 Titular Professor, Composites Materials Group, CENM, Universidad del Valle, Cali, Colombia, Received zzz, revised zzz, accepted zzz, Published online zzz.

3. AlirezaNajiGivi 1, Suraya Abdul Rashid 2, Farah Nora A. Aziz 3, Mohamad AmranMohdSalleh 2, "Contribution of Rice Husk Ash to the Properties of Mortar and Concrete: A Review" Journal of American Science, 2010;6(3).

4. P. Chindaprasirt a, C. Jaturapitakkul b, U. Rattanasak c,*, "Influence of fineness of rice husk ash and additives on the properties of lightweight aggregate" Fuel 88 (2009) 158–162.

5. Paratibha Aggarwal*, Yogesh Aggarwal, S M Gupta, R Siddique, "Properties of Self-Compacting Concrete – An Overview" 30th Conference on Our World in Concrete & Structures: 23 – 24 August 2005, Singapore.

6. S. D. Nagrale1, Dr. Hemant Hajare2, Pankaj R. Modak3, "Utilization Of Rice Husk Ash" International Journal of Engineering Research and Applications (IJERA) ISSN: 2248-9622, Vol. 2, Issue 4, July-August 2012, pp.001-005.

7. Sumrerng Rukzon1, Prinya Chindaprasirt2, and Rattana Mahachai3, "Effect of grinding on chemical and physical properties of rice husk ash" International Journal of Minerals, Metallurgy and Materials Volume 16, Number 2, April 2009, Page 242.

8. Maurice E. Ephraim, Godwin A. Akeke and Joseph O. Ukpata, "Compressive strength of concrete with rice husk ash as partial replacement of ordinary Portland cement" Scholarly Journal of Engineering Research Vol. 1(2), pp. 32-36, May 2012.

9. A. Ramezanianpour1,*, M. Mahdi khani2, Gh. Ahmadibeni3, "The Effect of Rice Husk Ash on Mechanical Properties and Durability of Sustainable Concretes" International Journal of Civil Engineerng. Vol. 7, No. 2, June 2009.

10. Md. Harunur Rashid, Md. Keramat Ali Molla, Tarif Uddin Ahmed, "Durability of Mortar in Presence of Rice Husk Ash" World Academy of Science, Engineering and Technology 43 2010.

11. Dr. Hemant Sood1, "Incorporating European Standards for Testing Self Compacting Concrete in Indian Conditions" International Journal of Recent Trends in Engineering, Vol. 1, No. 6, (May 2009).

12. Mixture proportioning procedure for Self-compacting concrete, The Indian concrete journal, Aug 2004.

SMART SOIL EXAMINER TO ASSIST FARMER IN THE FIELD OF AGRICULTURE

Mr. Soheb Akkalakot, Ms. Soumya Ghongadi, Ms. Shweta Rayar, Ms. Shruthi E, Prof. Rudrappa Gujanatti

ECE Department, KLE Dr. MSSCET, Belagavi

Abstract - This technical assistance program will help farmers to improve the crop yield by providing information with regard to soil testing based on wireless sensor network in agriculture such as monitoring environmental conditions like soil moisture, soil temperature and soil fertility. It also tries to maintain database of farmer, their field with present, previous and standard crop details. Using "Information decision making technology" farmers are guided to improve their agricultural production and they are also provided with the information related to current crop rates in marketing sector through direct link to government marketing sites. And the results are messaged to the farmer with the help of GSM.

Keywords - Crop yield, soil testing, soil moisture, soil temperature, soil fertility, soil nutrients (NPK), database, zigbee.

INTRODUCTION

Nowadays farmers are facing many problems due to shortage of soil testing units and lack of knowledge to utilize the technology. Because of wrong predictions desired yield is not been obtained. For ages, agriculture has always had a very special place in the life style of an Indian Agriculture and its associated activities contribute about 5.7% of Indian gross domestic products. However, in spite of all the development, the agriculture methods that Indians use are still way old. Soil fertility is the measure factor to be looked for getting better yield. Measure constrain in promoting balanced use of fertilizers includes inadequate soil testing facilities, wide gap in dissemination of knowledge, lack of awareness among farmers about benefits of balanced fertilization.

This technical program maintains database of farmer, their field with present, previous and standard crop details. Using "Information decision making technology" farmers are guided to improve their agricultural production and they are also provided with the information related to current crop rates in marketing sector through direct link to government marketing sites.

With the proposed work crop health and yield shall be improved and farmers are updated regularly with cultivation information and marketing through media. Using these inputs farmer can grow the suitable crop and can get desirable yield & profit.

LITERATURE SURVEY

Muhamd Azman Miskam, et.al. , published a paper entitled "Preliminary Design on the Development of Wireless Sensor Network for Paddy Rice Cropping Monitoring Application in Malaysia" [1]. This paper presents the preliminary design on the development of WSN for paddy rice cropping monitoring application. The propose WSN system will be able to communicates each other with lower power consumption in order to deliver their real data collection. The main objective of the new design architecture is to cater the most important and critical issue in WSN, that is power consumption.

Narasimhan , v. Lakshmi, et.al. , published a paper entitled "Greenhouse Asset Management Using Wireless Sensor-Actor Networks" [2]. Greenhouse plays an increasingly important role in modern horticulture in order to meet the needs of the world's growing and demand driven economy. The primary issue of greenhouse based horticulture is to manage the greenhouse environment optimally in order to comply with the economic and environmental requirements.

Hui Liu, et.al. , presented a paper entitled "Wireless sensor network technology" [3]. This paper can provide optimal and integrated solution for distributed data collecting, delivering and analyzing in tough croplands environment. A wireless sensor network for cropland environmental monitoring is designed according to cropland application requirements. It consists of a set of sensor nodes for data sensing, a sink node for data aggregating and long-distance transmitting, and a base station for data storing and analyzing.

BLOCK DIAGRAM

Figure 1 show the block diagram of sensing unit used in this project. This uses simple components like sensors, display units, RF Tx & Rx, ARM7 processors, Voice Bank and speaker etc., which are easily available in market and smaller in size which makes it portable. The sensor section used in this system gives accurate values of all the parameters necessary to test the soil fertility. Once the necessary parameter values are obtained they are sent to Technical Base Station via zigbee transmitter, those values are processed using all the necessary information given by the software.
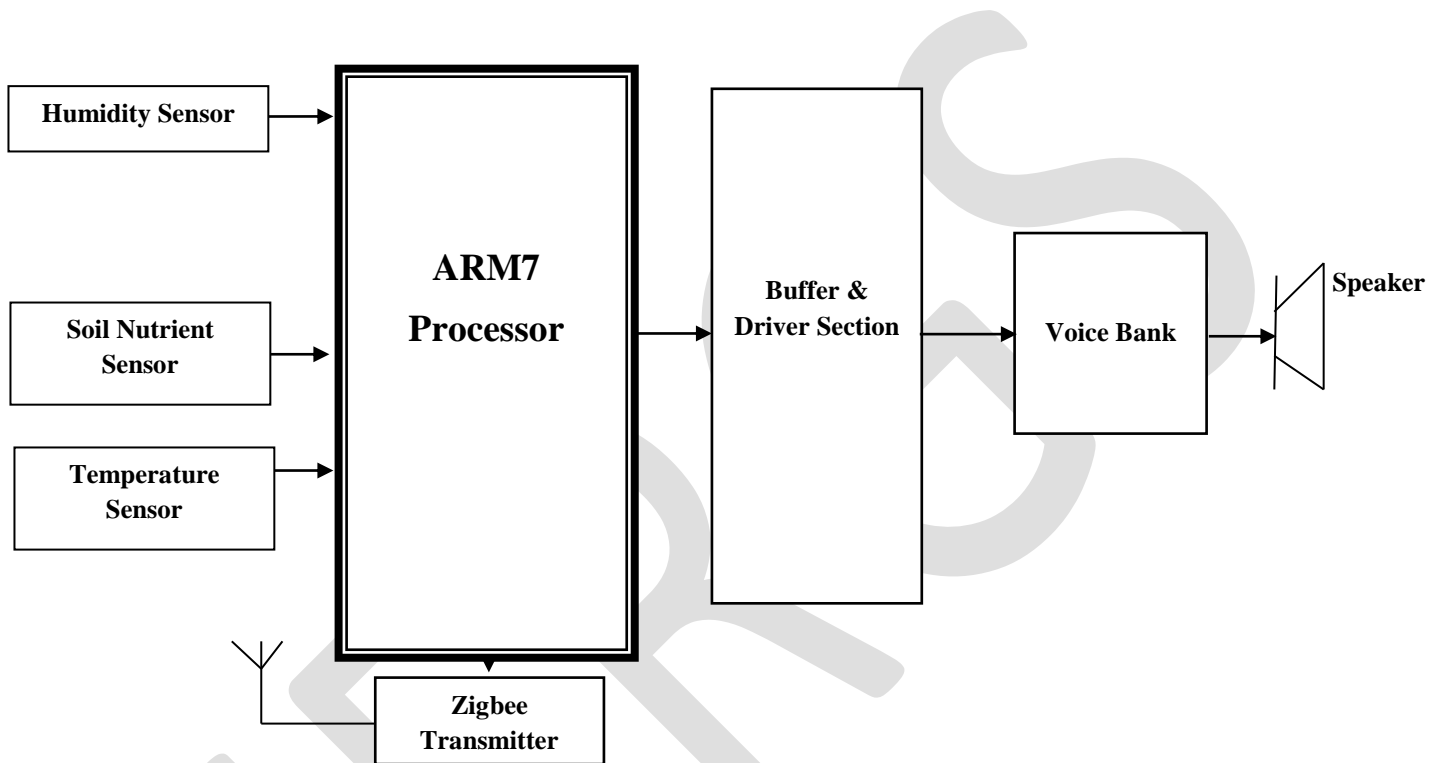
Figure 1: Block Diagram of the Sensing Unit

Figure 2 shows block diagram of the technical base station used in this project, where zigbee receiver receives the parameter sent by transmitter and these values are compared with the standard crop details when the user presses the button on the sensing section, the respective responses are obtained quickly. The necessary assistance information stored in voice bank is triggered by RF unit as a voice output. And also an alert message is sent to the farmer's cell phone.
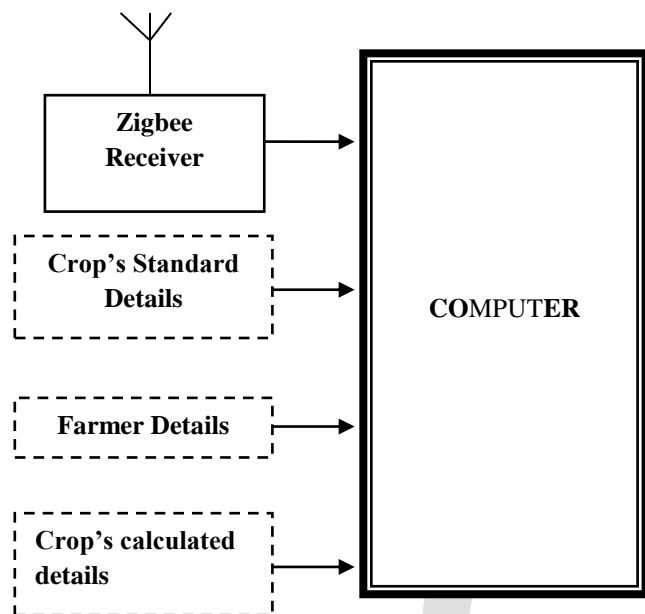
Figure 2: Block diagram of the Technical Base Station

FLOWCHART
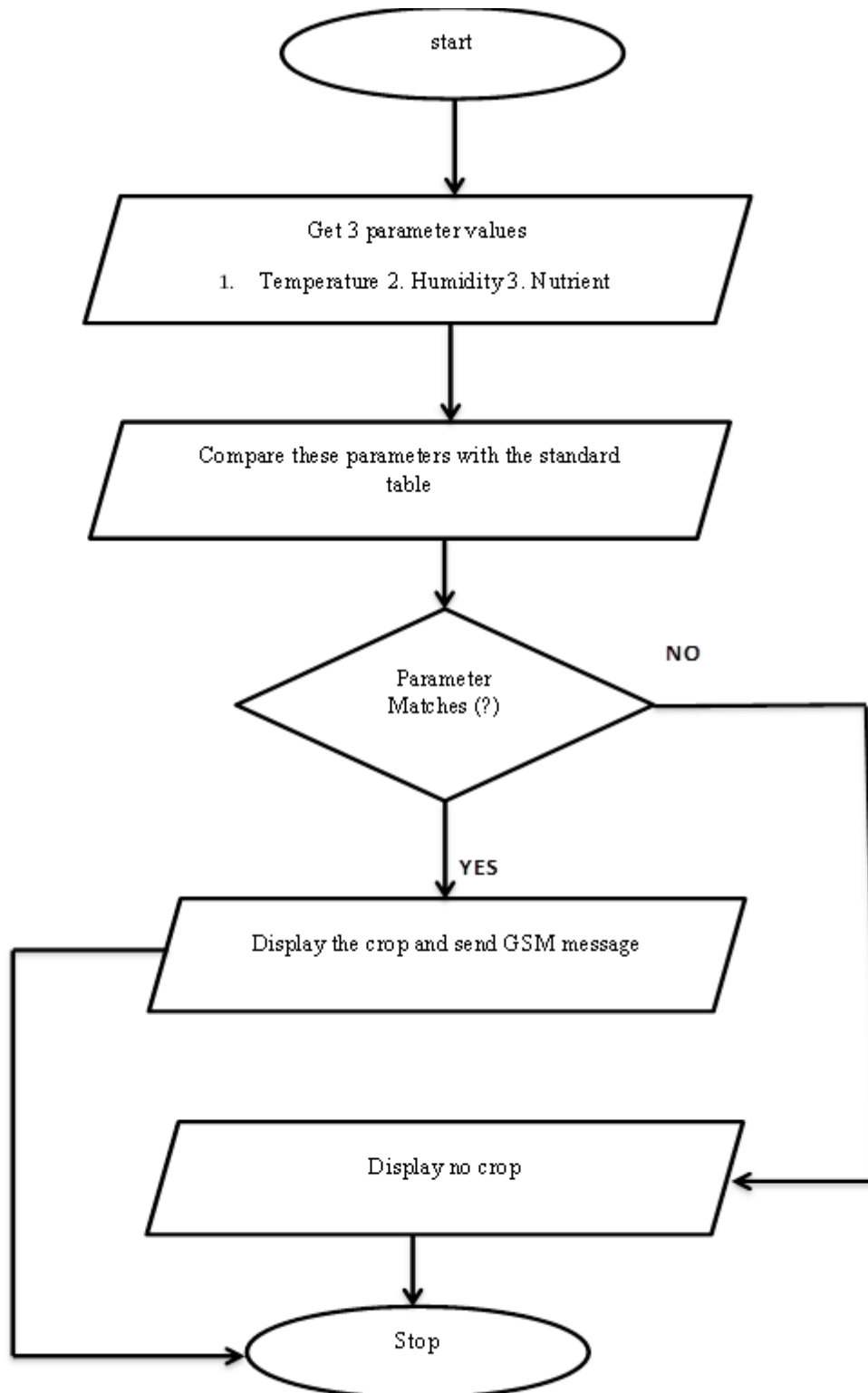
Figure 3 shows the flowchart of the project

Figure 3: Flowchart of the project

ADVANTAGES

[1] Easy to implement and portable: This project uses simple components like sensors, display units, electrodes etc which are easily available in market and smaller in size which makes it portable.

[2] Economic and User-friendly: As we are using low cost materials in the system, it makes it economic and its operation is simple so that farmers can easily use it.

[3] Approximately accurate results: The sensor used in this system gives accurate values of all the parameters necessary to test the soil fertility.

[4] Correct assistance with respect to derived results: Once the necessary parameter values are obtained on display, those values when entered in the Base Station, all necessary information will be given by the software.

[5] Quicker result analysis: When the user presses the button on the keypad, the necessary values are obtained quickly. In assistance software too quick response can be obtained.

[6] Robust and Long-life: Since maintenance is less and no hazardous components are used, makes this system effective and reliable.

APPLICATIONS

[1] In Agriculture to help Farmers for testing soil fertility.

[2] To survey land without any others help.

[3] Determination of type and quality of soil before cultivation.

[4] Horticulture.

[5] Nursery plantation.

[6] In maintenance of farmer details.

[7] It can be used to provide details about estimated yield to the government.

RESULTS

Figure 4 shows the result displayed on the GLCD for the parameters namely temperature=31^0C, humidity=16 and pH level=20, whenever user presses the switch at the sensing unit.
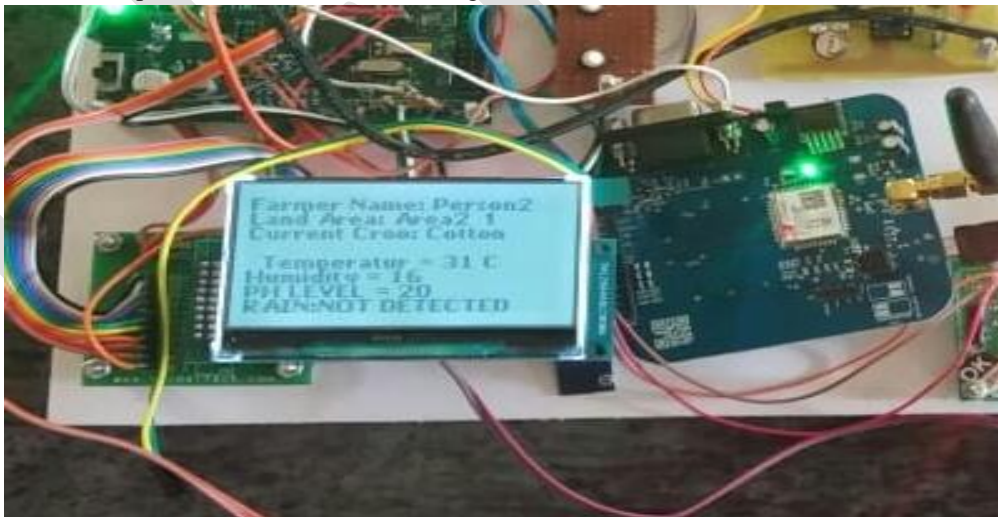
Figure 4: Result for temperature=310 C, humidity=16, pH=20

Figure 5 shows the result displayed on the GLCD for the parameters namely temperature=14^{0}C, humidity=17 and pH level=20, whenever user presses the switch at the sensing unit.

Figure 5: Result for temperature=14^0 C, humidity=17, pH=20

Figure 6 shows the message alert for the parameters temperature, pH level, and humidity which is sent by GSM modem
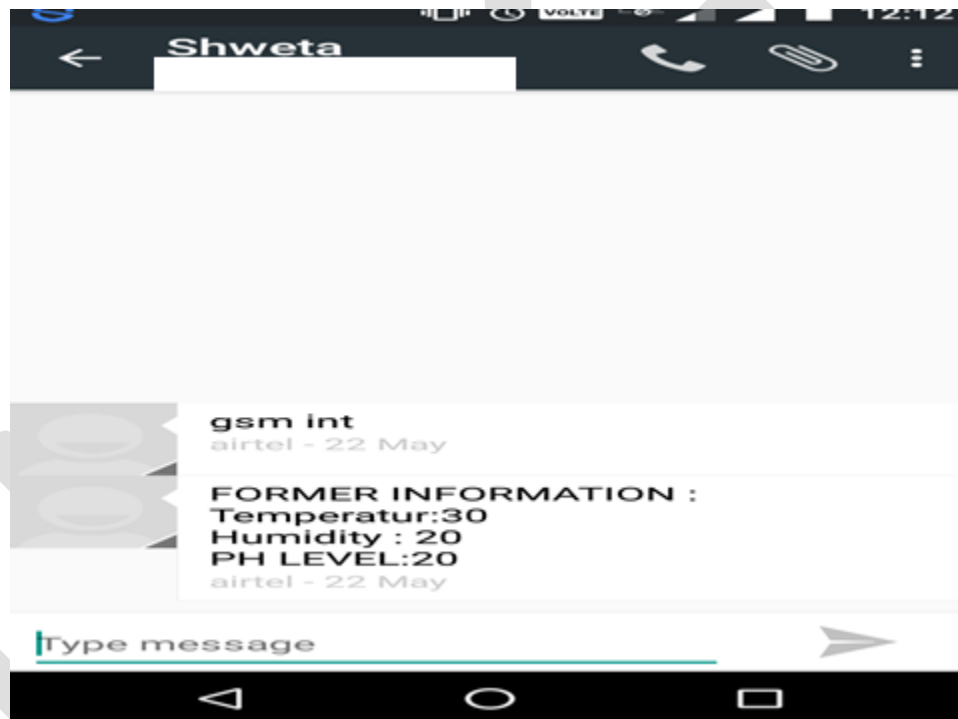

Figure 6: GSM message alert

ACKNOWLEDGMENT

CONCLUSION

In this project, we proposed real-deployment of smart soil examiner to assist farmer in the field of agriculture which is designed and implemented to realize agriculture. The end users can modify the operation to a variety of experimental setups, which will allow the farmers to reliably collect the data from locations previously inaccessible on a micro-measurement scale. And such a system can be easily maintained and installed. This project successfully applies the wireless sensor networks on agro-ecology fields by investigating environmental situations. The complete real-time and historical environment information is expected to help the agro-ecological specialists achieve efficient management and utilization of agro-ecological resources.

REFERENCES:

[1] Miskam, MuhamadAzman, Azwan bin Nasirudin and InzarulfaishamAbd., Rahim "Preliminary Design on the Development of Wireless Sensor Network for Paddy Rice Cropping Monitoring Application in Malaysia", European Journal of Scientific Research Vol-37 No.4 (2009), pp .649-657, ISSN 1450-216X, 2009.

[2] Narasimhan, V. Lakshmi, Alex A. Arvind and Ken Bever, "Greenhouse Asset Management Using Wireless Sensor-Actor Networks", 2007.

[3] Hui Liu, ZhijunMeng, Maohua Wang, "A Wireless Sensor Network for Cropland Environmental Monitoring". International Conference on Networks Security, Wireless Communications and Trusted Computing, Vol-1, pp 65 – 68, 2009.

Optimization of Drill Process Parameters for Maximum Material Removal Rate using Taguchi and ANOVA

[1]Pradeep Mishra, [2]Dr. A.S Verma, [3]Avdesh Dixit

[1,2]Department of Mechanical Engineering, Kanpur Institute of Technology, Kanpur, U.P, India

[3]Department of Mechanical Engineering, Bhabha Institute of Technology, Kanpur, U.P, India

Abstract— An objective of this Experimental work was to optimize and analyzed process parameters namely point angle (deg), spindle speed (RPM) and feed (mm/Rev) in drilling operation of mild steel. In this work, experiments were carried out as per the Taguchi experimental design and an L9 orthogonal array was applied to study the influence of various combinations of process parameters for MRR. ANOVA (Analysis of variance) test was conducted to determine the percentage of contribution for each process parameters on drilling. The results indicate that feed is the most significant factor and point angle is the second most significant factor for Material removal rate. This work is useful for selection optimized values of various controllable process parameters that do not only maximize the MRR but also reduce the delimitation and improve the MRR.

Keywords—Drilling, DOE, Taguchi, ANOVA, Array, Mild Steel, MRR

1. INTRODUCTION

Drilling is widely used for machining processes to produce holes in various industrial parts. Drilling is a process of producing round holes in a solid material or enlarging existing holes with the help of multi-point cutting tools (drill bits). [1] Drilling is one of the widely used machining processes for various purposes. Nowadays it is frequently used in automotive, aircraft and aerospace and dies or mold industries, home appliances, and medical and electrical equipment industries. Thus, it needs to be cost-effective along with the assurance of the quality specifications within the experimental limit. In today's rapidly changing circumstances in manufacturing industries, applications of optimization techniques in metal cutting processes are essential for a manufacturing unit to respond efficiently to severe competitiveness and the increasing demand of the quality product in the market. Optimization methods in metal cutting processes, considered being a very important tool for continual improvement of output quality in products & processes [2]. The quality of drill depends on cutting tool geometry, workpiece materials, and input parameters.

2. LITERATURE REVIEW

Dr. Anant Guja et al. [3] in this study experiments were performed on SG500/7 plate using different twist drills under dry cutting conditions. The measured results were collected and analyzed with the help of the commercial software package MINITAB16. Analysis of variance (ANOVA) was employed to determine the most significant control factors affecting the surface roughness. The spindle speed (850, 1150, & 1440 rpm), feed rate (90,120 &135 mm/min) and tool material (HSS, Carbide and TiAlN Coated Carbide) were selected as control factors. The main and interaction effect of the input variables on the predicted responses are investigated. It is predicted that Taguchi method is a good method for optimization of various machining parameters as it reduces number of experiments. The results indicate the optimum values of the input factors and the results are conformed by a confirmatory test

S.V. alagarsamy et al. [4] the aim of this work was utilize Taguchi method to investigate the effects of drilling parameters such as cutting speed, feed and depth of cut on surface roughness and material removal rate in drilling of Aluminium alloy 7075 using HSS spiral drill. The Taguchi method, a powerful tool to design optimization for quality, is used to find optimal cutting parameters. Orthogonal arrays, the signal- to- noise ratio, the analysis of variance are employed to analyze the effect of drilling parameters on the quality of drilled holes. A series of experiments based on L16 orthogonal array are conducted using CNC vertical machining centre. The experiment results are collected and analyzed using statistical software Minitab16. Analyses of variances are employed to determine the most significant control factors affecting the surface roughness and material removal rate. ANOVA has shown that the depth of cut has significant role to play in producing higher material removal rate and cutting speed has significant role to play for producing lower surface roughness.

Vinod Kumar Vankanti et al. [5] objective of the present work is to optimize process parameters namely, cutting speed, feed, point angle and chisel edge width in drilling of glass fiber reinforced polymer (GFRP) composites. In this work, experiments were carried out as per the Taguchi experimental design and an L9 orthogonal array was used to study the influence of various combinations of process parameters on hole quality. Analysis of variance (ANOVA) test was conducted to determine the significance of each process parameter on drilling. The results indicate that feed rate is the most significant factor influencing the thrust force followed by speed, chisel edge width and point angle; cutting speed is the most significant factor affecting the torque, speed and the circularity of the hole followed by feed, chisel edge width and point angle. This work is useful in selecting optimum values of various process parameters that would not only minimize the thrust force and torque but also reduce the delimitation and improve the quality of the drilled hole

Ashish Tripathi et al. [6] the measurement of torque and thrust in drilling enable to find the amplitude of vibration produced that will decide the type of setup needed for the work. The objective of this research paper is to find thrust and torque in mild steel and aluminum 6061 and to find optimal values of drilling parameters so that minimum value of torque and thrust is obtained. After finding the values of thrust and torque in mild steel and aluminum6061 the comparison of values for both the materials has been presented. The lower value of thrust and torque will result into higher tool life and lower vibration in machine tool structure.

3. MATERIALS AND METHOD

3.1. Work Piece Material

Work piece material used for experiment was mild steel Table 1 shows the chemical composition of mild steel.

Table: 1 Chemical Composition of Mild Steel

Element	Composition (wt %)
C	0.16
Al	0.07
Si	0.168
Mn	0.18
P	0.025
Cu	0.09
Fe	Balance

Figure: 1. Mild Steel work piece after Drilling

3.2. Drill bits Material

High speed steel drill bits was used for drilling and every drill bit point angle was different i.e. 75, 118 and 130 deg.

Figure: 2. Different point angle HSS Drill Bit

3.3. Selection of Process Parameters

In this experiment machining process parameters like point angle (deg), Spindle Speed (rpm) and Feed (mm/rev) of the drill were considered. As per Taguchi's design of experiments for three parameters and three levels L9 Taguchi orthogonal array was selected. The number of factors and their corresponding levels are shown in Table 2.

Table: 2 Machining Parameters and Levels

Process Parameters	Level		
	1	2	3
Point Angle (deg)	75	118	130
Spindle Speed (rpm)	80	160	270
Feed (mm/rev)	0.45	0.86	1.42

4. METHODOLOGY

5.1. Taguchi Method

Taguchi approach was firstly introduced by Dr. Genichi Taguchi. Taguchi approach has three stage system design, parameters design, and tolerance design. Taguchi approach is a statically approach to improve the product quality and increases the production. A specially designed orthogonal array of Taguchi was used in this work to investigate the effects of the entire machining parameters through the small number of experiments and it takes less time for the experimental investigations.[7]**Smaller the better:** this is used where smaller value is desired.

S/N Ratio = $-10\log\frac{1}{n}\sum_{i=1}^{n} yi^2$ …………… (1)

Where y = observed response value and n = number of replications

Nominal the best: this is used where the nominal or target value and variation about that value is minimum.

S/N Ratio = $-10\log\frac{\mu^2}{\sigma^2}$ ……………………. (2)

Where σ = mean and μ= variance

Higher the better: this is used where the larger value is required.

S/N Ratio $= -10\log\frac{1}{n}\sum_{i=1}^{n}\frac{1}{yi^2}$ ………………… (3)

5.2. ANOVA (Analysis of Variance)

ANOVA is a statistical tool used to test differences between two or more means. It may seem odd that the technique is called "Analysis of Variance" rather than "Analysis of Means" The ANOVA is obtained by dividing the measured the sum of the squared deviations from the total mean S/N ratio into contributions by each of the control factors and the errors.[8] ANOVA identify the percentage of contribution of controlled process parameters.

Table: 3. Experimental Table with S/N Ratio

Sr. no	Point Angle	Spindle Speed	Feed	MRR	S/N Ratio
1	75	80	0.45	8.182	18.257
2	75	160	0.86	6.000	15.56303
3	75	270	1.42	11.250	21.02305
4	118	80	0.86	8.824	18.91285
5	118	160	1.42	10.000	20
6	118	270	0.45	10.714	20.59926
7	130	80	1.42	9.000	19.08485
8	130	160	0.45	13.125	22.36199
9	130	270	0.86	6.818	16.67337

5. RESULT AND ANALYSIS

Minitab17 was used has been used for analysis of the experiment. Minitab17 software analysis the experimental data and then provides the calculated results of signal-to-noise ratio. The objective of the present work was to maximize the MRR in drilling process optimization. The equations are an exception to the prescribed specifications of this template. The effect of different process parameters on MRR is calculated and plotted as the controllable process parameters change one level to another level. The average value of S/N ratios has been calculated to find out the effects of different parameters and as well as their levels. The use of both ANOVA technique and S/N ratio approach makes it easy to analyze the results and hence, make it fast to reach on the conclusion. Table III shows the experimental results for material removal rate and corresponding S/N ratios.

5.1. Analysis of Signal to Noise Ratio

Larger-the-best performance characteristic was selected to obtain material removal rate.

Table: 4. Response Table for S/N Ratio (MRR)

Level	Point Angle	Spindle Speed	Feed
1	18.28	18.75	20.41
2	19.84	19.31	17.05
3	19.37	19.43	20.04
Level	1.56	0.68	3.36
Rank	2	3	1

Table: 5. Response Table for Mean

Level	Point Angle	Spindle Speed	Feed

Level	Point Angle	Spindle Speed	Feed
1	18.28	18.75	20.41
2	19.84	19.31	17.05
3	19.37	19.43	20.04
Level	1.56	0.68	3.36
Rank	2	3	1

From the table IV &V and figure 3 & figure 4 that feed and point angle after that spindle speed play a important role for MRR, Point Angle = 118 deg, Spindle Speed = 270 RPM and Feed = 0.45 mm/rev
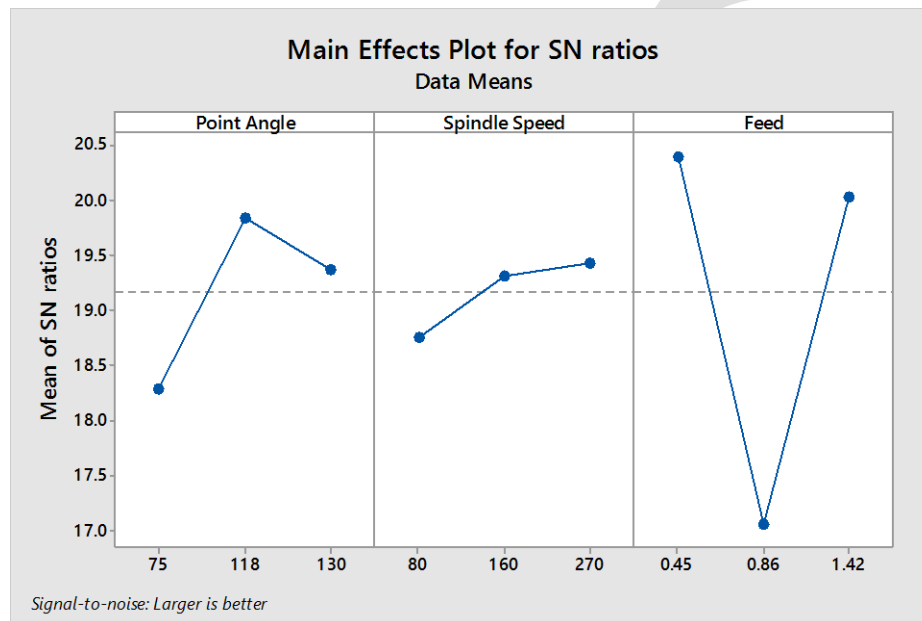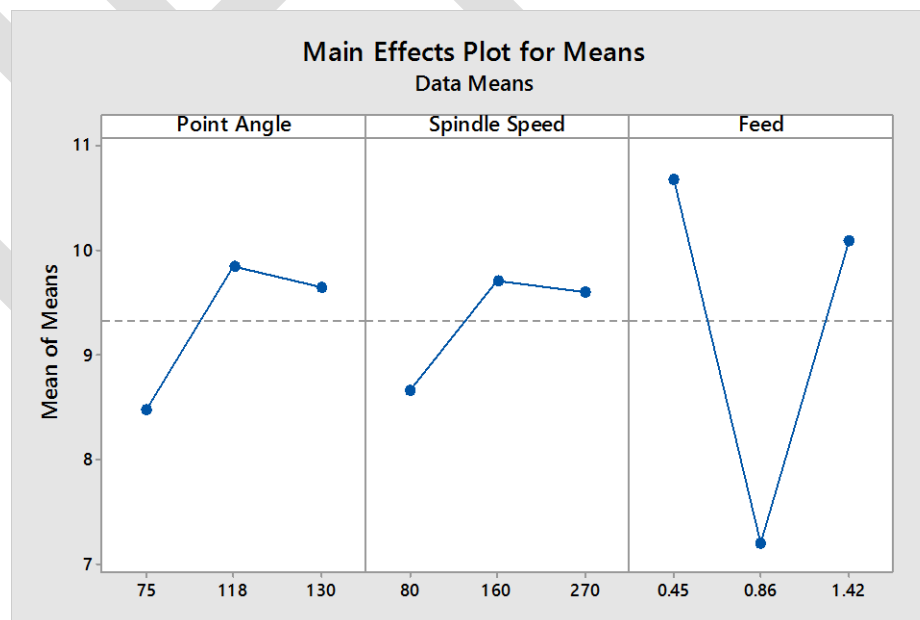

Figure: 3. Main Effect Plot for S/N Ratio of MRR

Figure: 4. Main effect Plot for Means

5.2. Analysis of Variance (ANOVA)

Minitab 17 was used to investigate the process parameters. ANOVA define the percentage of contribution for each process parameters.

Table: 6. ANOVA Result for MRR

Source	DF	SS	MS	F	P	%CON
Point Angle	2	8.282	1.6412	0.24	0.807	22.07
Spindle Speed	2	4.951	0.9757	0.14	0.876	13.19
Feed	2	20.552	10.2762	1.49	0.401	54.76
Error	2	3.749	6.8744			9.99
Total	8	37.534				100.00
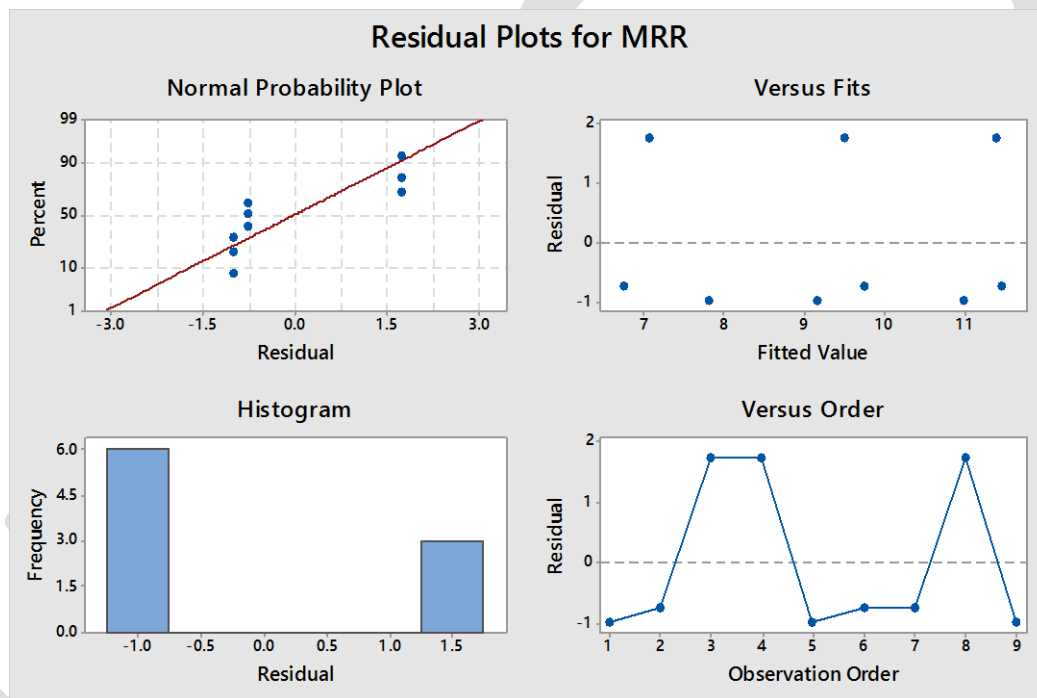
Figure: 5. Residual Plots for MRR

6. CONCLUSION

The optimize process parameters in the drilling of mild steel for optimized MRR are Point Angle 118, Spindle Speed 270 RPM and feed 0.45 mm/rev. ANOVA clearly identify that Feed is 54.76 %, point Angle 22.07 % and spindle speed 13.19 % contribute to maximum material removal rate

REFERENCES:

[1] Vinayak Samleti, Prof. V.V. Potdar "Optimization of Drilling Process Parameters Using Taguchi Method-A Review" August 2017, Volume 4, Issue 08 Jetir (Issn-2349-5162)

[2] Amarnath R. Mundheka, Subhash R. Jadhav "Optimization of Drilling Process Parameters: A Review" International Journal for Research in Applied Science & Engineering Technology (IJRASET) Volume 3 Issue II, February 2015 ISSN: 2321-9653

[3] Mr.Pruthviraj Chavan , Dr. Anant Gujar "Study the effect of Machining Parameter on Surface Roughness in Drilling of SG 500/7 Material" International Journal of Advance Engineering and Research Development Volume 3, Issue 7, July -2016 e-ISSN (O): 2348-4470 p-ISSN (P): 2348-6406 at: https://www.researchgate.net/publication/309211582 July 2017.

[4] S.V. alagarsamy, S. Arockia Vincent Sagayaraj, P. Raveendran "Optimization of Drilling Process Parameters on Surface Roughness & Material Removal Rate by Using Taguchi Method" International Journal of Engineering Research and General Science Volume 4, Issue 2, March-April, 2016 ISSN 2091-2730 https://www.researchgate.net/publication/304894900

[5] Vinod Kumar Vankanti, Venkateswarlu Ganta "Optimization of process parameters in drilling of GFRP composite using Taguchi method" Received 4 May 2013 Accepted 16 October 2013 Available online 21 November 2013 Elsevier. © 2013 Brazilian Metallurgical, Materials and Mining Association. Published by Elsevier

[6] Ashish Tripathi, Ranganath M Singari, Vipin Dahiya "Optimization of Process Parameters with Effect of Thrust and Torque in Drilling Operation" IJAPIE-2016-04-201,Vol 1(2), 1-12- t: https://www.researchgate.net/publication/301298419

[7] M. Balajia, B.S.N. Murthy, N. Mohan Rao "Optimization of Cutting Parameters in Drilling Of AISI 304 Stainless Steel Using Taguchi and ANOVA" 2212-0173 © 2016 The Authors. Published by Elsevier Ltd, This is an open access article under the CC BY-NC-ND license (http://creativecommons.org/licenses/by-nc-nd/4.0/)Peer-review under responsibility of the organizing committee of RAEREST 2016 doi: 10.1016/j.protcy.2016.08.217

[8] Weiran Duan, Yifan Dai, Yong Shu, Sherrington "Application of Taguchi methods and ANOVA in optimization of process parameters for surface roughness of fused silica in the Magnetorheological Finishing processes" Advanced Materials Research Online: 2013-02-13 ISSN: 1662-8985, Vol. 662, pp 449-452 doi:10.4028/www.scientific.net/AMR.662.449 © 2013 Trans Tech Publications, Switzerland

A Review on Gas Turbine Blade Failure and Preventive Techniques

Lakshay Bansal, Vineet kumar Rathi, Krunal Mudafale

Amity University Haryana, bansallakshaybansal@gmail.com

Abstract– With the increase in demand for power supply and more efficient turbojet engines, gas turbine designing is being pushed to its extremities. Turbomachines are becoming larger as compared to the machines of past decades. Due to increase in size, the cause and chances of failure have also increased. Gas turbine blade is the component which is exposed to extreme operating condition, thus experience different failure modes. Constant mechanical and thermal stresses act on different sections of blade. Newer super-alloys with enhanced metallurgical properties are being developed and tested to counter the stresses acting on the blades. Advance additive manufacturing techniques are used to produce next generation super-alloys. Failure due to mechanical and metallurgical anomalies are indirectly related to the high operational temperature and can be corrected up to a certain limit. Thus thermal protection is required for blades. Advance cooling techniques and coatings are being used for this purpose. Different literatures were combined to compile all the data analysed on blade failure and the preventive techniques being used.

Key Words– Gas turbine blades, Erosion, Fretting fatigue, Thermal stresses, Super-alloys, Hot corrosion, Film cooling, thermal barrier coating,

1. NOMENCLATURE

k_1 = Material constant

$f(\beta_i)$ = Empirical function of particle impact angle

V_{ti} = Tangent component of incoming particle velocity

V_{tr} = Rebound particle velocity

$f(V_{ni})$ = Component of erosion due to normal component of velocity

E = Erosion rate

K = Von Karman constant

ε = Eddy diffusivity for momentum

l = Mixing length

δ = Boundary layer thickness

P = Row spacing of coolant holes

D = Van Driest damping function

B_r = Blowing ratio

x = Stream wise distance from point of injection

y = dimensionless distance of first point off the blade surface

2. INTRODUCTION

A basic design (fig 1.) of gas turbine setup consists of compressor to increase the air pressure, combustion chamber where fuel is ignited with incoming air flow to increase the thermal and thus kinetic energy of the gases and turbine to produce mechanical output in form of shaft work. Gas turbines are used commonly for power generation and in air-breathing jet engines to power compressor [1]. To yield more output, the design and size of the turbines are increasing drastically resulting in increased stresses on the turbine blade.

Fig 1. Gas turbine
(https://www.turbinesinfo.com/gas-turbines/)
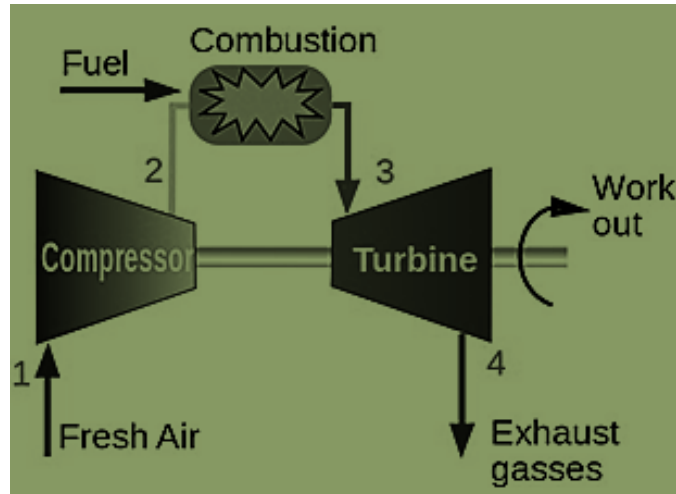
Turbine blades have to face large amount of vibrations due to critical operating conditions involving high rotary motion at tremendously high temperatures [2,3]. These factors result in common mode of turbine blade failure. Efficiency and the blade reliability reduces mainly due to mechanical and/or metallurgical anomalies such as fatigue, creep, corrosion and erosion. Other factors may be airborne pollutants, foreign object damage or poor manufacturing or irresponsible operating. Corrosion and fatigue being of main concern are most analyzed to improve the durability and enhance the operational life of the turbine blades. The material used for gas turbine blades should be hardened, heat resistant with very high melting point and corrosion resistant, thus cobalt-based and nickel-based super-alloys are mainly used [4].

Further to counter thermal stress, advanced cooling techniques like film cooling are being developed and used [5]. The purpose of this paper is to compiles all the major modes of turbine blade degradation leading to failure, preventive methods presently being used and highlight the recommended areas for future study.

3. MODES OF FAILURE AND BLADE DEGRADATION

Gas turbine blades are subject to extreme condition due to which the blades degradation occur. Degradation may be service induced which might be accelerated due to different factor. Damages may occur due to mechanical behavior of the material or the metallurgical properties influencing the blade life time [1,4]. Due to centrifugal and oscillatory actions at component contact, crack formation is found to be significant that this place [6].

3.1 Erosion

Removal of material from the surface by the action of solids or fluids moving in contact with that surface at high velocity resulting in a faster material loss than the expected duration is called *erosion*. Flow sometimes is accompanied by unwanted solid particles that cause cutting and deformation to not only turbine blades but other components of gas turbine also. Erosion in gas turbine blade have been a source of concern since last decades as the designing, efficiency and the economic aspect depend greatly on this factor [7]. I. Finnie [9] stated in his study that erosion is a complex function of particle velocity, angle, material and target properties. Simply, by applying the Grant-Tabaoff erosion model, the erosion of ductile metals and their alloys can be predicted. Assuming the dependency of erosion process on amplitude of angular impingement, the following equation is derived [9]:

$$E = k_1 \mathfrak{f}(\beta_i)(V_{ti}^2 - V_{tr}^2) + \mathfrak{f}(V_{ni}) \tag{1}$$

Considering the suction side of rotor blade i.e. the side of blade where the impact angle of striking trapped particle is higher than the maximum erosion angle, erosion rate can be reduced by increasing the mass flow. Whereas, the erosion rate is directly influenced by the rotor's rotational speed as the particles entering rotor domain directly hit the pressure side of the blade [10].
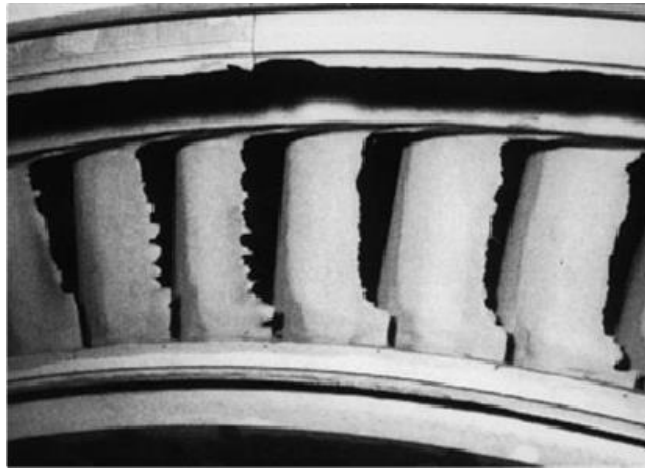

Fig 2. Turbine blades erosion
(https://www.researchgate.net/figure/Severe-erosion on-suction-side-of-steam-turbine-blades_fig2_276490146)

3.2 Fatigue

Fatigue is the weakening of a material due to repeated cycling loads or number of stress cycles it can survive. It is directly related to material properties. High cycle fatigue in turbine blades is one of the main cause of fatigue failure. Estimation of a blade's fatigue life can be made if the stresses acting on the blade and the material properties are known [1]. Blade failures due to fatigue are categorized as high cycle fatigue (HCF) and low cycle fatigue (LCF) [11,12]. Low cycle fatigue is due to stress applied on a body, high enough to produce plastic deformation whereas high cycle fatigue is characterized by the stresses for which S-N curve can be determined [13].

Point that experiences centrifugal and oscillatory vibration, such as component contact for example the region where blades are attached to the disk, are most vulnerable locations for cracking due to fatigue. A significant reduction in fatigue life is caused due to the micro slip experienced by the contact surface when subjected to fatigue. This is known as fretting fatigue. Fretting fatigue is the common cause for increased tensile and shear stresses which further leads to origin of crack, its growth and thus fracture [6]. Propagation of fret crack depends on the stress gradient, shape of contact, coefficient of friction and load applied. Compressor blade root joints are generally coated with Cu-Ni-In for fretting fatigue resistance [14].
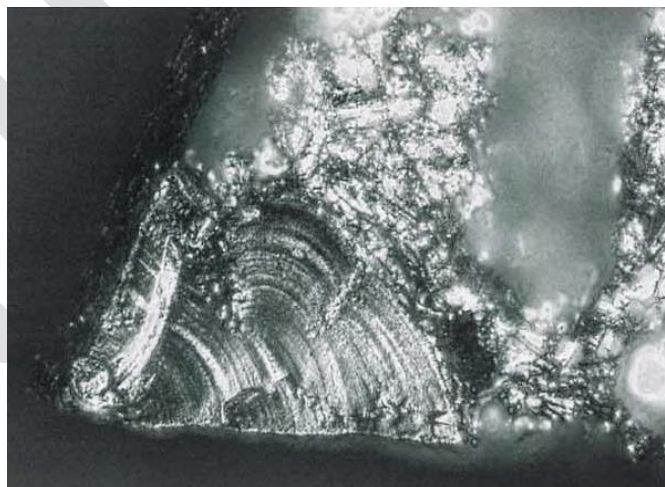

Fig 3. Crack propagation due to fatigue
(An investigation of fatigue failures of turbine blades in a gas turbine engine by mechanical analysis, Engineering Failure Analysis 9 (2002) 201–211)

3.3 Thermal stresses

Large amount of thermal stress is experienced by the turbine blades due to direct exposure to high temperature gases [15]. Components of first stage of turbine are exposed to large amount of thermal loads resulting in creep and thermal fatigue [16]. Particularly, the blade tips experience large thermal loads due to leakage of flow through the gap between the shrouded casing and the blade tip, increasing the chances of cracking. Large pressure gradient between the pressure side and suction side of blade results in acceleration of leak flow which leads to thin boundary layer formation and elevated heat transfer rate. This increases the turbine power loss and decreased efficiency [15]. Failures of even single crystal directional solidified alloy is majorly due to cracks caused by thermal fatigue. Alloy failure depend on the cyclic loading at elevated temperature [6].
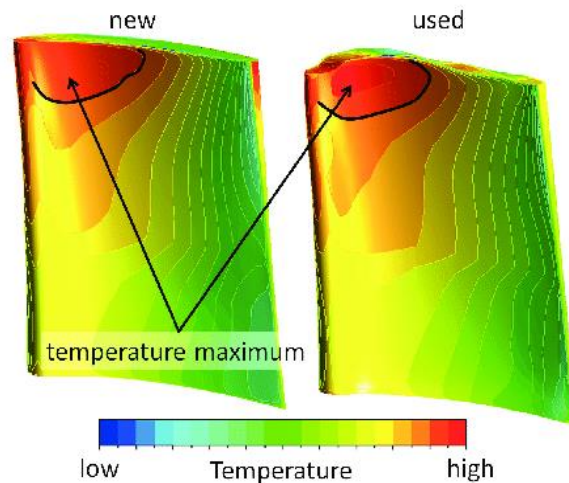
Fig 4. temperature variation on different section of gas turbine blade
(https://www.researchgate.net/figure/Total-pressure-and-temperature-distribution-on-the-new-and-used-turbine-blade_fig2_314197784)

Rhee and Cho [17,18] used a low speed turbine cascade to study the blade tip heat transfer characteristics. Coefficients of heat transfer at tip were found out to be 1.7 times higher compared to blade surface and shroud. As a consequence of reduction in leakage flow caused by the relative motion of case, the heat transfer at the stationary care was 10% more than rotatory case. Study of relation between rim height, tip clearance and heat transfer was done by Park et al. [19,20] which concluded that heat transfer is directly proportional to blade tip clearance and inversely proportional to rim height.
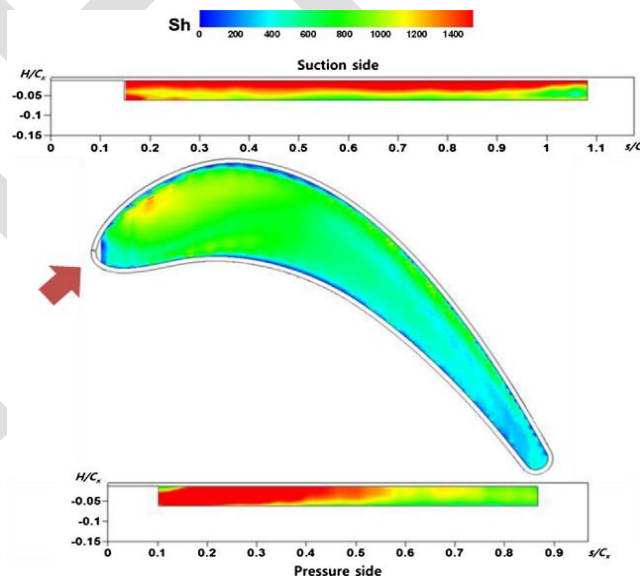
Fig 5. Heat transfer distribution on the tip surface and inner rim surfaces
(Heat transfer and film cooling effectiveness on the squealer tip of a turbine blade, Jun Su Park, Dong Hyun Lee, Dong-Ho Rhee, Shin Hyung Kang, Hyung Hee Cho, Energy 72 (2014) 331-343)

New heat resistant materials are being developed for replacing the current materials. Some of the examples are IN617, TOS1X-I and IN740 [21].

3.4 Material

Super-alloys are used for the application in high temperature operations and can be categorized by the base metal used: Nickel-based alloys, Cobalt-based alloys and Iron-based alloys. Super-alloys are used due to their excellent strength even at very high temperatures. Ni-based and cobalt-based super-alloys are mainly used for the fabrication of gas turbine blades. *IN738LC* is a nickel-based super-alloy with exceptionally high temperature and oxidation resistant properties. The alloy is strengthened by precipitating γ phase [7]. Hardness of IN738LC is due to fcc g-Ni matrix strengthened by solid solution and fine precipitations. Because of its alloying constituents and high g- γ, IN738LC is difficult to weld. Some more nickel-based super-alloys are developed such as IN718, IN6225, Hastelloy X, Waspalloy. Selective laser melting (SLM) can be used to improve tensile strength of IN738LC. Magnetic parts can be directly made using the additive manufacturing technique of selective laser melting [22].

Nickel-based single crystal super-alloys are divided further on the era they were developed in. First generation Ni-based alloy constituting mainly of Cr, Co, Mo, W, Ti and Ta. Cr is essential for hot corrosion resistance, Co and Mo are used due to their property of fcc matrix solid solution strengthening elements. Addition of *Rhenium* produced second generation alloy (Fig. 6) such as PWA1484, Rene N5, CMSX-4, SMP14. Third generation alloys (Fig. 7) like CMSX-10 and Rene N6 were developed by General Electric. New generation of alloys such as MC-NG, TMS75, TMS80 have been developed by Japan and France which show very high creep resistance and less density compared to third generation alloys [23].

Alloy	Cr	Co	Mo	Re	W	Al	Ti	Ta	Nb	Hf
CMSX-4	6.5	9	0.6	3	6	5.6	1	6.5	–	0.1
PWA 1484	5	10	2	3	6	5.6	–	8.7	–	0.1
René N5	7	8	2	3	5	6.2	–	7	–	0.2
SC180	5	10	2	3	5	5.2	1	8.5	–	0.1
SMP14	4.8	8.1	1	3.9	7.6	5.4	–	7.2	1.4	–
MC2	8	5	2	–	8	5	1.5	6	–	–

Fig 6. Chemical compositions (wt.%) of second generation Ni-based super-alloys for single crystal blades.

Alloy	Cr	Co	Mo	Re	W	Al	Ti	Ta	Nb	Hf
CMSX-10	2	3	0.4	6	5	5.7	0.2	8	0.1	0.03
René N6	4.2	12.5	1.4	5.4	6	5.75	–	7.2	–	0.15
Alloy 5A	4.5	12.5	–	6.25	5.75	6.25	–	7	–	0.15
TMS-75	3	12	2	5	6	6	–	6	–	0.1
TMS-80	2.9	11.6	1.9	4.9	5.8	5.8	–	5.8	–	0.1
MC-NG	Patent pending									

Fig 7. Chemical compositions (wt.%) of third generation Ni-based super-alloys for single crystal blades.

3.5 COROSION

Unwanted particles entering turbine are common cause for corroded turbine blades. It is clear from fig 8. that the crack originates from the site of noticeable carbide presence, leading to crack propagation and ultimately fracture [29]. Corrosion combined with high temperature environment becomes *hot corrosion* and is defined as the accelerated corrosion due to presences of salts such as Na_2SO_4, NaCl, and V_2O_5, which combine to produce molten deposits that damage the protective oxide layer on surface. Sodium sulphate is a well-known corroding agent produced during combustion process. Sodium chloride may enter the combustion chamber and Sulphur is a constituent of almost all fuels [28].
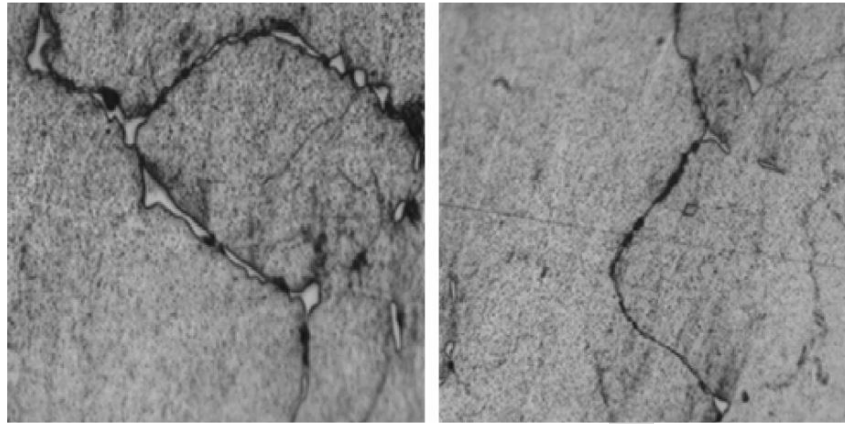
Fig 8. Continuous films of carbides in grain boundaries in two different zones
(Failure analysis of gas turbine blades in a thermal power plant, N. Vardar, A. Ekerim, Engineering Failure Analysis 14 (2007) 743–749)

3.5.1 Hot corrosion type 1

Extreme and rapid oxidation that occurs in presence of sodium sulphate and temperature range of 815 to 926 degree Celsius is known as *hot corrosion*. Main feature of this type of corrosion is that the base metal denuded surface experience an *intergranular* attack by sulphate particles as they are converted into complex unstable metal oxides. Similar behaviour is shown by potassium sulphate [28].

3.5.2 Hot corrosion type 2

This type of hot corrosion requires specific condition to attack at the most vulnerable site. Temperature between 593 to 760 degree Celsius and significantly pressurised SO_3 are the most favorable conditions along with the low melting constituents of nickel alloy like $NiSO_4$ and Na_2SO_4 that provide the need sulphate and oxygen compounds.

4. COOLING TECHNIQUE

First stage of any turbine encounters the highest temperature. In a gas turbine, blade tips are the most heated section of the entire blade. Cooling of components would protect them against overheating for safe operation as it would ensure limited thermal stresses which are experienced by the blades. This would result in proper cycle efficiency and enhanced component operational period. Steam turbine use cold steam as coolant, which is passed through the gaps between components. Gas turbine used film cooling technique for the purpose of blade cooling [24].

4.1 Film cooling

Film cooling works by injecting cool air through downwards inclined hole (fig 9.) in the boundary layer which covers the blade skin. This develops a cool film over the blade. Different hole patterns are used in modern film cooling to cover a full section of blade. This is known as full-coverage film cooling technique [25]. Study regarding the effects of tip clearance and blowing ratio on film cooling effectiveness, carried out by Kwah and Han [26] concluded that increase in effectiveness is directly proportional to both of the mentioned quantities. Factors influencing the film cooling performance are flow unsteadiness, compressibility, free stream turbulence, angle of ejection, three-dimensional external flow structure, hole size, location and shape, and wall curvature. Two dimensional injection model was developed by Tafti and Yavuzkurt that used two-dimensional Low-Reynolds number K-ε model boundary layer code for film cooling.

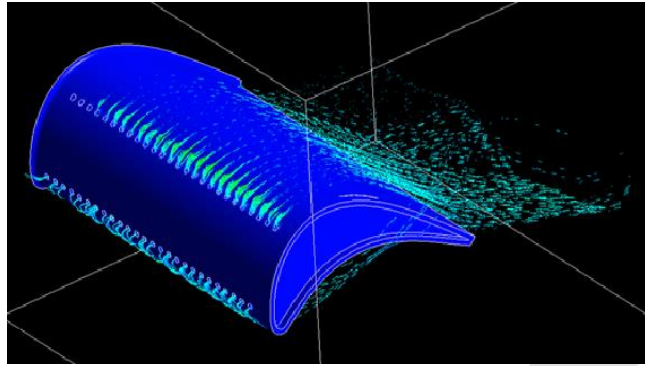**Fig 9.** Film cooling in turbine blade
(http://cfd2012.com/ansys-cfx-turbine-cooling.html)

In two dimensional boundary layer full-coverage film cooling, the prediction of heat transfer is done by using Crawford's model. It was used for augmentation of eddy viscosity on flat surface. Though applicable only for flat surface, this is the excepted model for present day calculations as no better model is available. Eddy diffusivity for momentum in presence of film cooling is determined by augmenting Prandtl mixing length using the following relation [27]:

$$\frac{l}{\delta} = \left(\frac{l}{\delta}\right)_{3D} + \left(\frac{l}{\delta}\right)_a \qquad (2)$$

Here '3D' refers to three dimensional mixing and 'a' refers to departure due to jet-boundary layer interaction given by:

$$\left(\frac{l}{\delta}\right)_a = \lambda_{max,a} * F * f , \qquad (3)$$

$$F = 2.718 \left(\frac{y}{PD}\right)^2 \exp\left[-\left(\frac{y}{PD}\right)^2\right], \qquad (4)$$

$$f = \exp\left[-\frac{\frac{x}{\delta}}{2}\right], \qquad (5)$$

$$\lambda_{max,a} = 0.0353 \exp(2.65B_r) \qquad (6)$$

$$\lambda_{max,a} = 0.0177 \exp(2.64B_r) \qquad (7)$$

$$\lambda_{max,a} = 0.0601 \exp(3.46B_r) \qquad (8)$$

Equation (6), (7) and (8) are for slant angled injection, compound angled injection and normal injection respectively [27].

4.2 THERMAL BARRIER COATING

Thermal barrier coating (TBC) is another method to provide thermal protection to gas turbine blades from high temperature gases. TBC is made up of low-thermal conductive ceramic material. Surface temperature reduction of underlying super-alloy is observed when used in thickness range of 100 to 500μm. TBC is made up of four structural layers, two ceramic layer and two metallic layers, namely, the substrate layer, the bond coating, the thermally grown oxide layer and the ceramic top coat layer. Due to the complexity of these layers, simultaneous occurring of phenomenon like plastic deformation, thermal expansion, phase transformation, diffusion, oxidation, elastic deformation, thermal conduction, radiation, fatigue and fracture can be seen.

The multi-material nature of TBC makes it more complex than any other coating and helps the material to withstand extremely high temperature cycling and stress conditions. With the use of TBC, materials used are expected to operate for about 30,000 hours in industrial gas turbines and last thousands of take-off and landing cycles in commercial jet engines [30].

5. CONCLUSION

From the above study it can be concluded that the metallurgical and mechanical causes of blade failure will always be present. It is observed that extremely high temperature of gases flowing in turbine contributes a lot in blade degradation and to lessen the chances of failure, thermal protection of gas turbine components is of most importance. Advanced thermal protection for blades and components exposed to these extremely hot gases are the main area of research. Thermal stresses are concentrated on particular sections of blade due to the fact that the sites for hot gases to escape are the most vulnerable points for attack of hot corrosion and other damaging factors in whole turbine. Concept of thermal barrier coating is also a good area for research as it has great potential for future advancements. Film cooling is being used for turbine and rocket components. Talking about the metallurgical aspect, new materials with high temperature resistant properties along with resistance to failure at high load and mechanical stress are being developed. Advance manufacturing techniques are adopted to develop new generation super-alloys. The studies conducted by different researchers and the models developed which show the significant dependency of heat transfer rate through the blade surfaces should be used to full extent. This along with other researches should be tested and implemented to reduce the chances and causes of turbine blade failure which would ultimately lead to more efficient and less hazardous turbomachines.

REFERENCES:

[1] A.A. Patil, U.M. Shirsat, "Study of Failure Analysis of Gas Turbine Blade", National Symposium on engineering and Research, IOSR Journal of Engineering, pp. 37-43.

[2] W. Sanders, "Steam Turbine Path Damage and Maintenance," Vol. 1: February 2001 and Vol. 2: July 2002, Pennwell Press, 2001.

[3] Jianfu Hou, Bryon J. Wicks, Ross A. Antoniou, "An Investigation of Fatigue Failures of Turbine Blades in a Gas Turbine Engine by Mechanical Analysis," Engineering Failure Analysis 9, 2002, pp. 201–211.

[4] E. Poursaeidi, M. Aieneravaie, "Failure Analysis of a Second Stage Blade in a Gas Turbine Engine", Engineering failure analysis, 2007, 15: 2008, pp 1111-1129.

[5] J. Ahn, S. Mhetras, J-C Han, "Film-Cooling Effectiveness on a Gas Turbine Blade Tip using Pressure Sensitive Paint", In: ASME conference proceedings, Vol. 41685, 2004, pp. 241-250.

[6] Rajni Dewangan, Jaishri Patel, Jaishri Dubey, Prakash Kumar Sen, Shailendra Kumar Bohidar, "Gas Turbine Blades –A Critical Review of Failure on First and Second Stages", International journal of mechanical engineering and robotics research, Vol. 4, No. 1, January 2015, pp. 216-223.

[7] M. Azimian, H.-J. Bart, "Investigation of Hydro-abrasion in Slurry Pipeline Elbows and T-Junctions," Journal of Energy Power Engineering, Vol. 8, 2014, pp. 65–78.

[8] I. Finnie, "Erosion of surfaces by solid particles," Wear 3, Vol. 2, 1960, pp. 87–103.

[9] D.G. Rickerby, N.H. MacMillan, "The Erosion of Aluminum by Solid Particle Impingement at Normal incidence," Wear, Vol. 60, Issue 2, May 1980, pp. 369-382.

[10] Mehdi Azimian, Hans-Jörg Bart, "Computational Analysis of Erosion in a Radial Inflow Steam Turbine", Engineering Failure Analysis, Vol. 64, 2016, pp. 26–43.

[11] TSR Reddy, et al., "A Review of Recent Aeroelastic Analysis Methods for Propulsion at NASA Lewis Research Centre", NASA Technical Paper 3406, 1993.

[12] DP Walls, RE Delaneuville, SE Cunningham, "Damage Tolerance Based Life Prediction in Gas Turbine Engine Blades Under Vibratory High Cycle Fatigue," Journal of Engineering for Gas Turbines and Power, 1997, 119:143–6.

[13] Ioannis V. Papadopoulos, Piermaria Davoli, Carlo Gorla, Mauro Filippini and Andrea Bernasconi, "A Comparative Study of Multiaxial High-Cycle Fatigue Criteria for Metals," International journal of fatigue, Vol. 19, no. 3, 1997, pp. 219-235.

[14] Loveleen Kumar Bhagi, Prof. Pardeep Gupta, Prof. Vikas Rastogi, "A Brief Review on Failure of Turbine Blades," Proceedings Smart Technologies for Mechanical Engineering, 25-26 Oct 2013 at Delhi Technological University, Delhi.

[15] Jun Su Park, Dong Hyun Lee, Dong-Ho Rhee, Shin Hyung Kang, Hyung Hee Cho, "Heat Transfer and Film Cooling Effectiveness On the Squealer Tip of a Turbine Blade," Energy 72, 2014, pp. 331-343.

[16] S. Holdsworth, M. Radosavljevic, P. Grossmann, "Effectiveness Verification of Creep-fatigue Assessment Procedures for Fast Starting Steam Turbines," et al., 2012, ASME Paper GT2012-68223, pp. 367-373.

[17] D-H Rhee, HH Cho., "Local Heat/Mass Transfer Characteristics on a Rotating Blade with Flat Tip in a Low-Speed Annular Cascade Part II: Tip and Shroud", ASME Paper GT2005-68724, pp. 653-662.

[18] D-H Rhee, HH Cho., "Effect of Vane/Blade Relative Position On Heat Transfer Characteristics in A Stationary Turbine Blade: Part 1 Tip and Shroud", International Journal of Thermal Sciences, Vol. 47, Issue 11, November 2008, pp. 1528-1543.

[19] Park JS, Lee DH, Lee WJ, Cho HH, D-H Rhee, SH. Kang, "Heat/Mass Transfer Measurement On the Tip Surface of Rotor Blade with Squlear Rim", In: AIP conference proceedings, Vol. 1225, 2009, p. 952.

[20] JS Park, DH Lee, WJ Lee, D-H Rhee, SH Kang, HH Cho., "Heat transfer characteristics on tip and inner rim surfaces of blade with squealer rim, In: Proceedings of ICHMT Turbine-09; 2009.

[21] N. Lückemeyer, H. Kirchner, H. Almstedt, "Challenges in Advanced-USC Steam Turbine Design for 1300°F/ 700°C," ASME Paper No. GT2012-69822, pp. 685-693.

[22] L. Rickenbacher, T. Etter and S. Hovel, K. Wegener, "High Temperature Material Properties of IN738LC Processed by Selective Laser Melting (SLM) Technology" , Rapid Prototyping Journal 19(4), June 2013, pp. 282-290.

[23] Pierre Caron, Tasadduq Khan, "Evolution of Ni-based Super-alloys for Single Crystal Gas Turbine Blade Applications," Aerospace Science and Technology, Vol. 3, Issue 8, December 1999, pp. 513-523.

[24] Wenhao Huo, Jun Li, Xin Yan, "Effects of Coolant Flow Rates on Cooling Performance of the Intermediate Pressure Stages for an Ultra-Supercritical Steam Turbine," Applied Thermal Engineering 62, 2014, pp. 723-731.

[25] E. R. G. Eckert,"Analysis of Film Cooling and Full-Coverage Film Cooling of Gas Turbine Blades," Journal of Engineering for Gas Turbines and Power, Jan 1984, Vol. 106, pp. 206-213.

[26] JS Kwak, J C Han, "Heat Transfer Coefficient and Film-Cooling Effectiveness On a Gas Turbine Blade Tip," In: ASME conference proceedings, Vol. 36088, 2002, pp. 309-318.

[27] Vijay K. Garg, Raymond E. Gaugler, "Effect of Velocity and Temperature Distribution at The Hole Exit On Film Cooling Of Turbine Blades," Journal of Turbomachinery 119(2), July 1995.

[28] M.R. Khajavia, M.H. Shariatb, "Failure of First Stage Gas Turbine Blades", Engineering Failure Analysis 11, 2004, pp. 589–597.

[29] N. Vardar, A. Ekerim, "Failure analysis of gas turbine blades in a thermal power plant", Engineering Failure Analysis 14, 2007, pp. 743–749.

[30] Nitin P. Padture, Maurice Gell, Eric H. Jordan "Thermal Barrier Coatings for Gas-Turbine Engine Applications", Science, New Series, Vol. 296, No. 5566, Apr. 12, 2002, pp. 280-284.

Effect of with and without cryogenic treatment on Tensile, hardness and impact on hybrid Aluminium-6061 metal matrix composites

Varun Chandra M, Sudarshan M, Sumantha H, Harshith Gowda K I

Vidyavardhaka college of engineering, varunchandra.m@gmail.com

Abstract— The metal matrix composite (MMC) have become the leading material in aerospace and automobile industries and particle reinforced aluminum MMC`s have received a considerable attention due to their excellent mechanical properties like hardness, high tensile strength etc. Aluminum matrix composites refer to the class of light weight high performance aluminum ceramic material systems. The purpose is to study above mechanical properties of Al-6061 with boron carbide and graphite in cryogenic condition by varying boron carbide with 0, 3, 6, 9 and 12% particulate using stir casting process. An improved mechanical property of composites makes them very useful for various applications in many areas from technological point of view. The microstructure and hardness of the fabricated composites were analyzed and reported.

Keywords— Tensile, hardness, Impact, Boron carbide, graphite, Al 6061, cryogenic condition, stir Casting, Metal matrix composites, Scanning Electron Microscopy

1. INTRODUCTION

Aluminum alloys reinforced with ceramic particulates have significant potential for structural applications due to their high specific strength and stiffness as well as low density. These properties have made particle-reinforced metal matrix composites (MMCs) an attractive candidate for the use in weight-sensitive and stiffness-critical components in aerospace, Transportation and industrial sectors. Corrosion behavior is very important parameter for assessing the application potential of composites as structural materials. Aluminum alloys reinforced with ceramic particulates have significant potential for structural applications due to their high specific strength and stiffness as well as low density. These properties have made particle-reinforced metal matrix composites (MMCs) an attractive candidate for the use in weight-sensitive and stiffness-critical components in aerospace, Transportation and industrial sectors. Corrosion behavior is very important parameter for assessing the application potential of composites as structural materials. Table 1 shows the composition of aluminum 6061.

Aluminum	95.85–98.56%
Silicon	0.4% - 0.8%
Iron	0% - 0.7%
Copper	0.15% - 0.4%
Manganese	0% - 0.15%
Magnesium	0.8% - 1.2%
Chromium	0.04% - 0.35%
Zinc	0% - 0.25%
Titanium	0% - 0.15%
Other elements	0.15%

Table.1 Composition of Al-6061 alloy

2. OBJECTIVE

The main objective of this work is to fabricate Al6061-B_4C-Gr metal matrix composite by stir casting process, to prepare specimens according to ASTM standards. To investigate tensile, hardness and impact properties with and without cryogenic condition.

3. MATERIAL AND METHODS

From literature survey it was cleared that, there is wide scope to studies on corrosion behavior of Al-B_4C-Gr hybrid metal matrix composites, so aluminium-6061 is chosen as matrix material, silicon carbide and graphite as reinforcement materials.
Table.2 shows Composition of Al 6061, B_4C and Gr for specimen preparation. The quantities of boron carbide and graphite were taken in a pan and were pre heated by placing the pan on crucible for 15 mins. Al 6061 was heated in the furnace at a temperature of 800ºC.The molten material was stirred with a stirrer speed of 220 rpm to create vortex, then the heated reinforcements were added and

stirred. The composites were cast using conventional methods. The specimens are casted in 4 different combinations and it is shown below in table 2. Fig 1 shows the stir casting apparatus required to fabricate specimens.

Sl.No	Reinforcement %
Specimen 1	0%
Specimen 1	3%
Specimen 2	6%
Specimen 3	9%
Specimen 4	12%

Table.2 Composition of Al 6061 & Sic and Gr for specimen preparation

Fig.1 Stir Casting Apparatus

4. TESTING

Tensile Test was carried out on a computerized UTM according to ASTM E8. Fig 2 shows the tensile test specimens details
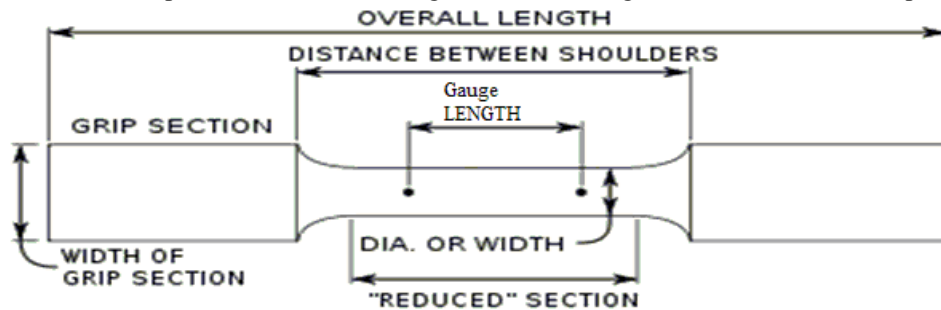
Fig.2 Tensile Test Specimens details

HARDNESS TEST

Hardness test was done with standard Rockwell Hardness Testing Machine. Test was performed according to ASTM E18.

IMPACT TEST

Impact test was done with Izod Testing Machine. Test was performed according to ASTM E23. Fig 3 shows the specimens prepared for hardness test.
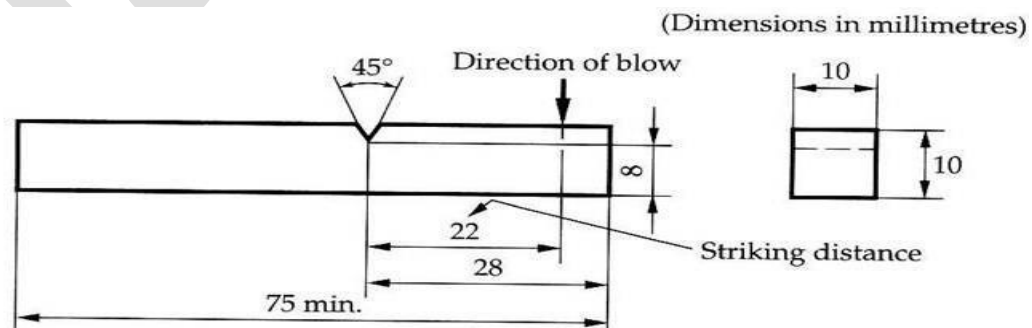
Fig.3 Impact Test Specimens details

5. RESULTS AND DISCUSSION

1. TENSILE TEST RESULTS

a. Before Cryogenic Treatment

Specimen	Tensile Strength in N/mm²
0%	80.265
3%	85.324
6%	93.168
9%	127.924
12%	121.131

Table.3 output data after tensile test

b. After Cryogenic Treatment

Specimen	Tensile Strength in N/mm²
0%	89.458
3%	96.739
6%	105.042
9%	138.97
12%	126.131

Table.4 output data after tensile test

	0%	3%	6%	9%	12%
WITHOUT CRYO TREATMENT	80.265	85.324	93.168	127.924	121.131
WITH CRYO TREATMENT	89.458	96.739	105.042	138.97	126.131
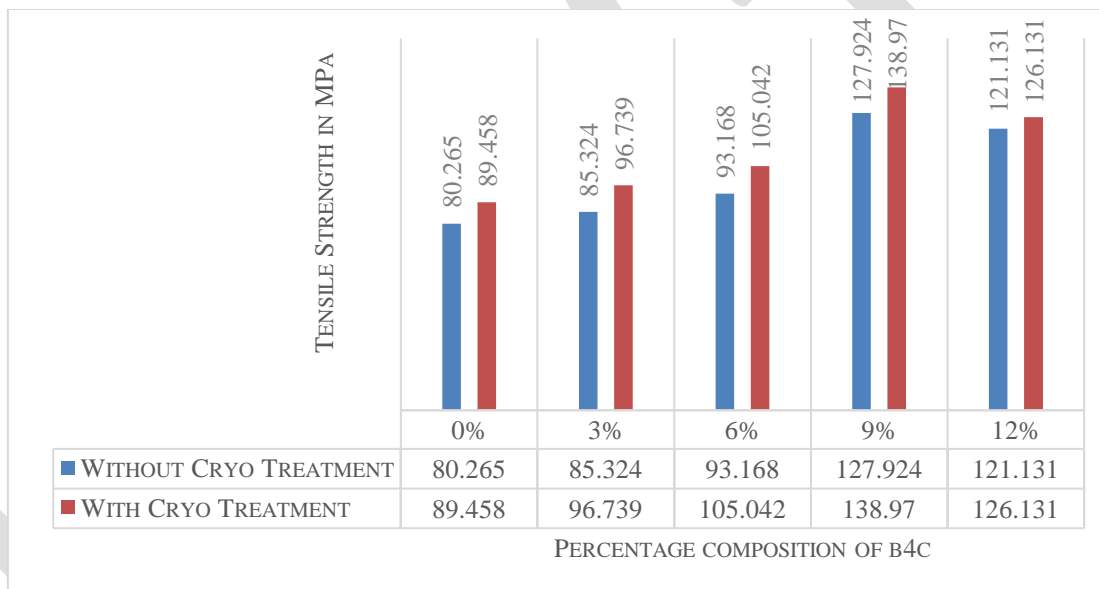
Fig.4 Variation of Tensile Strength and Peak load for different composition of B₄C

From above table/graph it shows that the B4C particles are very effective in improving the tensile strength of the composites. Tensile strength of the composite increases with increasing in particle size. The tensile strength of Aluminum metal matrix Composite was found to be maximum for the weight percentage of 9 and decreasing the strength gradually with the increase in weight percentage of the reinforcement. This is because the addition of B4C particles induces more strength to the matrix alloy by offering more resistance to the tensile strength.

When the material is cryogenically treated then the ultimate tensile strength and the yield strength increases with decrease in temperature. This is because the ultimate and yield strength of the material largely depends on the movement of the dislocation. At low temperature the internal energy of the atom is low. As a result, the atoms of the material vibrate less vigorously with less thermal agitation. When these agitations are low the movement of the dislocation is hampered. It requires very large stress to tear the dislocation from their equilibrium position. Therefore, the material exhibits increasing in ultimate and yield strength.

2. HARDNESS TEST RESULTS

a. Before Cryogenic Treatment

Specimen	Hardness Number (HB)
0%	26.87
3%	28.25
6%	32.75
9%	34.25
12%	36.58

Table.5 output data after hardness test

b. After Cryogenic Treatment

Specimen	Hardness Number (HB)
0%	28.62
3%	31.75
6%	35.73
9%	37.34
12%	39.84

Table.6 output data after hardness test

	0%	3%	6%	9%	12%
WITHOUT CRYO TREATMENT	26.87	28.25	32.75	34.25	36.58
WITH CRYO TREATMENT	28.62	31.75	35.73	37.34	39.84
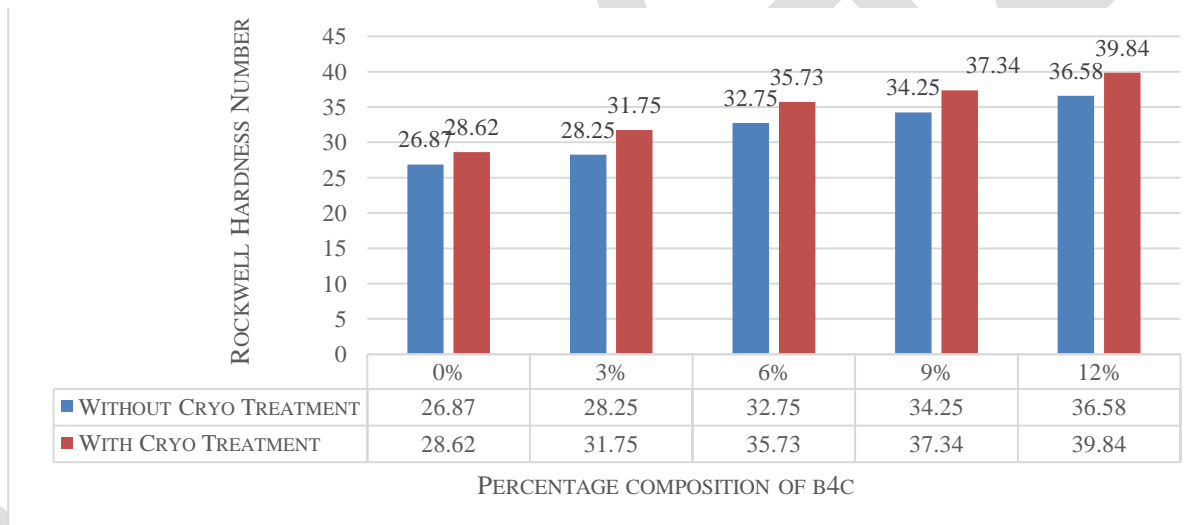
Fig.5 Variation of Rockwell Hardness Number for different composition of B_4C

The hardness of the AMC is increased with the increase in the particle size. The addition of the reinforcement particles in melt provides additional substrate from solidification to trigger, thereby increasing the nucleation rate and decreasing the grain size. For 12% of B4C the hardness was found to be maximum. With the presence of such hard surface, area of the particles offers more resistance to the plastic deformation which leads to increase in the hardness of composites. When the material is cryogenically treated, since the hardness is directly proportional to the ultimate tensile strength. It also follows the same trend as ultimate tensile strength.

3. IMPACT TEST RESULTS

a. Before Cryogenic Treatment

Specimen	Impact Value (Joules)
0%	2
3%	6
6%	4
9%	6
12%	12

Table.7 output data after impact test

b.   After Cryogenic Treatment

Specimen	Hardness Number (HB)
0%	1
3%	6
6%	4
9%	5
12%	11

Table.8 output data after impact test

	0%	1%	6%	9%	12%
■ WITHOUT CRYO TREATMENT	2	8	4	6	12
■ WITH CRYO TREATMENT	1	6	4	5	11

PERCENTAGE COMPOSITION OF B4C
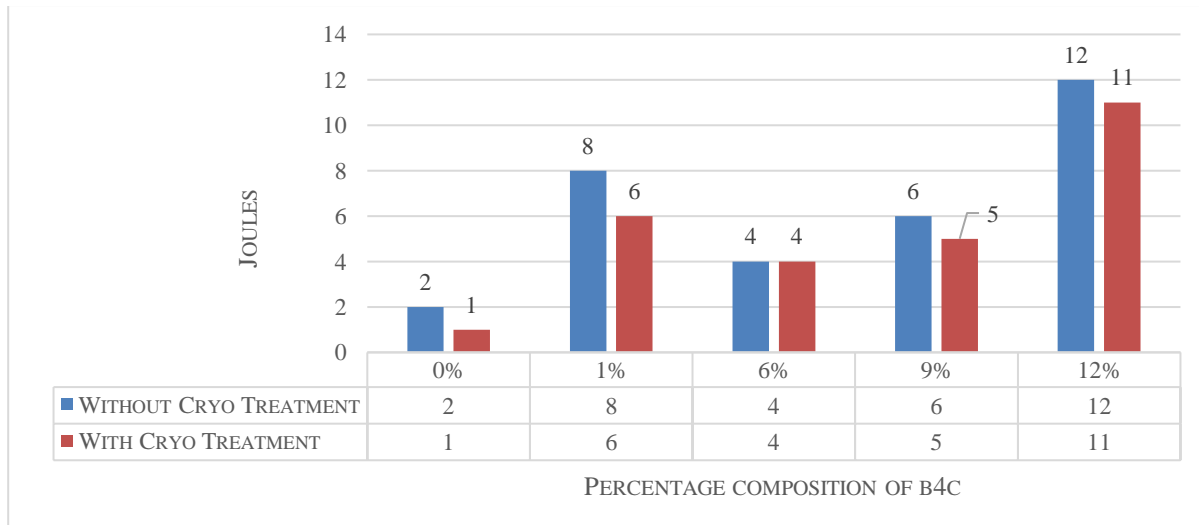
Fig.6 Variation of Impact test for different composition of B_4C

From the above graph it can be seen that the impact value is decreased and then increased with the increase in the percentage of reinforcement and the impact strength is less for cryogenically treated material because when the specimens are cryogenically treated the impact strength of material decreases with decreasing in temperature. This is because the material exhibits the ductile to brittle transition at low temperature.

6.   CONCLUSION

a)   The results from tensile test shows, the tensile strength increases have the percentage reinforcement increases and reaches the maximum at 9 wt% of reinforcement and then decreases gradually with increasing the reinforcement weight percentage.

b)   When the specimens are cryogenically treated the tensile strength increases with decreasing the temperature. It is found that the tensile strength is higher in case of cryogenically treated specimens on compared with non-cryogenically treated specimens.

c)   The results from the Rockwell hardness shows, hardness of the composites increases with increase in the percentage composition. For 12% composition hardness found to be maximum.

d)   In case of cryogenically treated specimens' hardness increases as the temperature decreases. On comparing with and without cryogenic condition, it is found that hardness increases for all wt% of reinforcement for cryogenic condition.

e)   The results from the Izod impact shows, the impact strength of the composite decreases with increase in the percentage composition but for 12% composition impact strength increases may because of presence of non-uniform distribution

f)   When the specimens are cryogenically treated, the impact strength decreases. This is because at low temperature the material exhibits ductile to brittle transition.

REFERENCES:

[1] R.M.Mohanty, K.Balasubramanian, Boron Carbide-nano particles reinforced hybrid Alumnium metal Matrix Composites: Fabrication and Properties, Materials Science and Engineering, 2007, A 498,42-52.

[2] Effect of deep cryogenic treatment on microstructure, mechanical and fracture properties of aluminium-al2o3 metal matrix composites by Panchakshari H.V., Girish D.P., M Krishn, ISSN: 2231-2307, Volume-1, Issue-6, January 2012.

[3] Panchakshari H.V, Dr. Girish D.P., ―Effect of cryogenic treatment on microstructure and microhardness of al6061-al2o3 metal matrix composites‖ Journal of Engineering Research and Studies E-ISSN0976-7916, JERS/Vol. III/ Issue I/January-March, 2012/105-107.

[4] Percentage reinforcement of b4c on the tensile property of aluminium matrix composites by Gopal Krishna U B, Sreenivas Rao K V and Vasudeva B, Vol. 1, No. 3, October 2012.

[5] S. Rama Rao, G.Padmanabhan, Fabrication and Mechanical Properties of Aluminium-Boron Carbide Composites, International Journal of Materials and Biomaterials Applications, 2012, 2(3),15-18.

[6] T.Raviteja, N.Radhika, R.Raghu, Fabrication and Mechanical Properties of Stir Cast Al-Si12Cu/B4C Composites, International Journal of Research in Engineering and Technology, 2013, 343-346.

[7] S.Prabagaran, G.Chandramohan, P.Shanmughasundaram," Influence of Graphite on the hardness and Wear behavior of AA6061–B4C Composite", Materiali in tehnologije / Materials and technology 48, 661–667, October 2014.

[8] Performance Investigation Of Cryogenically Treated Piston For Wear And Heat Distribution by S.Vijayraj, D.Venkatesh, S.Narayanan, G. Prabhu, 2015 October; 11(19): pages 102-110. 2015.

[9] Effect of cryogenic treatment on corrosion resistance of hybrid Aluminium7075 metal matrix composites by Arun C Dixit U Assistant Professor, Department of Mechanical Engineering, Vidyavardhaka College of Engineering, Mysuru, International Journal of Engineering Research and General Science Volume 4, Issue 3, May-June, 2016 ISSN 2091-2730.

[10] Cryogenic treatment on the mechanical and microstructural properties of aluminium alloys a brief study by Pavan.k.m, Sachin.L. S, Mayur.S, Chandrashekar.A, B.S. Ajaykumar.

DYNAMIC RESPONSE FOR DIFFERENT GEOMETRICAL SHAPE OF RCC SLABS

Aliyi Logita [1], Alemayehu Yilma Gebremikael [1]

Shashi Shekhar Singh [2]

Student of B.Sc., Department of Civil Engineering, Madda Walabu University, Bale Robe, Ethiopia [1]

Associate Professor, Department of Civil Engineering, Madda Walabu University, Bale Robe, Ethiopia [2]

shashi.mwu@gmail.com[2]

Abstract— Over the years, building slabs have been designed on the basis of equivalent static loading condition. It is assumed that the factor of safety taken during design process will take care of the variation that arises due to dynamic loading conditions. This process is appropriate for buildings with simple structural configuration – both in terms of geometry and material usage. The objective of this study is to carry out an analytical investigation to determine the realistic representation of modal properties of RCC slab (Different geometrical shape) and there by determine the best suited geometrical shape towards dynamic response.

Keywords— Modal Analysis, Dynamic Response, Finite Element Method, Rayleigh frequency, STAAD.PRO and Different Geometrical Shape.

INTRODUCTION:

Finite Element Method is universally accepted as a technique for numerical modelling to understand various structural behaviours, e.g. vibration characteristics, etc. To study an individual floor dynamics of a multi-storeyed building, modelling of the entire structure is not warranted. Therefore certain assumptions are to be taken for dynamic modelling of a floor slab.

Uncertainties to the shape of the slab also exist along with material property. The variation in stiffness of the floors due to improper assumption of shape of slab leads to variation in natural frequencies. Although a very realistic shape of slab selection depends entirely on the intuitiveness of the selector, no matter how good a selector may be, there always exist uncertainties in the results.

To resolve these uncertainties in selection of shape of slab, a Finite Element Analysis results is always necessary between the vibration parameters like natural frequencies, mode shapes etc.

METHODOLOGY:

To determine the shape of RCC slab towards dynamic response, Modal Analysis is performed to obtain the Rayleigh frequencies of the slab in different modes using STAAD.PRO software. These frequencies were obtained for all shapes (Circular, Regular Hexagonal, Regular Pentagonal, Regular Rectangular and Regular Triangular) of slab. In all of the cases, the frequencies are computed for keeping all the parameter constant. After obtaining these data, shape of slab v/s frequency graphs are plotted. The maximum frequency will give the familiar shape of slab towards dynamic response.

ANALYSIS OF RCC SLAB:

Dynamic force exerted on RCC slabs. In the current work Rayleigh frequency in fundamental mode is used to study the dynamic behavior of RCC slabs.

Following EBCS code are used for the analysis of RCC slabs.

      d)   EBCS-1:1995 , "Basis of design and actions on structures".

e) EBCS-2:1995, "Structural use of concrete".

f) EBCS-8:1995, "Design of structures for earthquake resistance".

PROBLEM – FOEMULATION:

Analyze the dynamic response for different geometrical shape of RCC slabs as per Ethiopian code of practice.
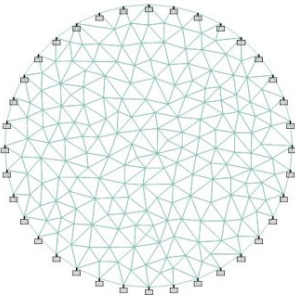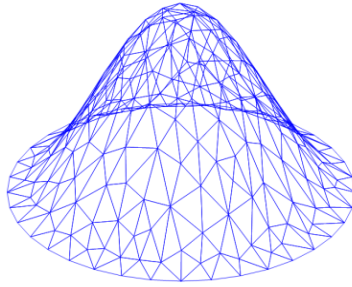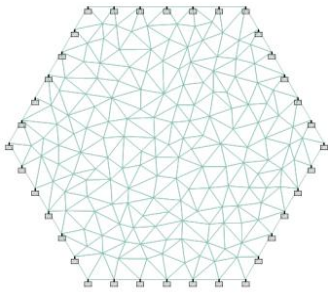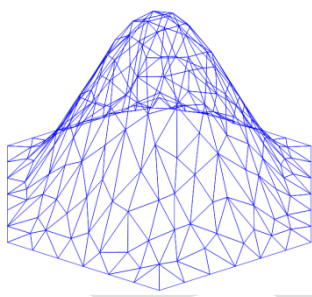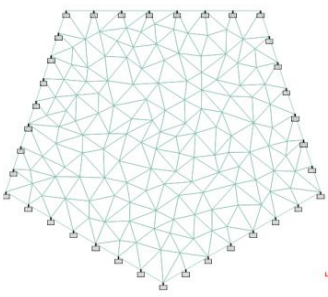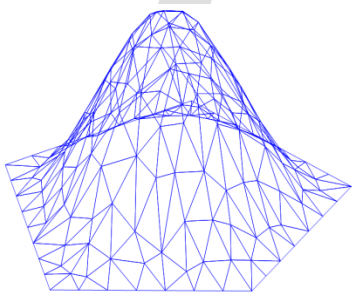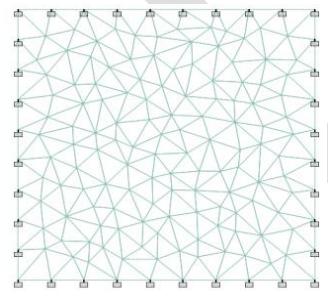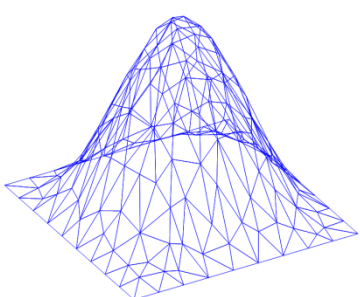
A. Detail of SLAB

- Type = RCC Slab with fixed Boundary condition.

- Surface area = 225m^2.

- Shape: Circular, Regular Hexagonal, Regular Pentagonal, Regular Rectangular and Regular Triangular.

- Thickness: 200 mm.

- Grade of Concrete: C30

- Material = Homogeneous and Isotropic.

- Young's Modulus of elasticity(E) = 3.2 x 10^{10} Pa

- Poisson's Ratio = 0.17

- Weight Density = 24kN/m^3

- No of division on Periphery = 36

- Meshing = Triangular

RESULT:

Fundamental mode shape and frequency in basic mode are tabulated in table-1 and table-2. Fig-1 shows the graphical representation of fundamental frequency for different geometrical shape of RCC slabs.

Table 1: Fundamental mode shape and frequency in basic mode for different geometrical shape of RCC slabs.

Shape of the Slabs (top view)	Detail of the RCC Slabs	Mode Shape (Fundamental mode)	Frequency (Hz) (Basic mode)
	1. Circular Slab 2. Surface area = 225m^2 3. Diameter = 16.92m 4. No of Division on Periphery = 36 5. Thickness = 200mm 6. Grade of Concrete = C30 7. Poisson's Ratio = 0.17		**4.787**

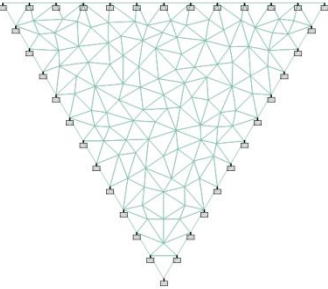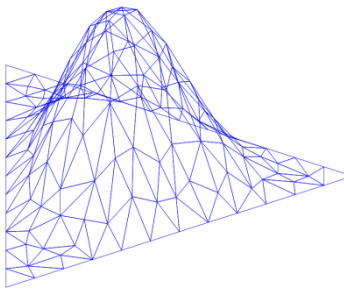|			
	8. Weight Density = 24kN/m^3 9. E = 3.2 x 10^{10} Pa		
	1. Regular Hexagonal Slab 2. Surface Area = 225m^2 3. Side = 9.309m 4. No of Division on Periphery = 36 5. Thickness = 200mm 6. Grade of Concrete = C30 7. Poisson's Ratio = 0.17 8. Weight Density = 24kN/m^3 9. E = 3.2 x 10^{10} Pa		**4.933**
	1. Regular Pentagonal Slab 2. Surface Area = 225m^2 3. Side = 11.4358m 4. No of Division on Periphery = 36 5. Thickness = 200mm 6. Grade of Concrete = C30 7. Poisson's Ratio = 0.17 8. Weight Density = 24kN/m^3 9. E = 3.2 x 10^{10} Pa		**5.343**
	1. Regular Rectangular Slab 2. Surface Area = 225m^2 3. Side = 15m 4. No of Division on Periphery = 36 5. Thickness = 200mm 6. Grade of Concrete = C30 7. Poisson's Ratio = 0.17 8. Weight Density = 24kN/m^3 9. E = 3.2 x 10^{10} Pa		**5.315**
	1. Regular Triangular Slab		**6.319**

2. Surface Area = 225m^2

3. Side = 22.795m

4. No of Division on Periphery = 36

5. Thickness = 200mm

6. Grade of Concrete = C30

7. Poisson's Ratio = 0.17

8. Weight Density = 24kN/m^3

9. E = 3.2 x 10^{10} Pa

Table 2: Frequency in basic mode for different geometrical shape of RCC slabs

Sr. No.	Shape of the Slab	Frequency (Hz) (Basic mode)
1	Circular	4.787
2	Hexagonal	4.933
3	Pentagonal	5.343
4	Rectangular	5.315
5	Triangular	6.319

Dynamic Responce in Basic Mode

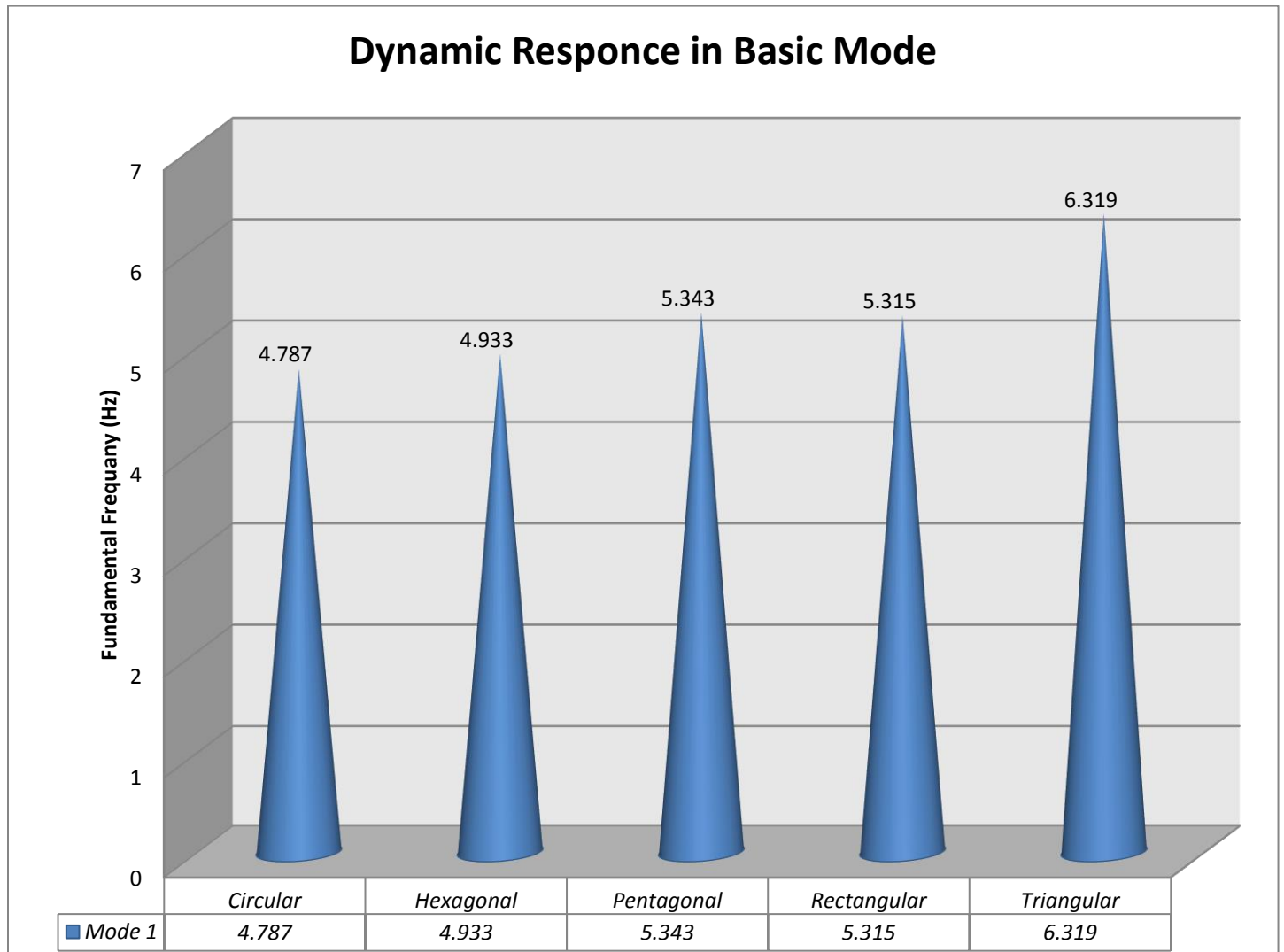|	Circular	Hexagonal	Pentagonal	Rectangular	Triangular
■ Mode 1	4.787	4.933	5.343	5.315	6.319

Fig-1 Fundamental frequancy for diferrent geomerical shape of slabs

CONCLUSION:

Following conclusions are obtained from all above graphical representations:

1. Fundamental frequency of Regular Triangular slab is 6.319 Hz which is highest among the entire slab.
2. Fundamental frequency of Circular slab is 4.787 Hz which is lowest among the entire slab.
3. Fundamental frequency of Regular Triangular slab is 32% more than Circular slab, 28.09% more than Regular Hexagonal slab, 18.26% more than Regular Pentagonal slab and 18.88% more than Regular Rectangular Slab.
4. Regular Triangular slab is best suited geometrical shape towards dynamic response among the entire slab.
5. Fundamental frequency of slab are decreasing if we are moving from Regular triangular slab to Circular Slab. But Fundamental frequency of Regular Pentagonal Slab (5.343 Hz) is more than Regular Rectangular slab (5.315Hz).
6. Regular Pentagonal Slab is better geometrical shape towards dynamic response than Regular Rectangular slab.

REFERENCES:

1. **Pavic A and Reynolds P (2001)**, "Dynamic modelling of post-tensioned concrete floors using finite element analysis", '*Finite Elements in Analysis and Design*', 37, 305-323.

2. **Blakeborough A. and Williams M. S.(2003)** , "Measurement of floor vibrations using a heel drop test", '*Structures & Buildings'*, 156(4), 367–371.

3. **Hanagan L M, Christopher H. R and Martin W. T.(2003)**, "Dynamic Measurements of In-Place Steel Floors to Assess Vibration Performance", '*ASCE Journal of Performance of Constructed Facilities*, 17(3), 126-135.

4. **Pavic A. and Reynolds P. (2003)**. "Vibration Serviceability of Long-Span Concrete Building Floors. Part 1: Review of Background Information. ", '*The Shock and Vibration Digest*, 34(3), 187–207.

5. **Pavic A. and Reynolds P. (2003)** ,Modal testing and dynamic FE model correlation and updating of a prototype high-strength concrete floor, '*Cement & Concrete Composites'* 25 ,787–799.

6. **Wolanski J A (2004)**, Ph.D thesis on, "Flexural behavior of reinforced and prestressed concrete beams using finite element analysis", '*Milwaukee, University of Wisconsin'*.

7. **Pavic A and Reynolds P (2007),** "Modal testing and FE model updating of a lively open-plan composite building floor", '*Journal of Structural Engineering'*, 133(4), 550-558.

8. **Mello da A, Silva da S (2008)**, "Modal analysis of orthotropic composite floors slabs with profiled steel decks", '*Latin American Journal of Solids and Structures'*, 5, 47-73.

9. **Ghada Saudi, Mohammed Zaki (2009),** "Finite-Element Model Tuning of Global Modes of a Grandstand Structure Using Ambient Vibration Testing", '*Journal of Performance of Constructed Facilities'*, 23(6), 467- 479.

10. **Krylov vv, Pickup s (2010)**, "Calculation of ground vibration spectra from heavy military vehicles", '*Journal of Sound and Vibration'*, 329, 3020-3029.

11. **Shashi Shekhar Singh (2011)**, M.tech thesis on, "Modal Testing of Reinforced Concrete Building Floors using Reaction Mass Shaker", 'IIT Kharagpur, India'.

12. **Ayush Srivastava, Belal Farooqi, Shashi Shekhar Singh (2016), "**Technique to determine the exact boundary condition of an existing RC building slab", 'International Journal of Civil Engineering and Technology ' , 7(6), 328-334.

13. **Aliyi Logita, Alemayehu Yilma Gebremikael, Gudisa Yadeta Galmesa, Nuguse Hailu Sime, Ajabi Bedada (2018),** B.Sc. thesis submitted on, "Dynamic Response for Different Geometrical Shape of RCC Slabs", 'MaddaWalabu University, Bale Robe, Ethopia.

The role of *T. viride* in deterring *F.roseum* aggressiveness on maize seedlings

Bouziane Z.*, Dehimat L. and Kacem Chaouch N

Laboratory of Applied Microbiology and Biotechnology, Constantine. Algeria.

Email; zh_bouziane@yahoo.fr

Abstract- The direct confrontation between *T. viride* and the various fungi tested *in-vitro* showed that it had a high capacity for competition, either by invading the entire surface of the petri dish, or by stopping the growth of pathogenic fungi at a distance. When inoculating maize plants with a concentration of 10^5 spores / ml by *F.roseum* by spraying the aerial parts, after 14 days of infection, the symptoms of the disease appeared on most maize plants, as did the length of the roots and the measurements of all the vegetative parts decreased significantly compared to control plants. *T. viride* was tested against *F.roseum* where *T. viride* was treated with a concentration of 10^6 spores / ml.

After 22 days of treatment, the symptoms of the disease were disappeared, and the measures of root length and aerial parts were close to those of the control. It is an effective fungus against phytopathogens because it secretes several enzymes that degrade fungal or bacterial cells through the use of parasitism mechanism.

Key words: *F.roseum*, *T. viride*, maize seedlings, growth degradation, biological control.

1-Introduction

The corn plant is of great agricultural and biotechnological importance (conversion of the product into bioethanol). It was also considered the first cereal plant, which was changed in its genotype GMO. However, this plant remains vulnerable to many abiotic factors (drought, pollution of the oceans .....) and biotic factors (harmful insects and fungi ...). Abiotic factors influence the development of the maize plant, facilitating its infection by various fungal pathogens and bacteria (Ristanovic, 2001). These diseases also lead to loss of yield of the nutritional and commercial value of dry matter loss or inability to germinate, analysis of sugars, fats and proteins. As research a progress, another method of control has been discovered, biological control, this is normally present in ecosystems that rely on the surveillance of pathogens by other organisms, including arthropods, nematodes (Lee and Lee, 2007). For this reason, this study was conducted to demonstrate the ability of the fungus *Trichoderma viride* to inhibit the growth of phytopathogenic fungi.

2-Materials and Methods

2.1-Preparation of corn seedlings

Under good sterilization conditions, corn kernels were put in a petri dish containing hypochlorite of sodium 10% for two minutes, in order to sterilize the surface to remove both microbes and the pesticide used when

treating the seeds. The latter have been dried by being placed inside a sterile filter paper, their transferred to petri dishes containing sterile filter paper saturated with sterile physiological water. Twelve grains were put systematically in the dish on the filter paper surface. After that, the grains were covered with another paper saturated with moisture. The dishes were incubated at a temperature of 22°c for 7 days (Benhamou and *al*., 1997).

After germination, the germinated seeds were transferred into pots containing 50 g of sterile soil and humus, where 10 seeds were put in earth pot. Twelve pots were prepared to realize the experiment, and five replications were made as control experiment. The pots were placed under normal conditions of lighting, ventilation and temperature (25-28°c) according to the weather conditions of May and June (2011). The seedlings were regulatory watered by plain water twice a week with about 50 ml for each pot once a week (Knop, 1965).

2.2-Inoculating the seedlings by pathogenic fungus *Fusarium roseum*

2.2.1-Preparing the sporal solution of *F.roseum*

Under good sterilization conditions, the sporal solution of *F.roseum* fungus was prepared by adding 5 ml of sterile distilled water to the fungal colony and then scraping the surface with an inoculation needle having the L shape; in order to obtain inicial solution of the sporal solution of *F.roseum*. After that, decimal dilutions (10^{-3}, 10^{-2}, and 10^{-1}) were prepared. After the preparation of the sporal solution, the spores of *F.roseum* were calculated using Thoma slice to obtain the concentration of 10^5 spore/ ml, and then the seedlings were inoculated (Gnancadja,2002).

2.2.2-Spraying the vegetative total with the suspension sporal of pathogenic fungi:

During the 04-leaf stage of maize seedling development, their leaves were sprayed with 50 ml of the sporal suspension of *F. roseum* at a concentration of 10^5 spores / ml (Woo and *al*., 2006).

2.2.3-Through the preparation of the sporal solution of the *Trichoderma viride*

The sporal solution of *T.viride* had been prepared in the same way that sporal fungal solution of *F.roseum* was prepared with an average of 10^6 spore/ ml and kept in the refrigerator till use (Rojan, 2010).

2.2.4-Treatment of maize plants by spraying the aerial part with the *T. viride* spore solution

After the onset of disease symptoms, the infected maize seedlings were sprayed with 50 ml of the sporal solution of *T. viride* at a concentration of 10^6 spores / ml (Windham and *al*., 1986).

3- Results

3.1- Inoculation of corn plants with *F.roseum* by spraying the aerial parts

After 14 days of inoculation of maize seedlings, record a clear difference in growth and morphology of the infected plants for the three samples tested compared to the control plants. On the other hand, the appearance of the red color on the limb of the tested plant leaves, the latter have been wrapped and take the pale yellow color (figure 1et 2). Statistical analysis shows at the level of 95% and 2 degrees of freedom that the tested plants differ from those of the control plants by the calculated value of (0, 03-0.,003-0,029- 0,025) for each of the (roots, stems, leaves, and the distance between the nodes), respectively, and are less than 0.05. Therefore, there is a difference between the average length of the plant parts of the tested samples and the control sample is different from zero, indicating the effect of *F.roseum* on the growth of maize plants. The root length of the infected plant samples (1 - 2 - 3) was (13 – 8, 33 - 10) cm. The length of the stems was estimated at (13-08- 07) cm, while the length of the limb was (23-17-17) cm finally, the distance between the nodes was estimated at (1, 81-2, 21 and 2, 28) cm respectively. The control plants reached a total root length of 19 cm, 20 cm legs, 55 cm leaves and finally the distance between the contractures of 4.75cm (table1), (figure 3, 4).

Table 1: Length of roots and aerial parts (cm) of maize plants after 14 days of *F.roseum* infection

plants parts The samples	Total root length (cm)	Length of stems (cm)	Length of leaves (cm)	Distance between nodes (cm)
Control	19	20	55	4,75
Sample 1	13	13	23	1,81
Sample 2	08,33	08	17	2,21
Sample 3	10	07	17	2,28

Figure1: Growth comparison of control plants with corn plants inoculated with *F.roseum* after 14 days of aerial spraying infection ((a) *F.roseum* infected plants, (b): control plants).

Figure2: Manifestation of the symptoms of *F.roseum* on the aerial parts, disappearance of the green color of the plants tested after 14 days of infection, ((a): disappearance of the green color of the leaves and lack of expansion of the blade with leaf curling, (b): yellowing of leaf margins with irregular white spots on the surface of some leaves, (c): burns in the center of the main leaf vein).
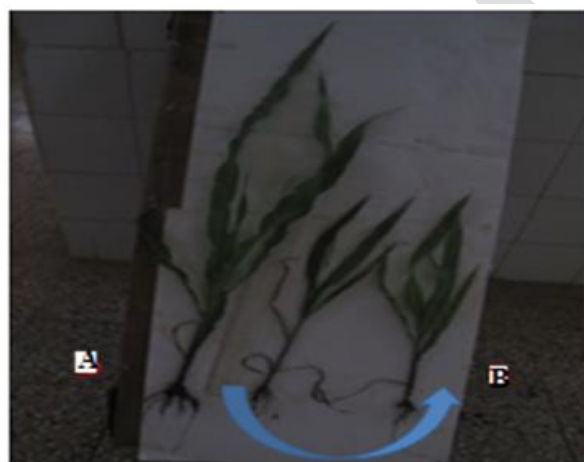

Figure3: Comparison of the length of the roots and stems of the control plants with those inoculated with *F.roseum* after 14 days of infection by aerial spraying ((a): plants infected with *F.roseum*, (b): control plants).
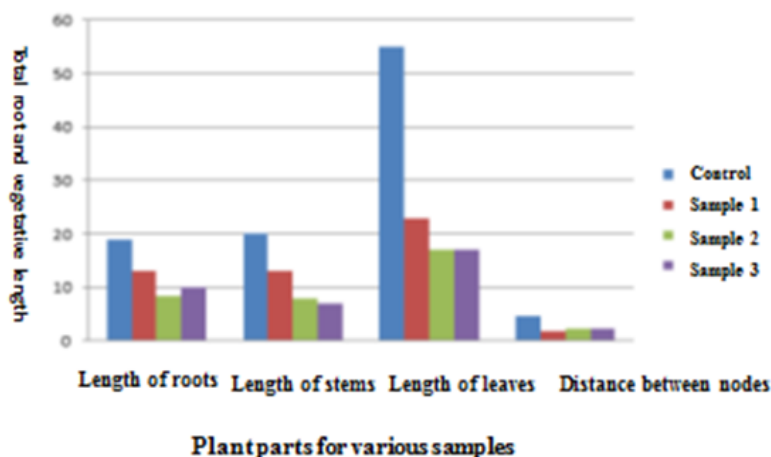

Figure4: Comparison of the length of roots and stems (cm) of corn plants inoculated with *F.roseum* by spraying the aerial parts with the control.

3.2- Treatment after infecting corn plants of *F.roseum* by spraying the overhead parts

Fourteen days after infection of *Fusarium*, all plants were treated with a spore suspension of *T. viride* (10^6 spores / ml), thus spraying all aerial parts.

After 22 days of treatment, several observations were recorded concerning the morphological characteristics of the plants (figure 5), it was noted the disappearance of the red color on the surface of the leaves and the stems of the plants, as well as the majority of seedlings took the green color after yellowing during infection (figure 6). The statistical analysis of the results at 95% level and the degree of freedom 2 refers to the calculated values 0,171- 0,233- 0,044- 0,270 for the parts of the plant tested (roots, stems, leaves, and the distance between the nodes) respectively, these values is greater than 0.05, Therefore, there is a difference between the average lengths of the tested plant samples, after being inoculated with *F.roseum*, and then treated with *T. viride,* this confirms the effect of *T. viride* on *F.roseum.* This results in the apparent regression of the symptoms of the disease and the increase in the length and size of the stems after they were thin. The length of the roots treated samples (1-2-3) reached (26, 5 – 31, 5 – 32, 5 cm) the length of the stems reached (20- 23, 5 – 23) cm the length of the leaves estimated from (55, 33 – 46, 36 – 53, 33) cm and finally the distance between the nodes was (2.42 - 3.35 - 3.21) cm respectively. In comparison with those of the control, in which the length of the roots was 34.5 cm, the stems with 23.5 cm, the leaves with 66 cm and the distance between the nodes estimated at 3.14 cm (table 2), (figure 7, 8).

Table 2: Length of roots and aerial parts of plants (cm) after 22 days of treatment of *T. virid*e by spray

Plants parts / The samples	Total root length (cm)	Length of stems (cm)	Length of leaves (cm)	Distance between nodes (cm)
Control	34,5	23,5	66	3,14
Sample 1	26,5	20	55,33	2,42
Sample 2	31,5	23,5	46,36	3,35
Sample 3	32,5	23	53,33	3,21

Figure5: Comparison of the growth of control plants to those which treated with *T. viride* after 22 days of spray treatment of aerial parts of plants ((a) plants treated with *T. viride*, (b): control plants).

Figure6: Disappearance of characteristic symptoms of *F.roseum* after 22 days of treatment with *T. viride* ((a, b, c): widening of leaf surface, disappearance of spots and yellow color, disappearance of burns at limb margins, and leaves recovered the color green).

Figure7: Comparison of length of roots and aerial parts of control plants to those treated with *T. viride* after 22 days of spray treatment of aerial parts ((b): treated with *T. viride*, (a): control plants).
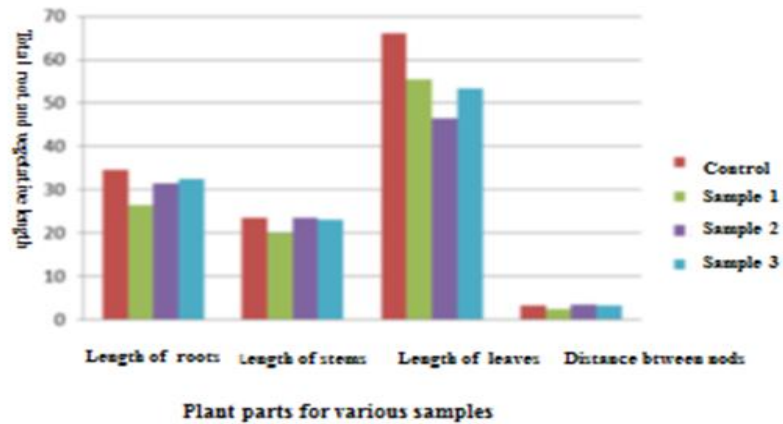
Figure8: Comparison of root length and aerial parts (cm) treated of *T. viride* untreated plants.

5- Discusion

Infection of the corn plant by a large number of fungi during their development can result in a loss of yield. *Fusarium* is probably infective to the roots, then develops and progresses densely, which stimulates their proliferation and causes the infection of neighboring plants. The pathogenic fungus continues to spread and infect from one year to the next, because of the germs found on plants or in the soil (Caron 2000).

Fusarium causes several diseases of the corn plant, including melting of seedlings, rot of stems and roots due to seed contamination. The disease is often observed in wetlands, and there is another source of fungi, the soil, where the fungus remains for a long time in the form of clamydospore. Seedling mildew disease is established in dry areas, which results in dryness in young seedlings in case of severe injury, and lateral roots fall in young stages (Gargouri, 2003).

In some cases, as the plant grows older, the fungus invades the stems, especially the young organs that constantly evolve and appear as white spots inside the marrow, often accompanying the dark red color on all parts of the plant. (Popescu, 2005) also points out those characteristic symptoms of the disease appear on the leaves during ripeness. During the interaction between the plant and *Trichoderma*, it contributes to the protection and enhancement of plant growth and soil fertilization. *Trichoderma* strains break down easily and also affect pathogenic fungi.

The ability of *Trichoderma* antagonism, is not only limited as a biological control agent, but it is considered a qualified agent for soil fertilization, preserves the integrity of the environment and helps to increase the fruit production and reduce the treatment of chemical compounds (Schirmbock and *al*., 1994)

Trichoderma is characterized by the production of large amounts of hydrolytic enzymes, which contribute to parasitism and secretion of enzymes (CWDE) capable of lysing the cell membrane of various hosts, including chitinase, 1,3-glucanase and proteases (Kubicek and *al*., 2001).

6- Conclusion

In the case of infection of *F.roseum* by spraying the aerial parts of the tested plants, after 14 days the manifestation of the characteristic disease symptoms of the inoculated fungus, consisting of leaf rolling and yellowing of the latter, was observed appearance of red color on the leaves of infected plants but less frequently, than it was when inoculating corn plants at ground level. There was a significant decrease in root length measurements, stems, leaves, and the distance between nodes compared with control.

After treatment of *T. viride*, there was a significant increase in measurements of different organs of the treated plants. Thanks to all these measurements and morphological characteristics, it can be said that the *T. viride* fungus plays an effective role in improving plant growth and also has the ability to resist fungal diseases associated with plants.

To demonstrate the effectiveness of *T.viride* against pathogenic fungi of plants in the applied field, we suggest future prospects:

- The study of the mechanical effect of *T.viride* on stopping the growth of pathogenic fungi.
- Determination of the tolerant range of pathogenic fungi and their susceptibility against *T. viride*.
- The use of *T. viride* in the field of agriculture to fight against fungal diseases
- Biotechnology study of *T. viride* leads to the extraction of their secondary metabolites, identifying these metabolites and then applying them in agriculture.

REFERENCES:

1- Benhamou, N., Rey, P., Cherif, M., Hoclenhul, J. and Tirilly, y. (1997). Treatment with the mycoparasitic *Pythium obligandrum* triggers inductionot defence- related reaction in tomato roots when challenged with *Fusarium oxysporium f.sp.radias- lycopersici. Phytopathology*, 87 p. 108-121.

2- Caron, D. (2000). *Fusarium* spikes or their agricultural perspective development January 2000, pp. 56-62.

3- Gargouri, S. (2003).Evaluation of the incidence of wheat foot rot and population structure of *Fusarium* species associated with the disease. Thesis in plant biology, Faculty of Sciences of Tunis, Tunisia. 9pp.- Popescu, Gh. (2005).Tratat de patologia plantelor, vol II, *Agricultura. Ed. Eurobit, Timisoara*, 54-63.

4- Gnancadja-André (L.S). (2002). Study of the mycoflora responsible for tarnishing of rice grains. Same. DE SA, Univ. Ibn Tofail, Fac. Sci. Kenitra, Morocco, 2002, 40 p.

5- Knop, W. (1965). Quantitative untersuchungen über die Ernährungosprozesse der pflanzen. Landwirtch. Vers. Stn, 7: 93-107.

6- Kubicek, C.P., Mach, R.L., Peterbauer, C.K. and Lorito, M. (2001). *Trichoderma*: from genes to biocontrol, *J. Plant Pathol*, 83 (2001) 11-23.

7- Lee, Y.S. and Lee, M. W. (2007). Biological control of various diseases of major vegetables in Korea. In: Chincholchar, S.B. and Mukerji, K.G (eds): Biological control of plant diseases [pp. 283-318]. The Haworth Press. Inc. New York.

8- Ristanovic, D. (2001). Mains (Zea mays L.). In Raemaekers, R.H.(2001). Agriculture on Afrique Tropicale. Eds Greoking Graphics. Bruxelles, Belgique, pp.44-69.

9- Rojan, P.J., Tyagi, E.D. ,Prévost, D., Satinder, K.B., Pouleur, S. and Surampall, R.Y.(2010).Mycoparasitic *Trichoderma viride* as a biocontrol agent against *Fusarium oxysporium f.sp.adzuki* and *Pythium arrhenomanes* and as a growth promoter of soybean.*Elsevier.Crop.Protection*,29(2010).1452-1459.

10- Schirmbock, M., Lorito, M., Wang, Y-L., Hayes, CK., Arisan-Atac, I., Scalar, F., Harman, GE. and Kubicek, CP. (1994). Parallel formation and synergism of hydrolytic formation enzymes and peptaibol antibiotics, molecular mechanisms involved in the antagonistic action of *Trichoderma harzianum* against phytopthogenic fungi. *Appl Environ. Microbial* 60: 4364-4370.

11- Windham, MT. Elat, y. and Baker, R. (1986). A mechanism for increased plant growth induced by *Trichoderma spp*. *Phytopathology*, 76, p.518-521.

12- Wood, M. (2002). Gene Jockey fights *Fusarium* head blight. *Agriculture Research*, 50: 12-13.

International Journal of Engineering Research and general science is an open access peer review publication which is established for publishing the latest trends in engineering and give priority to quality papers which emphasis on basic and important concept through which there would be remarkable contribution to the research arena and also publish the genuine research work in the field of science, engineering and technologies